THIOGLYCOSYLATED PHORPHYRIN, CHLORIN, BACTERIOCHLORIN AND ISOBACTERICHLORIN AS PHOTODYNAMIC THERAPEUTIC AGENTS AND THEIR POSSIBLE USE AS BIOIMAGING AGENTS

by

SEBASTIAN THOMPSON

A dissertation submitted to the Graduate Faculty in Chemistry in partial fulfillment

of the requirements for the degree of Doctor of Philosophy,

The City University of New York

2009

This manuscript has been read and accepted for the
Graduate Faculty in Chemistry in satisfaction of the dissertation
requirement for the degree of Doctor of Philosophy.

_____ _____

Date

Dr. Charles Michael Drain
Chair of Examining Committee

_____ _____

Date

Dr. Mahesh Lakshman
Executive Officer

Dr. Frida Kleiman

Dr. Derrick Brazill

Dr. Sushmita Mukherjee

Dr. Michele Vittadello

Supervisory Committee

Abstract

THIOGLYCOSYLATED PHORPHYRIN, CHLORIN, BACTERIOCHLORIN AND ISOBACTERICHLORIN AS PHOTODYNAMIC THERAPEUTIC AGENTS AND THEIR POSSIBLE USE AS BIOIMAGING AGENT

by

Sebastian Thompson

Adviser: Professor Charles Michael Drain

Since first used about a hundred years ago, photodynamic therapy is now a well-established treatment for a variety of cancers and other diseases, and is emerging as new treatments for a broad range of other cancers, antibiotics, and antivirals. In terms of cancer therapy, a dye capable of photosensitizing the formation of singlet oxygen and/or producing reactive oxygen species is delivered to the cancer tissues. Upon activation by either a band or a specific wavelength of light, the reactive oxygen species produced will oxidize nearby biomolecules such as aromatic amino acids, double bonds in lipids, and nucleic acid with diffusion limited kinetics. The resulting oxidative stress induces necrosis or apoptosis depending on a variety of factors including degree and location of the damage. Currently, about four drugs are approved to treat several different types of

cancer, these are porphyrinoids or porphyrin precursors, but none have cancer cell targeting motifs appended to the dye.

To improve the photodynamic therapy efficacy, significant research is focused on development of new photosensitizers that may have advantages over the ones currently used. Major research thrusts include: (A) improving dye light absorption in the 650 nm – 850 nm region for activation deeper into tissues and tumors, (B) improve selectivity towards cancer cells, and (C) faster biodistribution and clearance from the body after treatments. Together with these objectives, it is also important to understand the mechanism of action in terms of how the photogenerated toxic species initiate the different pathways for cell death. This latter information is important for the design and development of new compounds, and to understand how the cancer cells respond to this method of treatment.

Our lab developed a series of glycosylated porphyrins using a thioether linkage. The thioglycosylated phorphyrins are nonhydrolysable under physiological conditions and have been shown to be active photodynamic therapeutics, but only weakly absorb light above 650 nm. The chlorin, bacteriochlorin, and isobacteriochlorin derivatives are presented as new photodynamic therapy and dual-function imaging/therapeutic agents with photophysical properties that afford significant advantages over the parent compound, both in terms of light activation and imaging. The effectiveness of photodynamic treatment in initiating necrosis and apoptosis are analyzed and described. In addition, the isobacteriochlorin is presented as a two photon active compound, wherein it is activated by two photons between 780 nm and 880 nm. The two photon absorption property of the isobacteriochlorin is an important feature that allows optimal wavelengths

to be used and is part of a burgeoning field in photodynamic therapy. Considering the different photophysical properties of this compound, the possibility to use this compound as a dual function bioimaging/therapeutic agent is discussed.

Acknowledgments

I would like to thank Prof Drain, Prof Frida Kleiman, Prof D. Brazill, Prof Sushmita Mukherjee, Prof Frederick Maxfield, all the people at Hunter College, Cornell University and everyone who attend my defense.

This work was supported by the NSF (CHE-0554703) to C.M.D. Hunter College science infrastructure is supported by the National Science Foundation, the National Institutes of Health including the RCMI program (G12-RR-03037), and the City University of New York. S.T is thankful for suppor. of the Clinical and Translational Science Center at Weill Cornell Medical College(UL1RR024996)

Table of Contents

List of Tables

List of Figures

.

List of Abbreviations

PDT ..... Photodynamic therapy

ER ..... Endoplasmic reticulum

NMR ..... Nuclear magnetic resonance

$PGlc_4$……..Thioglycosylated porphyrin

$CGlc_4$..... Thioglycosylated chlorin

$IGlc_4$ .....Thioglycosylated isobacteriochlorin

$BGlc_4$.....Thioglycosylated bacteriochlorin

PARP ……...……. poly-(ADP ribose) polymerase

PS…… ……..photosensitizer dye

2PM……... Two photon microscopy

1PM……... One photon microscopy

2PA……...Two photon absorption

Apaf-1……..Apoptotic protease activating factor-1

Pro-caspase-9…….……. Cysteine aspartate-specific protease

DMEM…….……Dulbecco's Modified Eagle Medium

CHOP……...Growth arrest and DNA damage/C/EBP homology protein

DNA…….……..Deoxyribonucleic acid

ATP…….……Adenosine triphosphate

Chapter 1:

OVERVIEW OF THE PHOTODYNAMIC THERAPY OF CANCER AND TWO PHOTON IMAGING.

1.1 Introduction

Cancer is a disease where one or several cells develop new proprieties, such as uncontrolled growth, invasion and, in the worst of the cases, they have the propensity to produce metastasis – secondary tumor sites. The changes that produce these new cell behavior/properties rely on a specific suite of genes[1] that control growth and differentiation. In 2002 about half million of people died from cancer in the United States,[2] and while in most cases cancer is still an implacable disease, a growing number of cancers can be cured if diagnosed in an early stage. Currently, one of the most promising approaches for diagnosing the disease is the detection of biomarkers for a particular cancer. However, variations in genetic patterns among patients, along with the difficulty of finding new biomarkers for a particular cancer type, are important issues to be overcome for the widespread application of genomic and proteomic tools in cancer diagnosis.[3] Broadly, there are more than twenty different treatments against cancer that include, for example surgery, radiation, chemotheraphy, and photodynamic therapy.

Photodynamic therapy (PDT) is one of the current anticancer treatments that is finding a growing number of applications[4] – especially when other procedures are disfiguring or exceedingly painful such as head and neck cancers. PDT involves the

delivery of a photosensitizer dye (PS) to the cancer cell followed by irradiation with either white light or a specific wavelength of light.[5] The current embodiment of PDT is that the patient is dosed with a photosensitizing dye and the specificity arises largely from the selective irradiation of target tissue with light in the visible region of the electromagnetic spectrum. Upon irradiation the dye becomes reactive and/or toxic, or it photosensitizes the formation of reactive and/or toxic species such as reactive oxygen species (e.g. singlet oxygen, hydroxyl radicals) in vivo. It is commonly accepted that the toxic species generated in situ will cause damage to vital cellular components (e.g. aromatic heterocycles, double bonds, redox enzymes, membranes) which then activates one of the different cell death pathways: apoptosis or/and necrosis[6]. Concerning the photosensitizer, there are several characteristics that they need to possess to be considered a good agent for photodynamic therapy. (A) Although in PDT there is possibility to deliver the light to only the cancer cells, the drug selectivity for cancer cells and uptake should be optimized to minimize possible damage to healthy tissue surrounding the tumor. (B) The sensitizer needs to be able to absorb the light, and 600 nm to 800 nm is considered the optimal “therapeutic window” because this light penetrates deepest into tissues.[7] (C) In addition to these important characteristics, the kinetics of uptake and elimination from the human body should be fast enough to reduce the possible secondary effects such as damage caused by sun exposure.

1.2 Apoptosis Overview

Apoptosis is considered more than simply cell suicide, but is more accurately refered to as “programmed cell death.”[8] Apoptosis is the most important studied mechanism of cell death, and several million cells in the human body undergo

apoptosis every second. Insufficient apoptosis may prompt oncogenesis by allowing cell accumulation, while excessive apoptosis may be the basis of degenerative diseases such as Huntington's and Alzheimer's.[9] Apoptosis is manifested by both biochemical and morphological changes including: cell shrinkage, chromatin condensation, DNA fragmentation, plasma membrane blebbing and vesiculating, and phosphatidylserine lipid redistribution to the cell surface. Apoptosis plays an important role in the balance between cell death and cell growth.[10] Of the vast number of reports on apoptosis, there are a few on the induction of apoptosis by photodynamic treatments. Cellular responses to photodynamic therapy depend on the cell type, the specific photosensitizer, the dosage of both photosensitizer and light, and other factors[4]. The specific subcellular localizations of the photosensitizer dictates the sites of primary photo damage, thus the potential apoptosis initiation point(s). To date, the photosensitizers used in PDT are found to localize mostly in the mitochondria, lysosomes, endoplasmic reticulum (ER), and cell membranes. Concerning apoptosis, after its activation, the mitochondrial potential is lost, which is followed by the release of cytochrome c to the cytosol. Cytochrome c, upon binding to apoptotic protease activating factor-1 (Apaf-1) and pro-caspase-9 (cysteine aspartate-specific protease), activates the caspases. The activation of caspase-9 then triggers a cascade of proteases. The induction of the caspases also triggers a variety of other responses in the cell via signaling pathways, such as chromatin condensation, DNA cleavage, and the cleavage of repair enzymes such as poly-(ADP ribose) polymerase (PARP). The detection of these activities is generally considered as biochemical markers of apoptosis. Release of cytochrome c from between the inner

and outer membranes of the mitochondria has been shown to accompany apoptosis in every circumstance with every cell line studied to date, though the mechanism of the release of this enzyme remains a topic of interest. Generally, the photosensitizes that localize in the endoplasmatic reticulum[11] and/or mitochondria[12] initiate apoptosis after they have been activated by irradiation with light.

1.3 Necrosis

While apoptosis is programmed cell death, necrosis is cell death produced by external factor(s). These external factors include infection, trauma, toxic species, and lack of blood irrigation. Generally, cell necrosis is not considered beneficial for the human body since it is an uncontrolled process and several chemicals may be released from the dead or dying cells to the tissue that may trigger other biological responses. For example, necrosis is produced when the plasma membrane is compromised or the production of ATP is interrupted. Another important difference between these two cell death pathways is that necrosis is produced rapidly after the external factor is manifested, while apoptosis is generally a much slower process that can take several hours to observe changes in cell morphology.[13]

As with apoptosis, necrosis can also be activated using PDT, and each has advantages and disadvantages in terms of treatment.[14] Although less studied than apoptosis, necrosis is activated usually when the photosensitizer is located at the plasma membrane and/or the endosomes/lysosomes.[15] Although not a strict rule, it is often considered that low light power and low PS concentration are two conditions that will induce apoptosis while the opposite conditions will activate necrosis.[6]

In the cases where the PS concentrates in different organelles, there are important possibilities to induce necrosis or apoptosis depending the protocol used to deliver the PS to the cell. Protocols that involve shorter incubation times will kill the cell by necrosis, since the plasma membrane will be the primary location where the PS will concentrate. On the other hand, apoptosis will be activated with protocols using longer incubation times because this allows the time needed for the PS to concentrate in organelles such as the mitochondria or the endoplasmic reticulum.

1.4 Two Photon Microscopy

Two photon microscopy (2PM) was first introduced by Denk et al at Cornell University, and although the theory of 2PM is not yet complete, it is presumed that two photons are absorbed at the same time.[16] Since the probability of a molecule absorbing two photons in the same quantum event is low, femto-second laser pulses are needed to deliver enough photon flux to increase this possibility. After the simultaneous absorption of two photons, the molecule is in an excited state that follows the normal relaxation processes that occur after single photon excitation.[16]

Two photon microcopy in biological systems has several advantages compared with standard, one photon microscopy (1PM). First, the photons used in 2PM have lower energy (usually half) than those used in 1PM, and for this reason they are likely located in the “therapeutic windows” of the light spectrum. Secondly, because of the necessary high light flux, the excitation is confined only the small volume where the laser is focused, and it is almost zero where the laser is not focused.[16] Both the highly localized light and the red photons used considerably decrease the damage to healthy surrounding tissues when 2PM is applied to biology samples, i.e. only cells containing a good two

photon absorbing (2PA) dye will be effected. As mentioned above, the use of light in the therapeutic window allows treatments deeper into the body. Although advantages of using 2PM to detect and treat cancer via PDT (over the traditional single photon absorbing dyes) exit, there are several unresolved problems concerning 2PM – PDT. Though there has been recent progress,[17] most photosensitizers have poor two photon cross sections (low two photon absorbance). Secondly, the instrumentation to deliver a sufficient light flux for 2PA is not as simple as the corresponding microscopes and endoscopes used for standard single photon imaging and treatments. Issues of light scattering and localized heating affected by two photon light sources versus penetration into the various parts of the body are not well characterized, and so for the present restrict the possible applications of 2PM and two photon absorbing dyes for photodynamic therapy[18].

1.5 Summary

Although photodynamic therapy is one of the promising anticancer treatments, there are several points that current research is focused to improve them. First of all, the second generation of PS are designed to absorb (and emit) light at lower energy (wavelengths greater than 600 nm) where the light has more penetration into tissue and produces less damage to nearby healthy cells. For this reason, Chapter 3 describes the discovery and characterization of three porphyrin derivates with stronger and/or longer wavelength absorption above 600 nm; specifically, a chlorin, an isobacteriochlorin, and a bacteriochlorin. Of special note is the bacteriochlorin, since this compound has a strong single photon absorption band near 740 nm. To take advantage of two photon activation of the PS for therapy and for microscopy, there are several compounds currently under

investigation designed to be used as two-photon photodynamic therapeutics.[19] Concerning our compounds, the isobacteriochlorin is practically active in two photon microscopy using 750 nm to 880 nm light where there are no single-photon absorption bands. Interestingly, with 750 nm to 880 nm light the bacteriochlorin may be activated in both single-photon and two-photon excitation, or alternatively the compound may have a small amount of a single photon absorption band in this spectral region. An understanding of how the PS activates cell death is an important tool for both improving PS efficacy and to develop the best protocol for drug delivery. Our research described in Chapters 2 and 4 was mainly done to characterize uptake and evaluate the extent of apoptosis and necrosis for the tetraglycosylated porphyrin and tetraglycosylated chlorin. While apoptosis is activated for the population that is located in the endoplasmic reticulum, necrosis is presented when for the PS concentrated in the plasma membrane.

(15) Ahn, WS; Bae, SM; Huh, SW; Lee, JM; Namkoong, SE; Han, SJ; Kim, CK; Kim, JK; Kim, YW Int. J. Gynecol. Cancer 2004, 14: 475-482.

(16) Denk, W; Strickler, JH; Webb, WW; Science 1990, 248: 73-76.

(17) Starkey JR, Rebane AK, Drobizhev MA, Meng F, Gong A, Elliott A, McInnerney K, Spangler CW. Clin Cancer Res. 2008, 14: 6564-73.

(18) Karotki, A; Khurana, M; Lepock, JR; Wilson, BC Photochem. Photobiol. 2006, 82: 443–452.

(19) Ogawa, K; Kobuke, Y Org. Biomolecular Chem. 2009, 7: 2241 – 2246.

Chapter 2

APOPTOSIS ACTIVATION BY A NON-HYDROLYSABLE TETRA GLYCOSYLATED PORPHYRIN AFTER PHOTODYNAMIC TREATMENT: LOCALIZATION, PATHWAYS AND CONDITION

2.1 Abstract

A water-soluble tetra-S-glycosylated porphyrin ($PGlc_4$) is absorbed by MDA-MB-231 human breast cancer cells whereupon irradiation with visible light causes necrosis or apoptosis depending on the concentration of the porphyrin and the power of the light. With the same amount of light irradiation power (9.4 W m^{-2}), at 10-20 µM concentrations necrosis is predominantly observed, while at <10 µM concentrations, apoptosis is the principal cause of cell death. Of the various possible pathways for the induction of apoptosis, experiments demonstrate that calcium is released from the endoplasmic reticulum, cytochrome c is liberated from the mitochondria to the cytosol, pro-caspase-3 is activated, poly-(ADP-ribose) polymerase is cleaved, and the chromatin is condensed subsequent to photodynamic treatment of these cells. Confocal microscopy indicates a substantial portion of the $PGlc_4$ is located in the endoplasmic reticulum at <10 µM. These data indicate that the photodynamic treatment of MDA-MB-231 cells using low concentrations of the $PGlc_4$ porphyrin and low light induces apoptosis mostly initiated from stress produced to the endoplasmic reticulum

2.2 Introduction

Apoptosis, programmed physiological cell death, is an essential and well-regulated cell function that allows for the ordered removal of superfluous, aged, or damaged cells.[1,2] Several million cells in the human body undergo apoptosis every second. Insufficient apoptosis may prompt oncogenesis by allowing cell accumulation, while excessive apoptosis may be the basis of degenerative diseases such as Huntington's and Alzheimer's. Apoptosis is manifested by both biochemical and morphological changes including: cell shrinkage, chromatin condensation, DNA fragmentation, plasma membrane blebbing and vesiculating, and phosphatidylserine lipid redistribution to the cell surface. In contrast, the pathology of necrosis is characterized by significant degradation of membrane integrity and leakage of cell contents.

Photodynanmic therapy (PDT) is an approved treatment for a variety of cancers that can be exposed to a high flux of light[3] – either white or a band centered at a particular wavelength. The concept is that the patient is dosed with a photosensitizing dye and the specificity arises largely from the selective irradiation of target tissue with light in the visible region of the electromagnetic spectrum. Upon irradiation the dye becomes reactive and/or toxic, or it photosensitizes the formation of reactive and/or toxic species in vivo. The chromophores used in current technologies, and those in the immediate pipeline, are generally not selective for cancer tissue beyond what would be expected from the greater metabolism. These agents are generally believed to photosensitize the formation of singlet oxygen.

Singlet oxygen then reacts with a variety of cellular components including, aromatic amino acids, double bonds in lipids, a variety of redox enzymes and cofactors, and both the bases and the phosphate backbones of DNA and RNA. The mechanism(s) of action of PDT agents arise from both the photophysical properties of the chromophore and the specific localization of the porphyrin in the cell or tissue. The uptake and localization of the photodynamic agent in the cell depends exquisitely on the exact chemical structure of the dye and any covalently bound auxiliary motifs.[4]

The initiation of apoptosis using low concentrations of a non-hydrolyzable tetraglycosylated porphyrin with low light irradiation is presented in this chapter. Phototoxicity studies reveal that as the concentration of P-Glc_4 decreases from 20 μM to 10 μM the percentage of immediately necrotic cells decrease and the percentage of cells that exhibit a delayed response increase. Studies at 5 μM show less necrosis and the percentage of apoptotic cells is less, and at 1 μM neither necrosis nor apoptosis are indicated. As illustrated below, the specific concentration and localization of the photodynamic chromophore, as well as the light intensity, dictate the mode of cell death.

Of the vast number of reports on apoptosis, there are a few on the induction of apoptosis by photodynamic treatment. Cellular responses to photodynamic treatment depend on the cell type, the specific photosensitizer, the dosage of both photosensitizer and light, and other factors. The specific subcellular localizations of the photosensitizer dictates the sites of primary photo damage, thus the potential apoptosis initiation point(s). To date, the photosensitizers used in PDT are found to be localized mostly in the mitochondria, lysosomes, endoplasmic reticulum (ER), and

cell membranes. Concerning apoptosis, after its activation, the mitochondrial potential is lost, which is followed by the release of cytochrome c to the cytosol. Cytochrome c, upon binding to apoptotic protease activating factor-1 (Apaf-1) and pro-caspase-9 (cysteine aspartate-specific protease), activates the caspases. The activation of caspase-9 then triggers a cascade of proteases. The induction of the caspases also triggers a variety of other responses in the cell via signaling pathways, such as chromatin condensation, DNA cleavage, and the cleavage of repair enzymes such as poly-(ADP ribose) polymerase (PARP). The detection of these activities is generally considered as biochemical markers of apoptosis. Release of cytochrome c from between the inner and outer membranes of the mitochondria has been shown to accompany apoptosis in every circumstance with every cell line studied to date, though the mechanism of the release of this enzyme remains a topic of interest.

The entry and partition of photosensitizers in cells is a complex issue that depends on nonspecific properties such as hydrophobicity and the subtituents on the molecule that may target specific cell membrane structures. It may be that many compounds enter into cells via more than one pathway and partition into several cellular components with a time-dependence. Some photosensitizers preferentially bind the plasma membrane, where a number of signaling pathways including apoptosis may be induced, though the mechanisms remain controversial. Apoptosis is rapidly induced at the plasma membrane level via activation of “death-inducing signaling complexes” (DISCs) that involve cell surface receptors such as Fas and tumor necrosis factor receptor (TNFR).

Research on porphyrins appended with sugar moieties has been of great interest in the last decade.[5] Glycosylated porphyrins can have greater water solubility than most naturally occurring and synthetic porphyrins. Amphipathic solubility can not only increase the efficacy of drug delivery but also assist the drug elimination from the organism after treatment. The proper amphipathicity of neutral saccharide conjugated porphyrins enables them to permeate better into both lipophilic and hydrophilic biological structures. Furthermore, they can have specific interactions with saccharide transporter and other proteins on cell membranes, and thus exhibit specific targeting of cancer cells

2.3 Experimental procedures

Materials. All chemicals were purchased from Sigma-Aldrich. Dulbecco's Modified Eagle Medium (DMEM) and antimycotic for cell culture were obtained from GibcoBRL. Bovine calf serum was obtained from HyClone. PBS (136 mM NaCl, 2.6 mM KCl, 1.4 mM KH_2PO_4, 4.2 mM Na_2HPO_4) was obtained from Invetrogen. The 13W fluorescent bulb was from Sanco. The antibodies against CHOP and eIF2 were a kind present from Dr. Alejandro Adam from SUNY. The ER-tracker Green and the Fluo-4 was purchased from Invitrogen. P-Glc_4 was synthesized as described previously, and has a fluorescence quantum yield in cell culture medium of about 5%.

Cell Culture. Cells were maintained in DMEM, 10% bovine calf serum, 1% antimycotic, at 37^0 C and 5% CO_2 atmosphere.[8] Typically, ~2 x 10^5 cells mL^{-1} were seeded in cell culture plates and allowed to grow for 24 hours. For experiments involving the porphyrin saccharide conjugate, PGlc_4 was added to the cells 24 hours

prior to the photodynamic experiments and biochemical assays to allow it to be taken up by the cells. The cultures were rinsed 2-3 times with fresh DMEM to remove any unbound porphyrinic compounds before proceeding to the various assays. Fluorescence microscopy indicates no unbound porphyrin remains.

Confocal Microscopy. Cells were plated onto cover slips in cell culture dishes. Porphyrins dissolved in methanol were added to the cultures to a final concentration of 10 μM (methanol concentrations were < 0.2%). After incubation for 24 hours the cells were rinsed, treated with ER-Tracker Green (final concentration 1 μM) in growth medium, and incubated for 30 minutes under conditions outlined above. Cells were then washed twice with PBS and incubated with a 4% paraformaldehyde solution in growth medium for 15 minutes at 37^0 C under cell growth conditions. Cells were then washed three times with PBS, mounted in Dako fluorescence mounting medium, and visualized using a Zeiss LSM510 laser scanning confocal microscope where images were captured. For MitoTracker green: excitation 476 nm, emission 490-510; for $PGlc_4$: excitation at 633 nm, emission 650-670nm.

Inverted epifluorescence microscope. Cells were plated onto cover slips in cell culture dishes. Porphyrins dissolved in methanol were added to the cultures to a final concentration of 10 μM. After incubation for 24 hours the cells were washed three times with PBS. The cells were incubated for 30 minutes in growth medium with Fluo-4 (final concentration 1 μM) for 30 minutes. Cells were then washed twice with PBS and incubated for another 30 minutes in normal growth medium. Images were taken using Nikon Eclipse TE 200 inverted epifluorescence microscope.

Western blots. Cells were treated with porphyrin for 24 hours, rinsed and

irradiated as described above. After a period of time appropriate for the given experiment, cells were washed with cold PBS twice before lyses with RIPA buffer (50 mM Tris-HCl, 1% NP40, 0.25% Na-deoxycholate, 150 mM NaCl, 1 mM EDTA, 1 mM PMSF, 1 μg mL^{-1} aprotinin, leupeptin, and pepstatin each, 1 mM Na_3VO_4, and NaF). The lysates were gently rocked at 4^0 C for 25 minutes, centrifuged at maximum speed for 10 minutes, and the supernatant applied to a western blot.[8] Equal amounts of protein were adjusted into gel-loading buffer (50 mM Tris-HCl, pH 6.8, 100 mM dithiothreitol, 2% SDS, 0.1% bromophenol blue, 10% glycerol), and heated for five minutes at 100^0 C prior to separation by SDS-polyacrylamide (8%) gel electrophoresis. After transferring to nitrocellulose membranes (Osmonics), membrane filters were blocked overnight at 4^0C with 5% non-fat dry milk in PBS. The nitrocellulose filters were washed three times for five minutes in PBS with 0.05% Tween-20 (Bio-Rad), before incubation with anti-CHOP, anti-eIF2, anti-cytochrome c, or anti-pro-caspase-3, or anti-PARP. Anti-mouse IgG conjugated with horseradish peroxidase was used as a secondary antibody. The bands were visualized using an enhanced chemiluminescent detection system (Amersham). In the assay for cytochrome c, the cytosol was further fractionated from the mitochondria with a kit designed for this purpose (purchased from Biovision) and both the cytosolic and mitochondrial fractions were examined by a western blot.

2.4 Results and Discussion

A previous report found that concentrations of $PGlc_4$ over ca. 10 μM form nanoscaled aggregates so may enter and partition into the cells differently than the non-aggregated compound.[6]

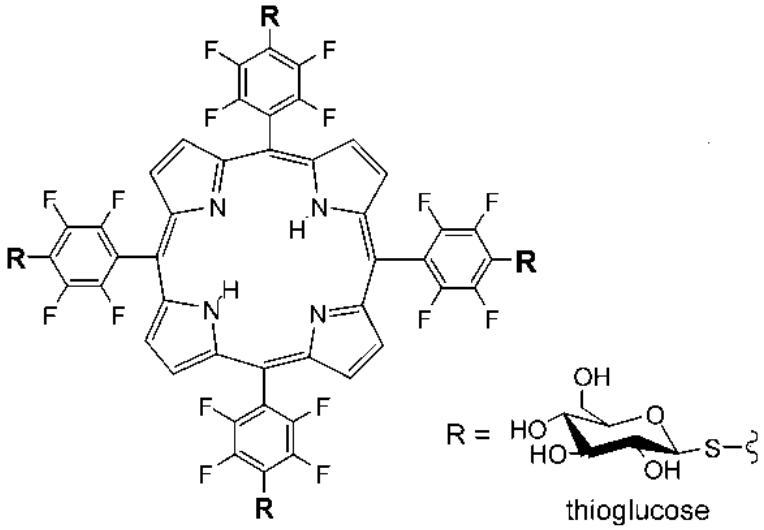

Figure 2.1. Structure of $PGlc_4$

The entry and partition of this compound depends both on concentration and incubation time. Our investigations on the mechanism of apoptosis induction by light and $PGlc_4$ in MDA-MB-231 breast cancer cells is evaluated by several assays. Confocal microscopy indicates that when treated with <10 μM, the porphyrin binds predominantly to the endoplasmic reticulum. Although the mechanism is partially unclear, it is known that stresses to the ER can activate apoptosis and that the release of calcium from the ER to the cytoplasm is one of the steps involved.[7] Several observations are consistent with our hypothesis that under low light and low concentrations, $PGlc_4$ induces apoptosis primarily by ER-stress in MDA-MB-231 breast cancer cells. This evidence shows that calcium is released from the endoplasmic reticulum, which subsequently is followed by cytochrome c release from the mitochondria.

Confocal fluorescence microscopy

ER-Tracker Green® (Molecular Probes) is a dye specific to endoplasmic

reticulum and luminesces green when exited with blue light, and the tetraarylporphyrin core of $PGlc_4$ fluoresces in the red region. The combination of the two dyes allows an evaluation of the location of the glycosylated porphyrin in MDA-MB-231 cells. Confocal fluorescence images of cells treated with both 10 μM $PGlc_4$ and with ER-tracker Green exhibit both the porphyrin fluorescence (red) and the ER Green fluorescence (Fig. 2.2). These experiments indicate that after exposure the cells to the PS, $PGlc_4$ is localized at the ER. This supports our hypothesis that photodynamic treatment of cells with P-Glc_4 can induce apoptosis by stress to the ER. Similar experiments using Mito-Tracker® (Molecular Probes) reveal only a small correlation with the fluorescence of $PGlc_4$ so the compound does not significantly localize in the mitochondria.

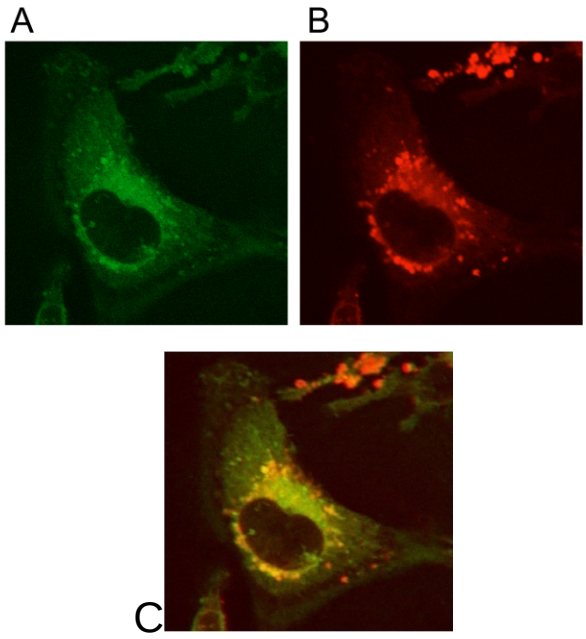

Figure 2.2. P-Glc_4 is mainly localized in endoplasmic reticulum in MDA-MB-231 cells. Cells were incubated with 10 μM $PGlc_4$ for 24 hours (red), rinsed, treated with ER Tracker Green, rinsed and fixed with 4% paraformaldehyde solution. Fluorescence of A: ER-Tracker Green, and B: $PGlc_4$. C: the overlapped image of A and B. Confocal fluorescence images were taken under identical conditions, magnification is 60x.

Release of calcium from the endoplasmic reticulum

To confirm the localization of the $PGlc_4$ and that free calcium is released from the ER upon photodynamic treatment, the calcium binding fluorophore Fluo-4 was used as an assay for monitoring intracellular free calcium[7]. The fluorescence of Fluo-4 significantly increases when bound to free calcium. Two different experiments were performed to measure the release of calcium from the ER to the cytoplasm. First, the MDA-MB-231 cells were treated with 10 μM of $PGlc_4$ for 24 hours, rinsed,

incubated with Fluo-4 as described in the methods section, and irradiated for 5 minutes or 10 minutes with white light from a 13 W fluorescent bulb. Control examined show no calcium release without both $PGlc_4$ and light. In the second experiment, MDA-MB-231 cells were treated with 10 μM of the $PGlc_4$ conjugate for 24 hours, incubated for 30 minutes with 1 μM of Fluor 4, rinsed three times, and incubated again for another 30 minutes with normal incubation conditions. Fluorescence images were then taken every minute while irradiating with low intensity white light to observe calcium release in the cells in real time; e.g. before and after the cells were irradiated with white light for 5 minutes (Fig. 2.3). Significant free Ca^{2+} are observed after photo irradiation of the cells in the presence of $PGlc_4$.

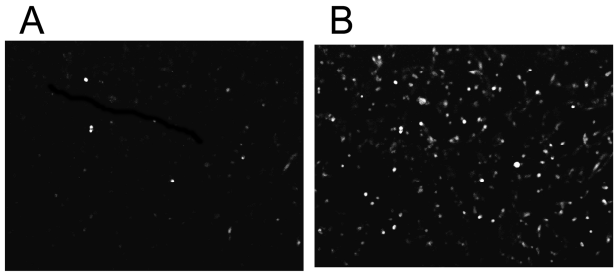

Figure 2.3. Release of calcium from the endoplasmic reticulum to the cytosol can be monitored in real time. Cells were incubated with 10 μM $PGlc_4$ and the Ca^{2+} sensor Fluo-4 , rinsed, placed under the microscope and images obtained every minute without moving the plate from the microscope, while the cells were irradiated with 0.84 mW/cm^2 (2.52 kJ/m2) white light. A: before irradiation, and B: after 10 minutes irradiation. Images are 20x and taken under identical conditions.

Release of cytochrome c from the mitochondria

If apoptosis proceeds through a mitochondria pathway, cytochrome c can be released to the cytosol, which in turn triggers caspase cascades and ultimately results in apoptosis. Though the mechanism of release remains under investigation, it has been demonstrated that two cytosolic proteins collaborate with cytochrome c to induce proteolytic processing and activation of caspase-3 in vitro[8]. To assay the mitochondrial involvement in apoptosis, the MDA-MB-231 cells were treated with 4 μM of the glucose-porphyrin conjugate for 24 hours, rinsed, and irradiated for 30 minute or 60 minute durations with white light from a 13 W fluorescent bulb. Five hours later a mitochondria/cytosol fractionation kit (BioVision) was used to separate the cytosol from the mitochondria. Western blots of the cytosolic and mitochondrial fractions were then used to detect cytochrome c. These results show that mild photodynamic conditions with P-Glu_4 cause cytochrome c release from the mitochondria to the cytosol (Fig. 2.4).

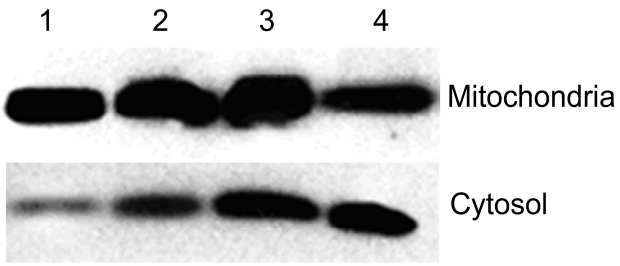

Fig. 2.4. Cytochrome c release from mitochondria to cytosol. 0 or 4 μM P-Glu_4 was incubated with human breast cancer MDA-MB-231 cells for 24 hours and after rinsing, irradiated with 13 W fluorescent white bulb for 30 or 60 min at 0.96 mW/cm^2 (17.28 or 34.56 kJ/m^2). Five hours later a mitochondria/cytosol fractionation kit was used to separate mitochondria and cytosol. The fractions were subjected to western blot to detect cytochrome c. Lane 1: control (no porphyrin, no light). Lane 2: control (4 μM porphyrin, no light) Lane 3: 4 μM porphyrin, 30 min irradiation. Lane 4: 4 μM porphyrin, 60 min irradiation.

Pro-caspase-3 cleavage/activation

Caspase-3 is activated during most apoptotic processes and is believed to be the main executioner caspase[9]. Caspase-3 activation is essential for DNA fragmentation as well as chromatin condensation and plasma membrane blebbing. Caspase 3 activation can be stimulated by cytochrome release c from the mitochondria via caspase-9/Apaf-1 or by other pathways. For these experiments the cells were treated with 0, 4, or 10 μM porphyrin conjugate, rinsed by exchanging the media, and irradiated for 20 or 40 minutes with white light. This experiment shows that pro-caspase-3 is indeed cleaved to yield the active caspase after mild photodynamic treatment of MDA-MB-231 cells in the presence of P-Glu_4 (Fig. 2.5).

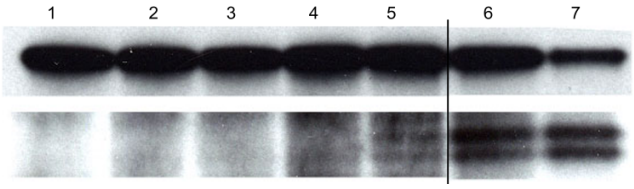

Fig. 2.5. Detection of pro-caspase-3 cleavage. 0, 4 or 10 μM P-Glu_4 was incubated with human breast cancer MDA-MB-231 cells for 24 hours and irradiated with 13W fluorescent white bulb for 20 or 40 min at 0.96 mW/cm2 (11.52 or 23.04 kJ/m2). Seven hours later, cells were collected and lysed. The supernatant of the lysate was applied to a western blot to detect pro-caspase-3. Lane 1: control (no porphyrin, no irradiation). Lane 2: control (no porphyrin, 20 min irradiation). Lane 3: control (4 μM porphyrin, no irradiation). Lane 4: 4 μM porphyrin, 20 min irradiation. Lane 5: 4 μM porphyrin, 40 min irradiation. Lane 6: 10 μM porphyrin, 20 min irradiation. Lane 7: 10 μM porphyrin, 40 min irradiation.

PARP Cleavage

Given the evidence of subcellular localization of P-Glu_4 at the endoplasmic reticulum, cytochrome c release, pro-caspase-3 activation, and chromatin condensation (see below), it not surprising to find that later stages of apoptosis, such as poly-ADP-ribose-polymerase (PARP) cleavage, are also observed[10] (Fig 2.6). PARP is one of the best-examined targets of activated caspases and is a common indicator of the action of caspase-3 in apoptosis

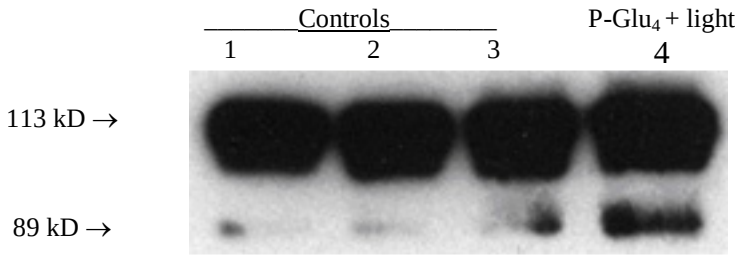

Figure 2.6: Detection of Poly-ADP-Ribose-Polymerase (PARP) cleavage in human breast cancer MDA-MB-231 cells as an indication of apoptosis. The cells were treated with 20 μM P-Glu_4 for 24 hours, irradiated with a 13W fluorescent light (0.27 mW cm^{-2} for 10 minutes; 1.62 kJ m^{-2}), and 9 hours after irradiation, cells were collected and lysed. The supernatant of the lysate was applied to western blot to detect PARP cleavage. Lane 1: with no irradiation or P-Glu_4; Lane 2: with irradiation but no P-Glu_4; Lane 3: with P-Glu_4 but no irradiation; Lane 4: with P-Glu_4 and irradiation.

DAPI staining

To examine the morphological changes in the MDA-MB-231 chromatin after photodynamic treatment in the presence of P-Glu_4, DAPI (4',6-diamino-2-phenylindole) staining experiments were used. DAPI binds to dA-T rich regions and is widely used as a DNA probe because of its large increase in fluorescence quantum yield upon DNA binding.[11] DAPI fluorescence images of the photodynamicly treated MDA-MB-231 cells reveal that the nuclei are condensed and split compared to a parallel control experiment (supporting information). The observed condensed and

split chromatin morphology is typical of apoptotic cells and further indicates that photodynamic treatment using low concentrations of the glycosylated porphyrin and low light irradiation is capable of inducing apoptosis.

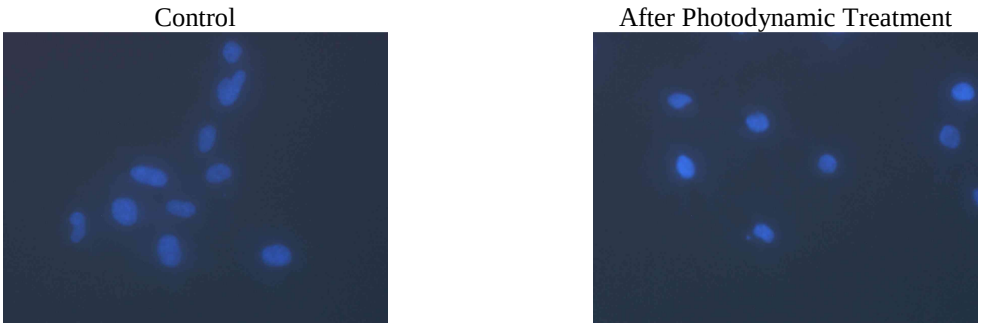

Figure 2.7. DAPI staining assays. 0 or 10 μM P-Glu_4 was incubated with human breast cancer MDA-MB-231 cells for 24 hours and irradiated for 5 min at 0.84 mW/cm^2 (2.52 kJ/m^2) under white light. 8 hours after irradiation, cells were fixed with 4% paraformaldehyde and stained with 1 μg/ mL DAPI solution. Fluorescence images were taken under identical conditions.

2.4. Discussion

Previous reports show that a tetraglucose-porphyrin conjugate, 5,10,15,20-tetrakis-(4-1'-thio-glucosyl-2,3,5,6-tetrafluorophenyl)-porphyrin, ($PGlc_4$) can be made in > 90% yield in two steps from commercially available meso-tetrakis(pentafluorophenyl)-porphyrin ($TPPF_{20}$) and a thioglucose derivative. The porphyrin-glucose bond of P-Glc_4 does not hydrolyze under physiological conditions. Human breast cancer MDA-MB-231 cells preferentially absorb tetraaryl porphyrins

with four glucose moieties 2-3 folds greater than the corresponding tetragalactose derivatives. It was also found that P-Glc_4 is also taken up by this cell line 2-3 times better than several well-studied hydrophilic porphyrin derivatives such as the tetracationic tetrakis(4-N-methylpyridinium)porphyrin. Additionally, $PGlc_4$ is highly selective toward $3Y1^{v\text{-}Src}$ transformed cells compared to normal 3Y1 cells.[6]

Doseametric studies reveal that these saccharide-porphyrin conjugates exhibit varying photodynamic responses depending on drug concentration and irradiation energy. (1) Using 20 μM conjugate and greater irradiation energy (> 22.56 kJ m^{-2}) induces cell death by necrosis presumably. (2) When 10-20 μM conjugate and less irradiation energy are used, both presume necrosis and apoptosis are observed. (3) Using < 10 μM and the least irradiation energy (< 0.75 kJ m^{-2}), a significant reduction in cell migration is observed, which indicates a reduction in aggressiveness of the cancer cells.

While greater concentrations of this porphyrin and greater irradiation with white light leads directly to necrosis, lower concentrations and less light lead to a delayed cell death predominantly by apoptosis. Confocal microscopy data indicates that at low $PGlc_4$ concentrations the porphyrin absorbed by MDA-MB-231 cells is localized at the ER, and calcium is released from the ER after the cells are exposed to the light. Thus, it is reasonable to conclude that a significant fraction of the observed apoptosis is a consequence of the stress induced to the ER after photodynamic treatment. The uptake of $PGlc_4$ by the ER is expected because the ER is known to use sugar for glycosylation and is a large inner cell structure.[12] The $PGlc_4$ stress to the ER releases calcium to the cytoplasm, cytochrome c is released from the

mitochondria, caspase 3 is activated, PARP is cleaved, and chromatin condenses[12] (Figure 2.8).

There are a variety of other cellular structures and/or functions that can serve as initiation points for the cascade of events that lead to apoptosis that can be affected by the remaining ca. 10% of $PGlc_4$ distributed throughout the cell. These include processes originating in the nucleus and some cationic porphyrins are well known to interact and cleave DNA under photodynamic conditions, but note that fluorescence microscopy indicates little, if any, whether or not $PGlc_4$ enters the cell nucleus. The 200 octanol/water partition coefficient for $PGlc_4$ between pH 7 and pH 4.75 renders the compound amphiphilic because the water soluble sugars at the 4-phenyl positions do not effectively surround the hydrophobic porphyrin core.

The enhanced activity of $PGlc_4$ relative to other saccharide conjugates can be attributed to several factors including the stability of the S-saccharide bonds to hydrolysis. The saccharide-porphyrin conjugates are more robust under light because of the added oxidative stability imparted by the 16 fluoro groups. The sugar moieties likely remain on the porphyrin even upon oxidation of the sulfur to the sulfoxide or sulfone. The reduced fluorescence intensity of $PGlc_4$ compared to many other meso tetraaryl porphyrins is indirect evidence of a greater triplet quantum yield, which results in greater yields of singlet oxygen and thus of oxidative stress in treated cells. These and previous results indicate that $TPPF_{20}$ may be an ideal scaffold to build a variety of porphyrin-saccharide conjugates and other biomolecular recognition motifs for diverse applications.

[A] PARP cleavage, cytochrome c release, caspase 3 activation data from: XIN CHEN, CUNY doctoral thesis, October 2005; Carbohydrate Conjugated Porphyrins Targeting Photodynamic Therapy (PDT): Potent Inducers Of Cancer Cell Death Both By Necrosis And Apoptosis; Solution-Phase Combinatorial Libraries With Whole Cell Selection Method

Since other cancer cell types take up different sugars such as galactose, this approach to the formation of PDT agents is amenable to the rapid synthesis and evaluation of compounds designed to be specific to a given cancer cell type or biomolecular target.

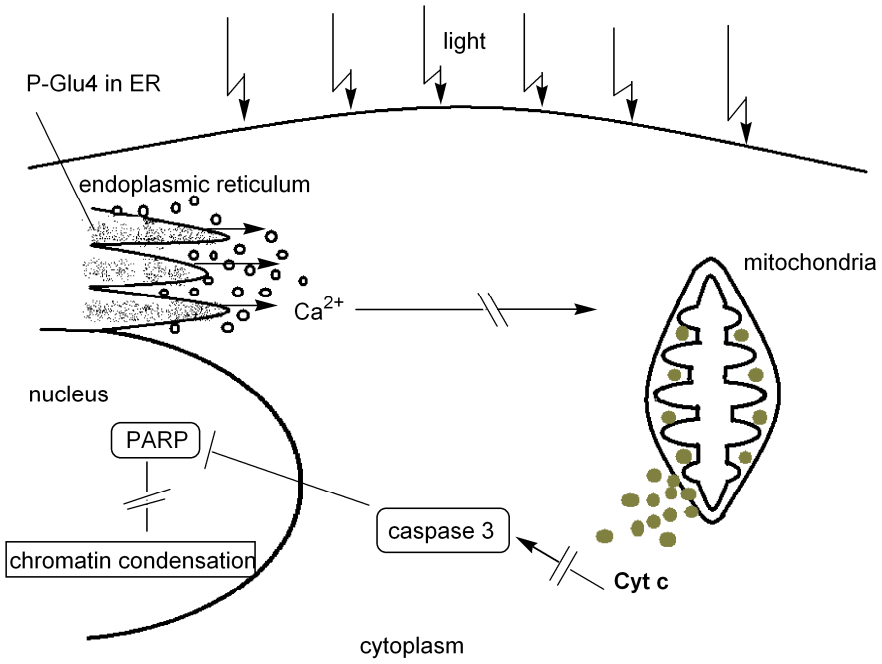

Figure 2.8. A proposed mechanism for the activation of apoptosis by $PGlc_4$ and light.

2.5 Conclusions

The various causes of MDA-MB-231 cell death mediated by the glycosyl-porphyrin conjugate depend both on light energy and drug concentration; nonetheless the elimination of cancer cells, via any mechanism, is the goal. These results indicate that highly vasculated tissues near surfaces accessible to light irradiation that receive greater doses of both drug and light may be eliminated by necrosis, whereas areas of

the tumor that absorb less drug and are further away from the light source may be eliminated by apoptosis. MDA-MB-231 cells are rendered less aggressive with yet less P-Glc_4 and lower light. Thus there is an array of responses by this breast cancer cell line that are elicited by this saccharide-porphyrin conjugate that depend on the amount of porphyrin absorbed and the amount of light reaching the cell.

Based on our results, when low doses of $PGlc_4$ (or under low light) are activated by light, apoptosis is initiated at the ER[13], and the release of Ca^{2+} then starts a cascade of events that leads to activation of caspase-3, significant cytochrome c release to the cytosol, PARP cleavage, and chromatin condensation (Scheme 2).

Appendix

CHOP expression

Note that the CHOP and eIF2α data were not used in the publication because the standard proteins were omitted from the gel.

Given the evidence of subcellular localization of P-Glc4 at the endoplasmic reticulum, and the subsequent stress produced to the ER when the glycophorphyrin is activated by light, different stress-response mechanisms may be activated.[14] One of these responses is the transcription factor C/EBP homologous protein (CHOP). It is reported[15] that ER stress is characterized by an increased level of the ER stress marker CHOP. The degree of CHOP expression was examined by Western blot, where it was found that the level of CHOP increased when $PGlc_4$ is activated by light. This means that CHOP is also part of the appoptosis pathways induced by the PDT using $PGlc_4$.

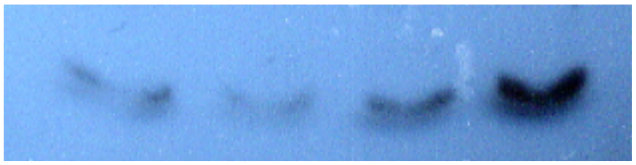

Figure A.1. CHOP expression. 0 or 10 μM $PGlc_4$ was incubated with human breast cancer MDA-MB-231 cells for 24 hours and after rinsing, irradiated with 13 W fluorescent white bulb for 30 or 60 min at 0.96 mW/cm^2 (17.28 or 34.56 kJ/m^2);the control is not irradiated. One hour later, the cells were collected, lysed, and the samples were subjected to western blot to detect the expression of CHOP. Lane 1: control (no porphyrin, no light). Lane 2: control (10 μM porphyrin, no light). Lane 3: 10 μM porphyrin, 15 min irradiation. Lane 4: 10 μM porphyrin, 30 min irradiation. Protein content was measured after lysis and 50 ug of total protein were loaded in each lane of an SDS-PAGE

eIF2 phosphorylation

Another ER-stress response involves the phosphorylation of the eukaryotic translation initiation factor 2 subunit α (eIF2α).[16] Under normal conditions, eIF2α is involved in transporting the initiator tRNA to the P-site of the pre-initiation complex. When the ER is under stress, eIF2α is phosphorylated thereby reducing the transformation of eIF2-GDP to eIF2-GTP required to bring initiator tRNA. Our result shows that the eIF2α phosphorylation occurs when light activates $PGlc_4$ in the cells.

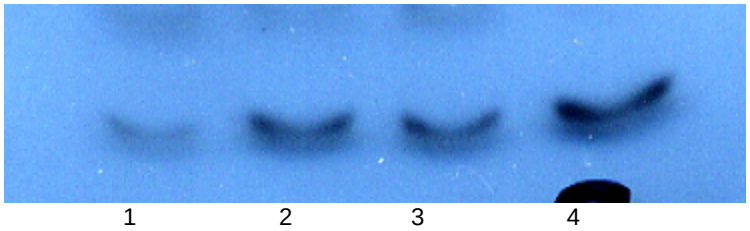

Figure A.2. eIF2α phosphorylation upon PDT treatment. 0 or 10 μM $PGlc_4$ was incubated with human breast cancer MDA-MB-231 cells for 24 hours and after rinsing, irradiated with 13 W fluorescent white bulb for 30 or 60 min at 0.96 mW/cm^2 (17.28 or 34.56 kJ/m^2). One control was not irradiated with light. After one hour , cells were collected and lysed. The samples were then subjected to western blot to detect the EIF2 phosphorylation. Lane 1: control (no porphyrin, no light). Lane 2: control (10 μM porphyrin, no light) Lane 3: 10 μM porphyrin, 15 min irradiation. Lane 4: 10 μM porphyrin, 30 min irradiation. Protein content was measured after lysis and 50 ug of total protein were loaded in each lane of an SDS-PAGE

Chapter 2 References

(1) Kroemer, G; Dallaporta, B; Resche-Rigon, M Annu. Rev. Physiol., 1998, 60: 619-642.

(2) Lawen, A BioEssays, 2003, 25: 888-896.

(3) Sternberg, ED; Bruckner, C; Dolphin, D Tetrahedron, 1998, 54: 4151-4202.

(4) Osterloh, J; Vicente, MGH J. Porphyrins Phthalocyanines, 2002, 6: 305-324.

(5) Chen, X; Drain, CM, Drug Design Reviews 2004, 1: 215-234.

(6) Chen, X; Hui, L; Foster, DA; Drain, CM Biochem., 2004, 43: 10918-10929.

(7) Xu, C; Bailly-Maitre, B; Reed, JC J. Clin. Invest. 2005, 115: 2656-2664.

(8) I. Yslas, M. G. Alvarez, C. Marty, G. Mori, E. N. Durantini, Rivarola V, Toxicology, 2000, 149, 69-74.

(9) E. A. Slee, C. Adrain, S. J. Martin, Cell Death and Differentiation, 1999, 6: 1067-1074.

(10) W. Yu, H. Wang, M. F. Poitras, C. Coombs, W. J. Bowers, H. J. Federoff, G. G. Poirier, T. M. Science, 2002, 297: 259-263

(11) B. S. P. Reddy, S. M. Sondhi and J. W. Lown, Pharmacology & Therapeutics, 1999, 84: 1-111.

(12) Caramelo, J; Parodi, AJ Seminars in Cell and Developmental Biology, 2007, 18: 732-742.

(13) Thompson, S; Chen, X; Hui, L; Toschi, A; Foster, DA. Drain, CM Photochem. Photobiol. Sci. 2008, 7: 1415-1421.

(14) Pino, SC; O'Sullivan-Murphy, B; Lidstone, EA; Yang, C; Lipson, KL, Jurczyk, A; diIorio, P; Brehm, MA; Mordes, JP; Greiner, DL; Rossini, AA; Bortell, R PLoS ONE. 2009; 4 (5):e5468

(15) Buytaert, E; Dewaele, M; Agostinis, P Biochim Biophys Acta. 2007, 1776: 86-107.

(16) Sun, GD; Kobayashi, T; Abe, M; Tada, N; Adachi, H; Shiota, A; Totsuka, Y; Hino O Biochem. Biophys. Res. Commun. 2007, 360: 181-187.

Chapter 3

MECHANISM OF NECROSIS: UPATAKE AND ACTYVITY OF A TETRAGLYCOSYLATED CHLORIN.

Abstract

Phorphyrins and their derivates are widely used for photodynamic therapy to treat different diseases, including cancer. Although the final goal of this anticancer treatment is the destruction of the cancer cells, this objective can be achieved by the activation of either apoptosis or necrosis. In the second chapter, the apoptotic pathways initiated by a tetraglycosylated porphyrin, $PGlc_4$, in MDM-MB-231 cells upon light illumination were described and analyzed. In this chapter we describe how necrosis is activated with a focus on the uptake of the photo sensitizers by the cells.

Overall, our results show that PGlc-4 and a tetraglycosylated chlorin, CGlc-4 a porphyrin wherein the macrocycle has one double bonds missing, cross the plasma membrane by endocytosis and they are retained in the endoplasmatic reticulum. Several assays also show that some of these photosensitizer compounds are also retained in the plasma membrane. Our results show that the photosensitizers located in the plasma membrane are the key activators of necrosis once activated by light. In terms of uptake, the possible interaction with glucose transporters is analyzed.

Introduction

As most widely practiced, photodynamic therapy of cancer uses a dye capable of photosensitizing the formation of singlet oxygen upon light illumination of the cells or tissues containing the dye. The resulting reactive oxygen species generated by the photosensitizers are the compounds that will damage different cellular organelles and molecules, that ultimately leads to cell death. Many research reports using a variety of cell lines and methodologies show that the resulting damage leads to cell death either by apoptosis[1], necrosis[2] or even autophagy[3]. In almost all of the cases studied so far, the primary place of damaged produced for these toxic compounds corresponds to the place that the photosensitizer (PS) is localized inside the cells[4].

Early work in our group found that simple click chemistry allowed the formation of a tetraglycosylated porphyrin, $PGlc_4$, wherein the sulfur attaching the sugar resists hydrolysis by acid/base and enzymes (Figure 3.1). This compound was also shown to be an effective PDT agent in a variety of cell lines. For example, our compound $PGlc_4$ localizes in the endoplasmatic reticulum and the apoptosis is activated when damage is performed to the same organelle.[1] It is commonly accepted that PSs localize in the endoplasmatic reticulum and/or mitochondria will activate apoptosis under photodynamic treatment, while the PSs confined in the plasma membrane or endosomes/lysosomes activate cell death by necrosis.[4]

$PGlc_4$ activates apoptosis when the dye concentration and the power of the light are relatively low, and this was mainly characterized in chapter two. Briefly, at low concentrations $PGlc_4$ is manly located in the endoplasmatic reticulum and once it is

activated by light, stress is induced to the ER, and several different biological signals show that apoptosis is activated. In this chapter we focus on how the molecules enter the cell and understanding how the process of necrosis is activated.

Because a minimum energy is needed to sensitize the formation of singlet oxygen and light penetration in tissue is greatest between 700 nm and 900 nm, the optimal absorption for this class of sensitizers is between ca. 650 nm and 800 nm. Thus, in order to make derivatives of $PGlc_4$ that have better light absorption properties in tissues – stronger absorption band(s) on the red side of the UV-visible spectrum – we made the chlorin ($CGlc_4$) and isobacteriochlorin ($IGlc_4$) derivatives. Chlorins are missing one pyrrole double bond and isobacteriochlorins are missing two on adjacent pyrroles (Figure

Figure 3.1 The glycosylated porphryinoids

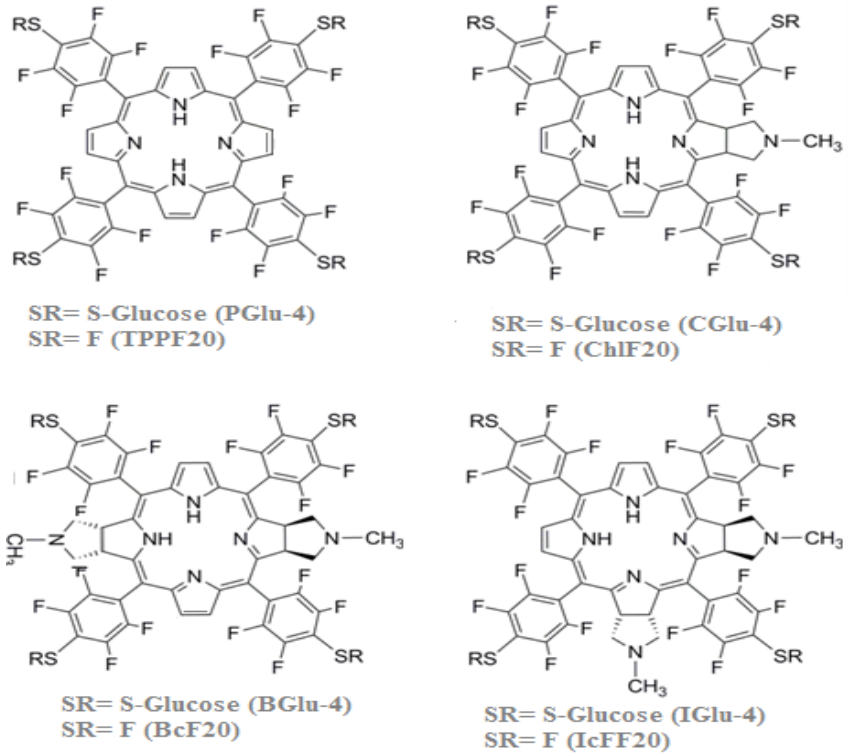

3.1). The synthesis and photophysical properties of these are reported in earlier chapters. In terms of uptake and localization, the hypothesis was that these derivatives would have similar properties. In terms of the photophysics, $CGlc_4$ is ca. 6-fold more fluorescent and $IGlc_4$ is ca. 11-fold more fluorescent than the parent $PGlc_4$ (quantum yields: 3% for $PGlc_4$, 17% for $CGlc_4$, 36% for $IGlc_4$). The triplet state, which is needed for the sensitized formation of singlet oxygen, correspondingly decreases, and it is reasonably to assume this is proportional.

In this chapter our data also demonstrated that $PGlc_4$, $CGlc_4$ and $IGlc_4$ are located, beside in the endoplasmatic reticulum, in endosomes/lysosomes, and/or the plasma membrane. The damage produced to the plasma membrane is the primary mechanism for the activation of necrosis. Since $PGlc_4$ has the greatest triplet quantum yield, it has the greatest potential to generate the reactive oxygen species. Though $CGlc_4$ and $IGlc_4$ (chapter 3) have reduced triplet quantum yields, under high power light conditions $CGlc_4$ and $IGlc_4$ also generate enough reactive oxygen species to produce the damage necessary to activate any of the cell death processes. Most of the experiments performed in this chapter were done using $CGlc_4$ because: (1) it is easier to make an purify, (2) its electronic absorption band at 650 nm is about 25-time greater than the parent compound, and (3) the proportionally greater emission above 600 nm facilitated fluorescence microscopy assays. Similar results were obtained using $PGlc_4$or $IGlc_4$.

Experimental procedures

Cell Culture. Chinese Hamster Ovary Cells (CHO) were maintained in F12, 5% Fetal bovine serum, 1% antimycotic, at 37^0 C and 5% CO_2 atmosphere. Typically, ~2 x 10^4 cells mL^{-1} were seeded in cell culture plates and allowed to grow for 24 hours. For experiments where endocytosis was inhibited, culture plates containing cells were placed on ice for at least half an hour and all the buffers were maintained at 4C. C-Glc_4 was dissolved in DMSO and added to the cells depending the protocol involved. The cultures were rinsed 2-3 times with fresh M2 to remove any unbound porphyrinic compounds before proceeding to the various assays.

Fluorescence spectroscopy

To detect necrosis, ethidium homodimer (EthD-1) from the LIVE/DEAD® Viability/Cytotoxicity Kit (Invitrogen) was used. The dye was added to cells in M2 medium for five minutes. The fluorescence emission of EthD-1 increases 5-fold when intercalated into DNA, and is extensively used to detect necrosis when the plasma membrane integrity is compromised. For experiments focusing on the plasma membrane, Cellmask® (Invitrogen) was used to dye the plasma membrane. The dye was added to the medium containing the cells at concentration of 0.5 ug/mL for five minutes. Both procedures followed the recommended protocols that come with the kits.

Fluorescence measurements were performed on dilute solutions, typically ~2 µM in phosphate buffered saline (PBS). Samples were excited at the same band (500 nm) where absorbencies ≤ 0.1 and were within 10% of each other. For emission spectra, both the excitation and detection monochrometors had a band pass of 1 nm. The corrected

emission (for instrument response) and absorption spectra were used. All experiments were carried out on the same day, using identical concentrations to minimize any experimental errors.

Fluorescence microscopy was performed using on an inverted Leica DM IL inverted instrument, exposure times were 100 miliseconds for imaging proposed and 30 sec for PDT, a Cy5 band pass (Excitation 580 nm to 640 nm - Emission 650 nm to 720 nm) for experiment involving $CGlc_4$ and filter TRITC (Excitation 500 nm to 550 nm - Emission 560 nm to 610 nm) for CellMask and EthD-1 experiments. Bright field images were taken on the same microscope. In general the activation of the dye used focused light from the microscope using the aforementioned Cy5filter band pass filter such that the power was 6mW.

Results and discussions

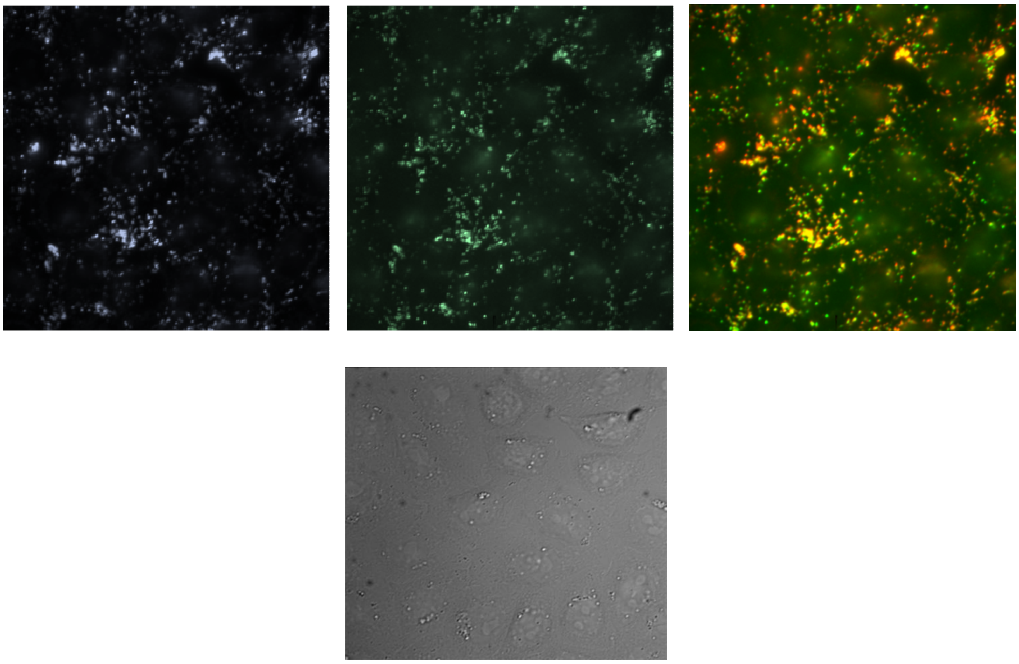

Figure 3.2. Fluorescence microscopy showing the localization of $CGlc_4$ in the endosomes and lysosomes of CHO cells: (A) high molecular weight dextrans (blue); (B) 1 μM CGlc-4 (green); and (C) the overlapped images. Images are 60x. Bright field image of the same samples (bottom).

Endosomal localization $CGlc_4$ The endosome/lysosome localization of both our compounds was indicated by colocalization with high molecular weight dextrans using a standard protocol[5] (Fig 3.2 A, B, C). It is known that many macromolecules that are internalized into cells by bulk phase endocytosis reside in the endosomes and since one of the limiting factors for the therapeutic efficacy of a drug is its ability to escape the endosomes, and translocate into the cytosol,[5] researchers have been experimenting with many alternatives to enhance this translocation efficiency. One such approach is termed

"photochemical internalization", where a photosensitizer is used to destroy the endosomal membrane in response to light, and release the drug into the cytosol[5]. The mechanism of release can be either activation of oxygen or localized heating of the endosome since aggregates of dyes often deactivate via vibrational processes.

Our results show that $CGlc_4$ can serve as its own photosensitizer, i.e., when $CGlc_4$ loaded cells were exposed to light, the integrity of late endosomes/lysosomes was compromised, as evidenced by the release of endosomal dextran and the dye into the cytosol (Fig 3.3 A, B, C). A shorter exposure to light of of the same wavelength and intensity on the same microscope was required to obtain a similar result for $PGlc_4$ contained in the late endosomes/lysosomes. Since $PGlc_4$ has a greater triplet quantum yield (ca. 95% vs. 70%), the latter result indicates the production of reactive oxygen species is a significant contributor to the release of dyes from the endosomes and lysosomes (Chapter 3).

Figure 3.3. Fluorescence microscopy of CHO cells treated with dextrans (μg/mL) and $CGlc_4$ (1 μM) shows that (A) using a A4 band pass (Excitation 455 nm to 495 nm - Emission 515 nm to 535 nm) band pass emission filter shows dextrans fluorescesnce is located in the endosomes; (B) after CGlc-4 is activated by the light from the microscope for 30 s; the endosomes are destroyed and the dextrans released to the cytosol; (C) The overlapped images of A and B shows dextran before the endosomes are destroyed (red) and after (green).

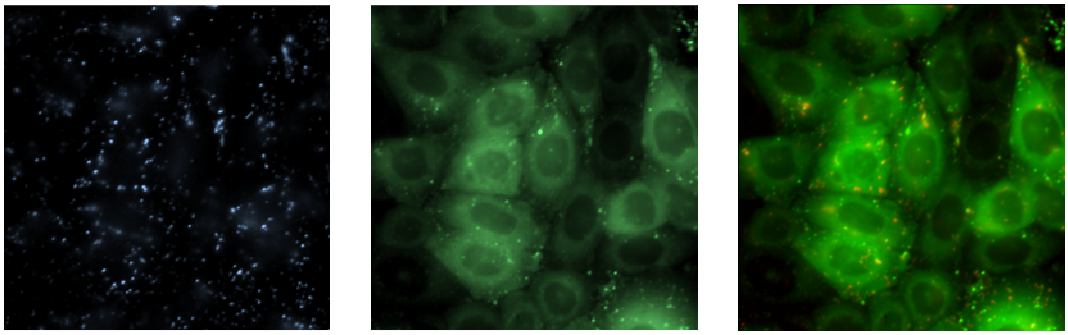

A B C

Necrosis activation by $CGlc_4$

PDT is followed by the activation of apoptosis, necrosis or even autophagy. Two important conditions will dictate the different cell death pathways: concentration of the photosensitizer (PS) and the light dose. High dose light and/or high concentration of PS will result in necrotic cell death cell4. To achieve necrosis in our experiments, the light used to activate our PS is focused white fluorescence light generate by a 150 W fluorescence lamp for 30 or 60 seconds, instead of a non-focused white fluorescence light generate by a 25 mW fluorescence lamp used in our apoptosis experiments.[1,4] As can be observed in the following images, the CHO cells are under significant stress after the PDT treatment.

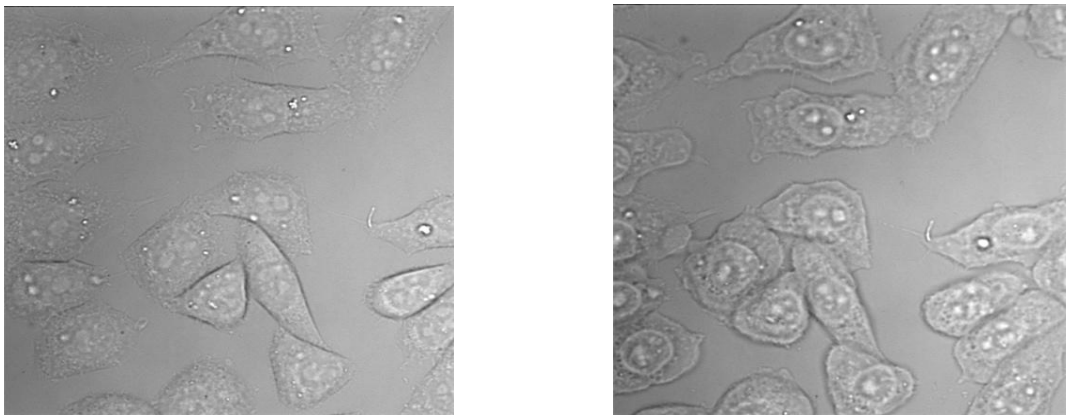

A B

Figure 3.4. CHO cells were incubated with 1μM $CGlc_4$ overnight, washed three times with M2 medium before imaging in the bright field (A) cells before activation of $CGlc_4$ with light, and (B) cells after irradiation with the microscope light (60 s, using a Cy5 filter, 6 mW). Post irradiation, the cells show obvious signs of stress as indicated by the swelling, blebbing, and other changes in morphology. Similar results were obtained with different incubation times with $CGlc_4$ (1hs, 4hs, 16hs, data not shown).

To confirm that the cells are undergoing necrosis, after the irradiation EthD-1 was added to the medium, and after five minutes the cells were washed again three times and images were obtained using this time TRIC filter to excite only the EthD-1. The fluorescence intensity EthD-1 increases several fold when the dye intercalates into DNA, and is generally used to recognize or detect necrotic cells after the integrity of the plasma membrane is damaged.[6]

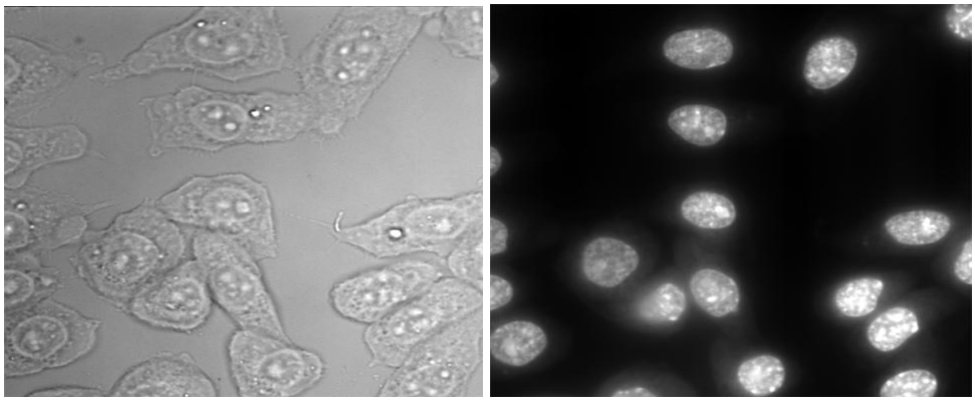

A B

Figure 3.5. CHO cells were incubated with 1 μM CGlc-4 overnight, washed three times with M2 medium. (A) Bright field image of the cells after irradiation and activation of the dye (see Fig. 3); and (B) fluorescence microscope image of the EthD-1 localized in the nucleus showing that the plasma membrane integrity and the cells are undergoing necrosis.

As shown in figure 3.5, the plasma membrane integrity is damaged when the PS was activated by light. These results indicate that some portion of the PS must be localized in the plasma membrane. These and previous results show that the nonhydrolysable glycosylated porphyrinoids $PGlc_4$ and $CGlc_4$ are taken up into the cell predominantly by endocytosis, and subsequently partitions or localizes in the endoplasmatic reticulum[6] while some remains in the plasma membrane. $CGlc_4$ can be detected in the plasma membrane as a weak fluorescence in the microscopy, when the cells are incubated at 37C.

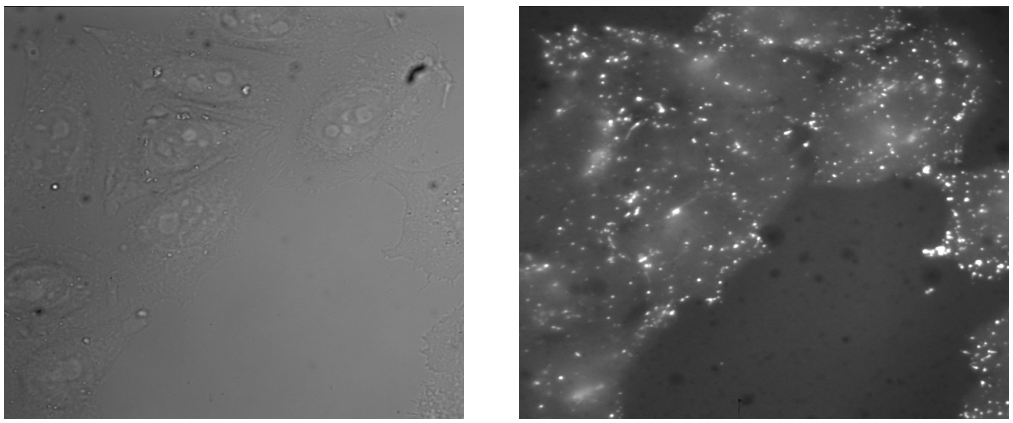

A B

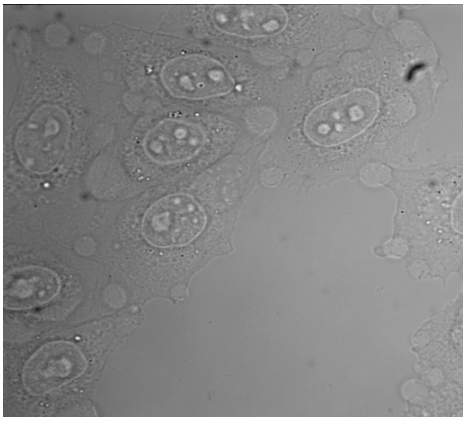

C

Figure 3.6. CHO cells were incubated with 1 μM $CGlc_4$ overnight, washed three times with M2 medium. The cells were maintained at 37 C. (A) bright field image of the cells and (B) fluorescence of $CGlc_4$ using a CY5 filter. The endosomes are the white spots and plasma membrane the smooth white areas. (C) Cell after been photodynamic treated.

When endocytosis is inhibited following a low temperature protocol where the cells were incubated with the $CGlc_4$ at 4 C for two hours,[7] the fluorescence of the dye is strongly

correlated with the plasma membrane (Figure 3.6).

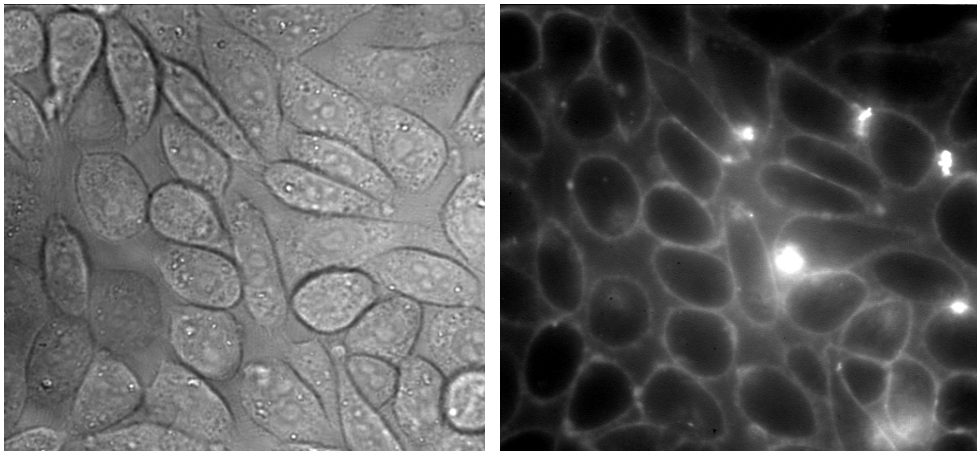

A B

Figure 3.7. CHO cells were incubated with 1 μM $CGlc_{-4}$ for two hours at 4 C, washed three times with cold M2 medium. (A) Bright field image of the cells, and (B) fluorescence of CGlc-4 using a CY5 filter on the emission side. This shows that the chlorin is localized only in the plasma membrane as indicated by the white lines surrounding the cells.

As expected, cells incubated for two hours at low temperature show that the PS is localized in the plasma membrane since endocytosis, the way that the cells uptake our PS, was inhibited. Thus, short incubation times result in the glycoconjugate porphyrins in the plasma membrane and in the endosomes/lysosomes.

Under the conditions studied, endocyctosis seems to be the major mode of uptake into the cells; however, the localization of some of the CGlc-4 in the plasma membrane

indicates that passive diffusion may also contribute somewhat to the uptake. Passive diffusion depends both on the kinetics (where longer incubation times may be necessary to get the dye into the cell), and on thermodynamics where the relative concentration of the dye and the physical properties of the dye are important. The octanol/water partition coeffecients for $PGlc_4$ is ca. 120 and for $CGlc_4$ ca. 40.

Necrosis activation by the PS located at the plasma membrane

In chapter two, apoptosis in MDS-MB-231 cells was observed when relatively low PS concentrations were used with low light doses. It was concluded that the stress produced to the endoplasmatic reticulum was the first step of the apoptosis pathway and the majority of the PS was located in the ER after the 24 hour incubation time. In addition, it was also concluded that when a greater power of light was used, necrosis was the major consequence after the PS activation. In this chapter, using the low temperature protocol described above and CHO cells, we find that when the $CGlc_4$ is delivered only to the plasma membrane, and activated by light necrosis was triggered.. These observations lead to the conclusion that CGl_4 activates necrosis by damaging the plasma membrane; the following experiments support this.

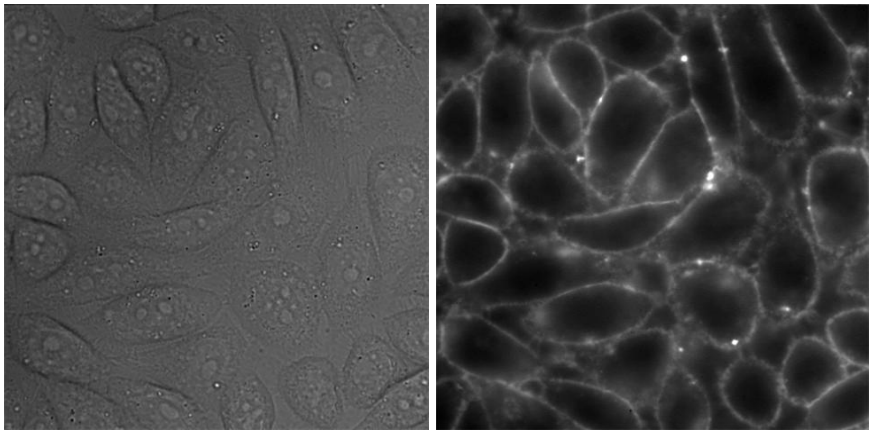

A B

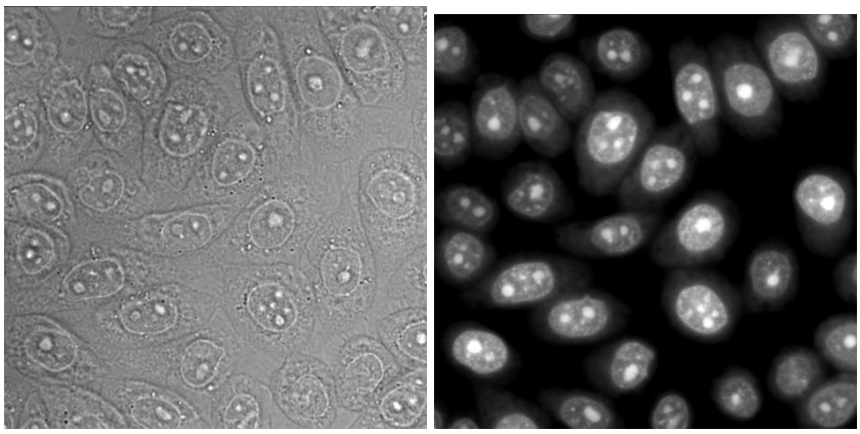

C D

Figure 3.8. CHO cells were incubated with 1μM CGlc-4 for two hours at 4 C, washed three times with cold M2 medium. (A) bright field image of the cells; (B) Fluorescence of the $CGlc_4$ using a CY5 filter on the emission side showing localization in the plasma membrane aswhite lines surrounding the cells; (C) cells after activation of CGlc-4 with focused light from the microscope through the cy5 band pass filter shows that the cells are under stress (bright field); (D) after image C was taken the cells were treated with EthD-1 using standard procedures and the fluorescence images show that EthD-1 is localized in the nucleus, indicating that the plasma membrane integrity is compromised and the cells are undergoing necrosis. For control experiment (no light/no porphyrin see Appendix).

CGlc-4 in the plasma membrane at 37 C Quenches CellMask™

To confirm our hypothesis that our $CGlc_4$ is located partially in the plasma membrane, quenching experiments were performed with a dye known to localize in the plasma membrane. In this assay, the quenching (reduced fluorescence) of a dye known to localize in the plasma membrane by energy transfer to a second dye, $CGlc_4$, indicates that

the second dye is localized in proximity[8]. This technique is often used in biological studies for imaging and demonstration of colocalization.[8,9] These requirements are satisfied in that the emission spectrum of CellMask™ overlaps well with the Q-bands of $CGlc_4$ (Figure 3.9). We observe fluorescence quenching when 1 equivalent of $CGlc_4$ are added to a PBS solution containing the same CellMask™, concentration used for cell experiments, implying that the two dye molecules interact sufficiently for energy transfer quenching. For the case that both dyes localize in the same place in a cell, a similar decrease in the fluorescence intensity from the CellMask™ should be expected.

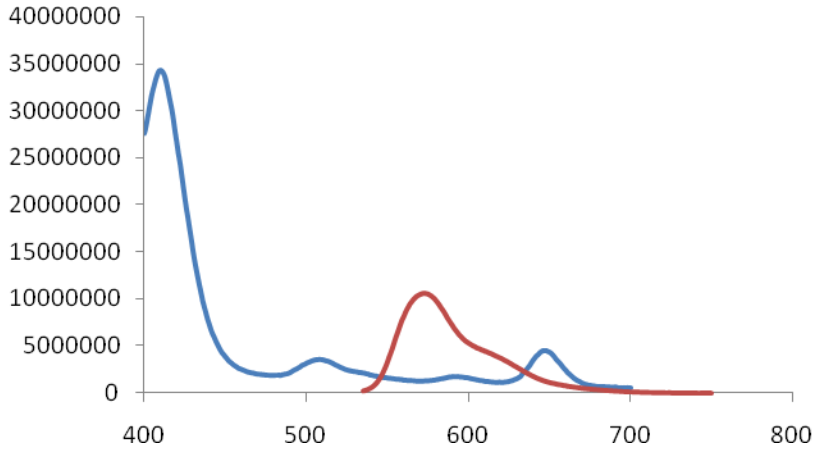

Figure 3.9. Blue line is the UV-visible spectra of CGlc-4 (3 μM), and the red line is the emission spectra of CellMask™ (3 μg/mL) in PBS. Note that the emission spectra of $CGlc_4$ has a peak centered at 650 nm with a small shoulder at 707 nm (see below).

Experiments performed with μM of the compounds dissolved in PBS demonstrate the quenching effect when $CGlc_4$ is added to the CellMask solution (Figure 3.9).

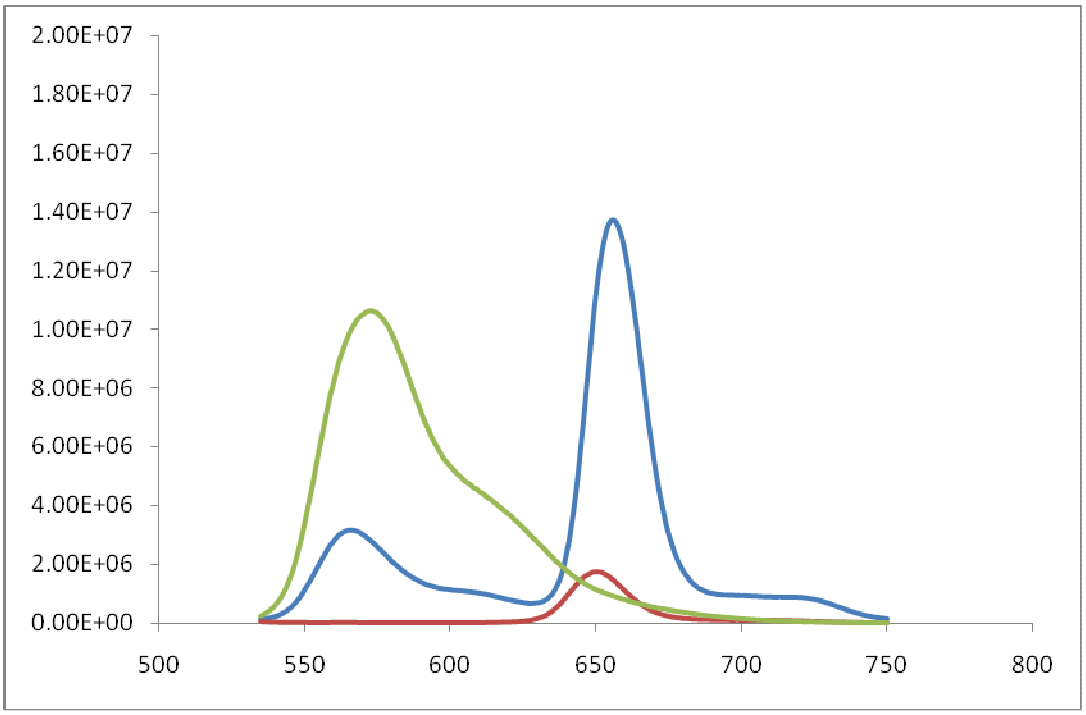

Figure 3.10. Emission spectra of the compounds in PBS; excitation at 500 nm. Green: 3 μg/mL CellMask™ Red 3 μM $CGlc_4$. Blue: Emission spectra of a solution containg both compounds at the above concentrations indicates energy transfer from the CellMask to $CGlc_4$.

As expected, the emission intensity of CellMask™ decreases when $CGlc_4$ is added to the solution and concomitantly the emission intensity of $CGlc_4$ increases, demonstrating energy transfer from the former to the latter compound. Once the quenching by energy transfer was demonstrated between CGlc-4 and CellMask™, the same experiments were performed in cell culture. Cells were loaded with CellMask™ following the recommended protocol to locate the compound at the plasma membrane[10] and the fluorescense intensity was compared when CGlc-4 was also added to the cells.

Thus, if $CGlc_4$ localizes in the plasma membrane, it should quench the fluorescence of the CellMask^{TM}. These experiments were performed at the two temperatures used above: where CGlc-4 is shown to remain in the plasma membrane at 4 C, and where it is endocytosed and taken up by the cells at 37 C.

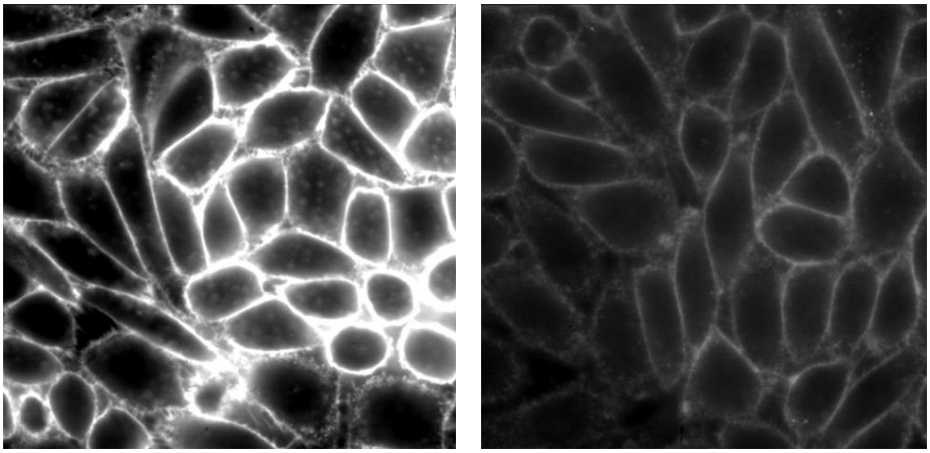

A B

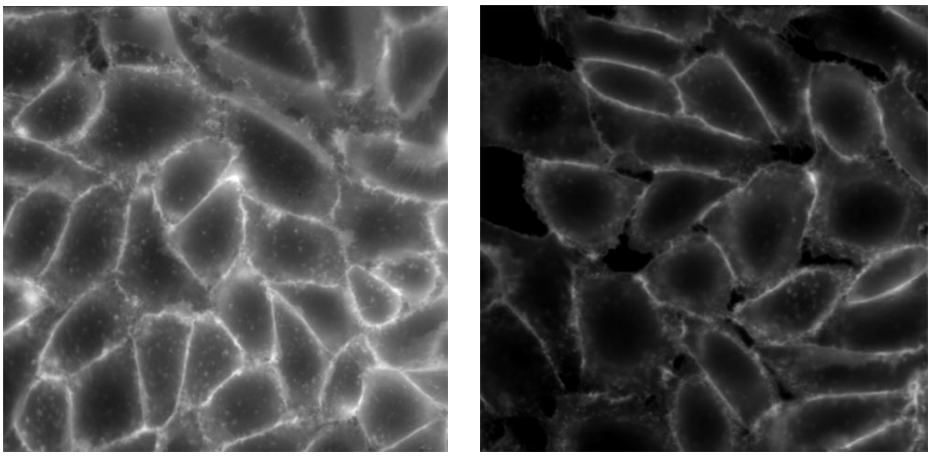

C D

Figure 3.11 CHO cells were incubated with CellMask™ 1 μg/mL for five minutes at 4 C, washed three times with cold M2 medium, and the fluorescenceimages obtained using a TRIC filter: (A) fluorescence of CellMask™ in the plasma membrane, (B) CHO cells were incubated for two hours with 1 μM $CGlc_4$ at 4 C, washed three times with cold M2 medium, and immediately afterwards treated with 1 μg/mL CellMask™ for five minutes at 4 C, washed three times with cold M2 medium, and images obtained using the TRIC filter, showing the quenching of the emission intensity of CellMask™ in the plasma membrane. (C) and (D) The same experiments but the incubation with $CGlc_4$ was performed at 37 C yield similar results.

Conclusion

The ultimate objective of PDT is to activate one or all of the cell death pathways. Most of the photosensitizing dyes currently under investigation activate apoptosis or necrosis depending on both the conditions used to deliver the dye and the light. In this chapter, it was described that $CGlc_4$ is endocytosed into the CHO cells and that a significant fraction also partitions into the plasma membrane where this population is

responsible of the activation of necrosis. Certainly, the plasma membrane integrity is altered and cell death immediately follows illumination of the cells containing $CGlc_4$. Knowing that $CGlc_4$ binds the plasma membrane and produced cell death when activated by light, opens up several different research objectives. First, the plasma membranes of cancer cells are significantly different from those from the corresponding healthy cells.[11] As demonstrated with the $PGlc_4$ derivative with MDA-MB-231, CHO, and other cancer cell lines,[12] the sugars impart significant selectivity to cancer cells, and are generally poorly taken up by non-cancer cell lines. The rapid, high-yield reactions to append other cancer cell targeting motifs, such as RDG and polylysine peptides, on the $TPCF_{20}$ core platform means that this photosentizer can be tailor made for a plethora of different cancers. This provides an alternative strategy for the few cancer types that do not take up the glycoconjugates.

The mechanism of absorption/binding of photosensitizers to the plasma membrane is dictated both by the chemical properties of the molecule and by the different components present in the medium.

Mechanisms of Binding to Cancer Cell membranes

Possible rolls of theactive glucose transporter (SGLT)

As demonstrated above, $CGlc_4$ binds the plasma membrane. Considering: (A) $CGlc_4$ has four non-hydrolysable thioglucose moieties appended to the periphery, (B) most cancer cell lines express glucose receptors and/or transporters in their membranes as a means to obtain additional source of energy, and (C) previous studies have

demonstrated that free thio-glucose can bind to and inhibit the active glucose transporter (SGLT) transporters,[14] there is a possibility that $CGlc_4$ binds the plasma membrane via an interaction with the active glucose transporter.

One circumstantial evidence that further supports this hypothesis is that Caco-2 cells present much larger amounts of our compounds on the plasma membrane (Figure 3.11), and are reported to contain several-fold more SGLT receptors on their plasma membranes compared to the CHO cells used above.

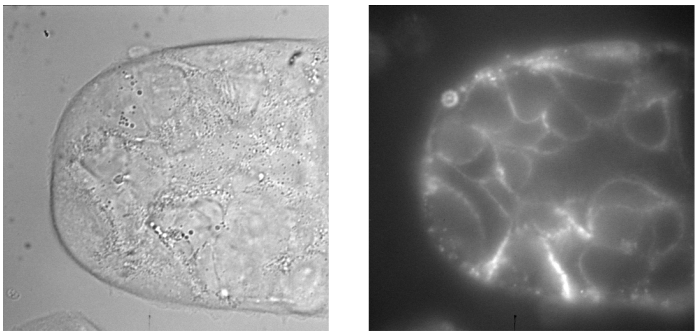

Figure 3.11. $CGlc_4$ is located on the plasma membrane on Caco-2 indicating that it is binding the SGLT transporter.

Another important information that supports this theory, it is the inhibition of necrosis when thio-glucose is added to the medium or in the case that the plasma membrane is washed five times with PBS 5% BSA. (See Appendix) .PDT is an increasingly popular therapeutic modality for various types of cancers. [16, 17] There are, however, several outstanding problems with the currently existing repertoire of PDT agents. Although the distribution within the tumor and not to the healthy tissue is not the

most important drawbacks of current PDT agents, better selectivity for tumor cells will improve PDT performance. We propose that $PGlc_4$ and CGlc-4 will be able to overcome this problem specifically in tumors that overexpress SGLT (by virtue of specific plasma membrane binding to these cells).

Interaction with Glucose presented in the medium

Glucose is one the most interesting compounds to be studied in terms of PS internalization, since most cancer cells over express glucose transporters with the aim to obtain more glucose to be used as an energy source.[18] To obtain information about the possible interaction in the uptake between $CGlc_4$ and the glucose transporters, MDA MB 231 cancer cells were pre-incubated with different glucose concentrations. The glucose concentration results show negative correlation with in the amount of $CGlc_4$ taken up into the cells. When no glucose is present in the medium, $CGlc_4$ is incorporated to a much greater extent than when glucose is present in the medium (Figure 3.12).

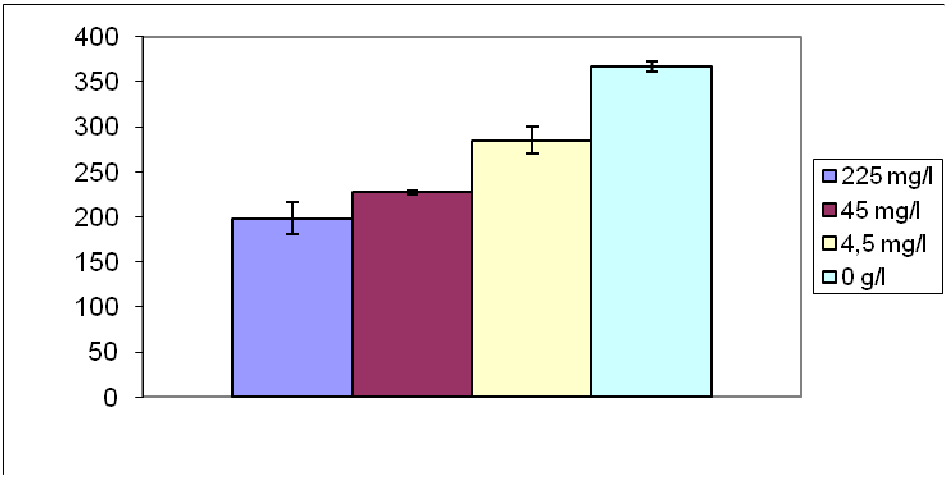

Figure 3.11: The relative amount of $CGlc_4$ up taken by MDA MB 231 cancer cells as a function of the glucose concentration in the medium. After 4 hs incubation, cells were

washed three times with PBS, lysis and the fluorescence intensity were measured as it was described in material and methods. Cell numbers were corrected using protein concentration.

The results show a direct effect of the glucose concentration in the growth medium and the incorporation of CGlc-4. This result is expected because of the four exocyclic thioglucose moieties. One of the important steps in drug uptake by cells in how the compound gets close to the cell to been incorporated. In the case where there is no glucose in the medium, the concentration gradient will facilitate the diffusion of $CGlc_4$ to the cells, but when glucose is present in the medium, the diffusion of the PS may not be as facile due to changes in viscosity and/or intermolecular interactions with the free glucose. However, the presence of various glucose transporters on cancer cells that significantly increases the local concentration of the dye around the cell. Because of the four glucose groups on these porphyrins, the effective concentration of the glucose is 4-fold greater. This increased local concentration around the cell and on the membrane may result in (1) aggregation of the dye such that nano-aggregates are formed and endocytosed, (2) blocking the uptake of free glucose from the medium. (3) increase the final uptake by the cancer cells by endocytosis. See appendix for the interaction with the albumin.

Appendix

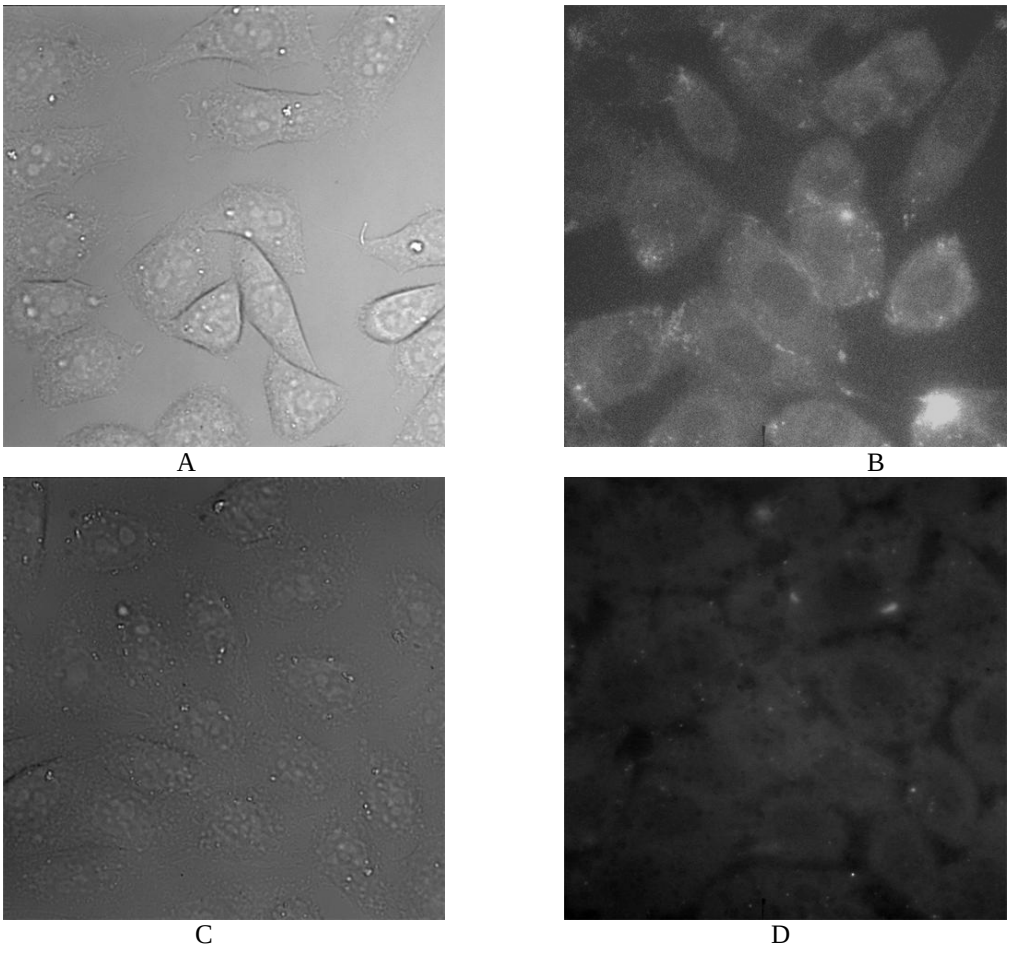

Figure A1. Control no light. CHO cells were incubated with 1 μM $CGlc_4$ (PS) overnight, washed three times with M2 medium before imaging the cells (A) in the bright field, (B) fluorescence microscope image of the EthD-1 using TRICT filter. Necrosis is not produced since the PS was not activated by light. Control cell without PS. Free PS label CHO cells washed three times with M2 medium before imaging in the bright field and irradiated as it was described in the materials and methods, (C) bright field image of cells

after radiation, (B) fluorescence microscope image of the EthD-1 using TRICT filter. Necrosis is not produced since there was no PS.

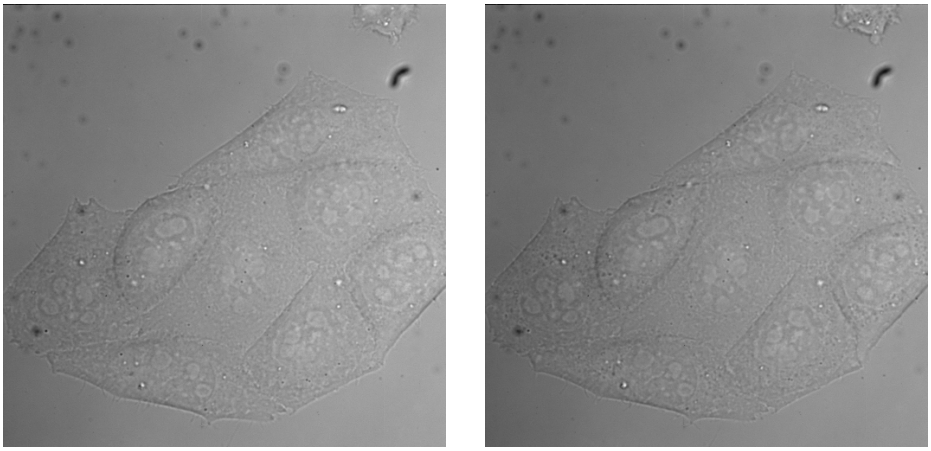

A B

Figure A2. CHO cells were incubated with 1μM $CGlc_4$ (PS) overnight, washed five times with PBS 5% (protocol used to wash the plasma membrane) and afterwards the cells were washed again three times with M2 medium before imaging inthe bright field (A) cells before irradiation as it was described in material and method (B) Cell after radiation showing no necrosis since there is no PS present in the plasma membrane. This experiment supports the idea that necrosis is activated by the PS located in the plasma membrane.

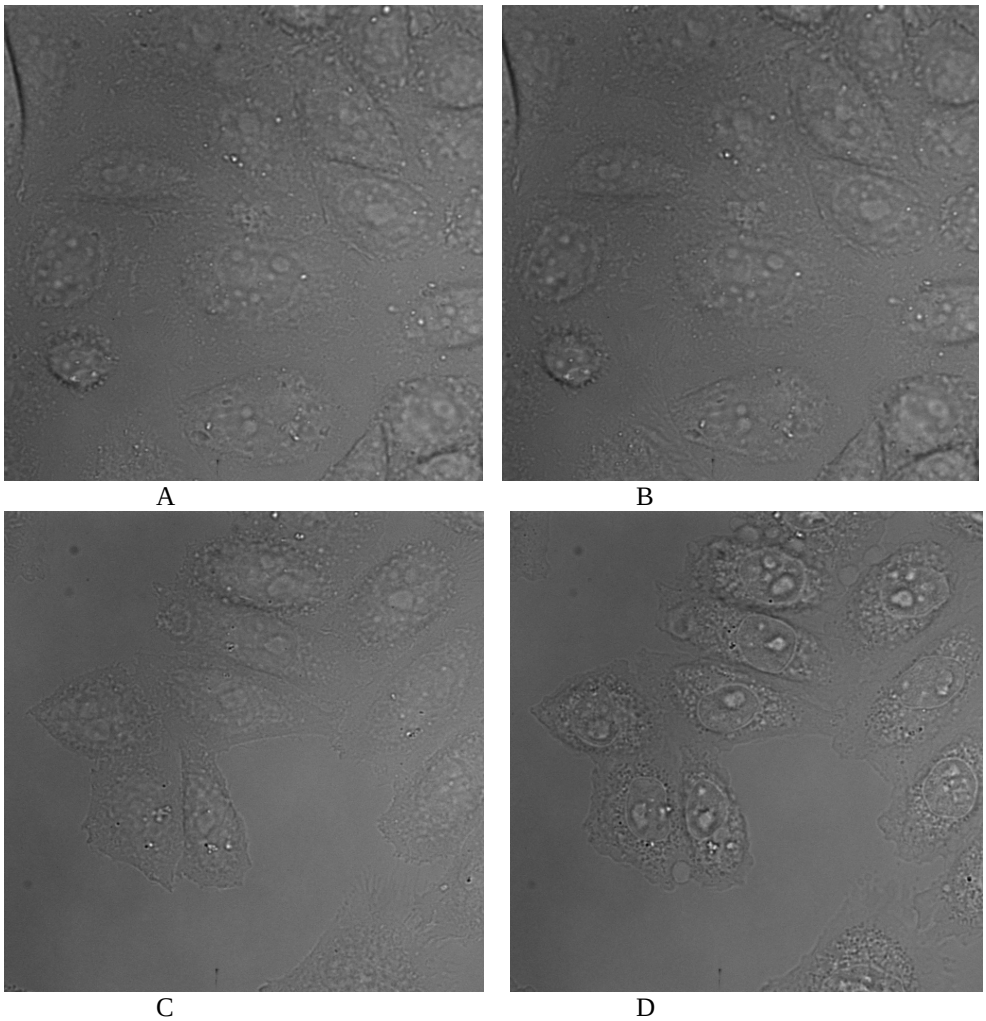

Figure A3. CHO cells were incubated with 1μM $CGlc_4$ (PS) 4 hours together with several concentrations of thioglucose, washed again three times with M2 medium before imaging in the bright field (A) cells before irradiation as it was described in the material and methods section; (B) cells after radiation showing no necrosis (1 mM thioglucose); (C) cells before irradiation as it was described in material and method (1μM thioglucose) (D) cell after radiation showing necrosis (1 μM). This experiment supports the idea that our PS may bind the active glucose transporters.

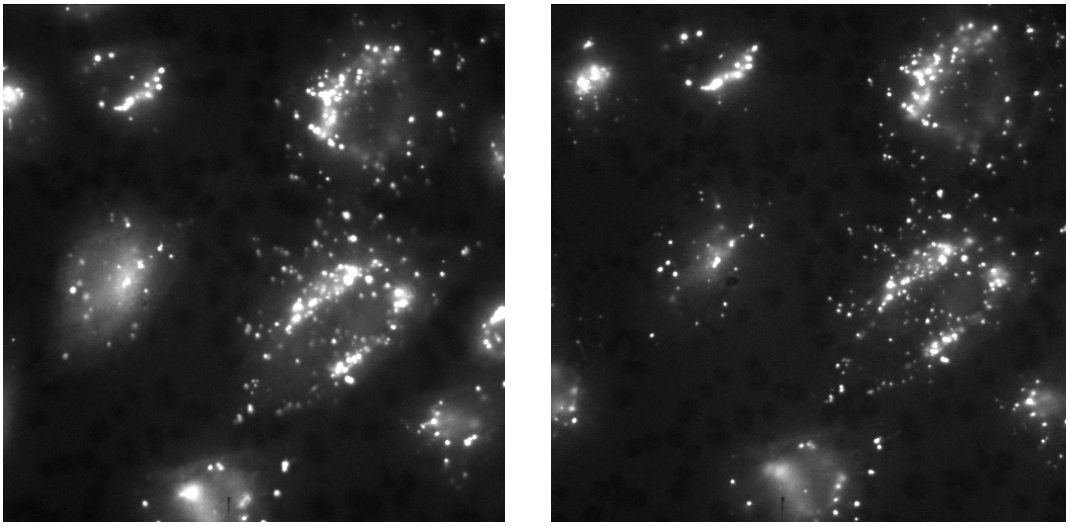

A B

Figure A4. CHO cells were incubated with 1μM $CGlc_4$ (PS) overnight, washed three times with M2 medium before imaging using CY5 filter (A) cells (B) cells after KI (0.3 mM) was added to the medium. The quenching of the PS located at the plasma membrane is observed.

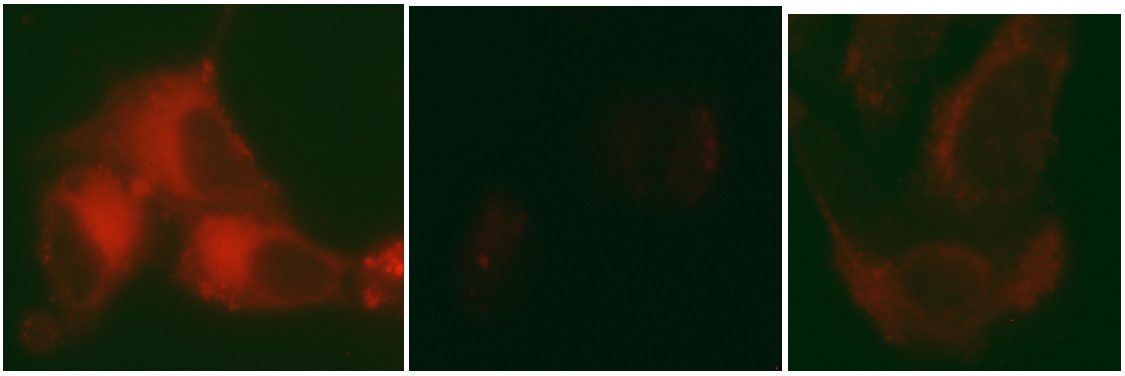

A B C

Figure A6. MDA MB 231 cancer cells were incubated for four hours with 1μM $CGlc_4$, washed three times and images were obtained under the same condition the same day to minimize possible variations. (A) cells incubated in DMEM medium with 10% serum. (B) cells incubated in DMEM medium 1% serum. (C) cells incubated with DMEM medium 1% serum and albumin.

Chapter 3 References

(1) Thompson, S; Chen, X; Hui, L; Toschi, A; Foster, DA; Drain, CM. Photochem. Photobiol. Sci. 2008, 7:1415-1421.

(2) Kessel, D; Luo, Y; Deng, Y; Chang, CK Photochem. Photobiol. 1997, 65: 422-426.

(3) Kessel, D; Vicente, MG; Reiners, JJ; J, Autophagy 2006, 2: 289-290.

(4) Buytaert, E; Dewaele, M; Agostinis, P; Biochim. Biophys. Acta. 2007, 1776: 86-107.

(5) Berg K, Folini M, Prasmickaite L, Selbo PK, Bonsted A, Engesaeter B, Zaffaroni N, Weyergang A, Dietze A, Maelandsmo GM, Wagner E, Norum OJ, Høgset A.; Curr. Pharm. Biotechnol. 2007, 8: 362-372.

(6) Markovits, J; Roques, BP; Le Pecq, JB; Anal. Biochem. 1979, 94: 259-264.

(7) Dunn, WA; Hubbard, AL; Aronson, NN J. Biol. Chem., 1980, 255: 5971-5978.

(8) Zucker, SD; Goessling, W; Bootle, EJ; Sterritt, C. J. Lipid Res. 2001, 42: 1377-1388

(9) Weissleder, R; Tung, CH; Mahmood, U; Bogdanov, A. Nat. Biotechnol. 1999, 17: 375–378.

(10) Pagano, M; Clynes, MA; Masada ,N; Ciruela, A; Ayling, LJ; Wachten, S; Cooper, DM Am. J. Physiol. Cell Physiol. 2009; 296: C607-619.

(11) Leth-Larsen, R; Lund, R; Hansen, HV; Laenkholm, A-V; Tarin, D; Jensen, ON; Ditzel, HJ Mol. Cellular Proteomics 2009, 8:1436-1449.

(12) Chen, X; Hui, L; Foster, DA; Drain, CM. Biochemistry 2004, 43: 10918-10929.

(13) Samaroo, D; Vinodu, M; Chen, X; Drain, CM. J. Comb. Chem. 2007, 9: 998-1011.

(14) Castaneda F, Burse A, Boland W, Kinne RK. Int. J. Med. Sci. 2007, 4: 131-139.

(15) Fritsch C, Lang K, Neuse W, Ruzicka T, Lehmann P. Skin Pharmacol. Appl. Skin Physiol. 1998, 11: 358-373.

(16) Dougherty TJ, Gomer CJ, Henderson BW, Jori G, Kessel D, Korbelik M, Moan J, Peng Q. J. Natl .Cancer Inst. 1998, 90: 889-905.

(17) Rastogi, S; Banerjee, S; Chellappan, S; Simon, GR Cancer Let. 2007, 257: 244-251.

Chapter 4:

PHOTONIC PROPERTIES OF THIOGLYCOSILATED CHLORIN, BACTERIOCHLORIN AND ISOBACTERIOCHLORIN FOR BIOIMAGING AND DIAGNOSTICS

Abstract

The facile synthesis of a non-hydrolysable thioglycosylated chlorin ($CGlc_4$) and isobacteriochlorin ($IGlc_4$) are reported. $CGlc_4$ and $IGlc_4$ have significantly enhanced fluorescence quantum yields compared to the corresponding porphyrin $PGlc_4$; ca. 6- and 12-fold in phosphate buffered saline, respectively. The uptake of these derivatives into cells such as human breast cancer MDA-MB-231 and K:Molv NIH 3T3 mouse fibroblast cells can be observed at nM concentrations with confocal fluorescence microscopy. In addition, bacteriochlorin (a secondary product of the isobacteriochlorin synthesis) is also presented as a novel PDT agent since its fluorescence quantum yield is similar than $PGlc_4$'s.

4.1. Introduction

For diagnostic and photodynamic therapeutic (PDT) applications the use of the lower energy light (red – near infrared) is an important characteristics that the new generation of compounds should possess[1] For this reason, porphyrinoids derivates such as chlorins and isobacteriochlorins are often synthesized because of their strong and/or redder lowest energy absorption band.[2] Chlorins and isobacteriochlorins are porphyrinoid derivates with one and two pyrrole double bond missing, respectively. Oxidative and more often reductive transformations are used to form the natural and synthetic chromophores.[2] Porphyrins, chlorins, and isobacterio-chlorins each have unique photophysical properties that are exploited by nature and can be used for diverse applications.[3] The intensity of the lowest energy UV-visible absorption band in the red region progressively increases in intensity and red shifts as the number of missing double bonds increases: porphyrins to chlorins to isobacteriochlorins. For diagnostic and photodynamic therapeutic (PDT) applications, the enhanced intensity of the low energy absorption bands allows more efficient use of wavelengths of light that penetrate further into tissues[2]. The excited state lifetimes, singlet and triplet quantum yields, and distortion upon metal ion binding are significantly different for these three types of porphyrinoid.

Photophysics. To understand the full potential of a given compound for use as Photodynamic theraphy agent, the triplet state quantum yield, and the quantum yield of singlet oxygen formation should be obtained and analyzed both in solution and in cells or tissue.[4] Photosensitisers remain at their electronic lowest or ground state energy level until a photon of light is absorbed and the subsequent promotion of an electron from the HOMO to the LUMO to produce the excited state. There several ways that the compound

may return to the ground state: (1) but the by emitting a photon (fluorescence), (2) by internal conversion with energy loss as heat, (3) entering the triplet state via intersystem crossing. Once the dye molecule is in the triplet state, it is possible to transfer the energy to another molecule in the triplet state – in this case ground state, triplet dioxygen. The result of the collision between the excited state triplet dye and the ground state triplet oxygen is that the energy is transferred from the former to the latter to result in the ground state singlet dye, and the excited state singlet dioxygen, which is widely referred to as sensitization. Dioxygen is unusual in that its ground state is a triplet. Singlet oxygen is a highly reactive oxygen species that reacts with diffusion limited kinetics to oxidize a variety of biomolecules and with water to generate other reactive oxygen species (ROS) such as hydroxyl radicals and peroxides. Cell stress and/or death results from oxidative damage at multiple sites including mitochondria, endoplasmic reticulum, cell membranes, etc.

The therapeutic applications of dyes as photosensitizers for the treatment of disease and infections (bacterial and viral) means that high triplet quantum yields should improve efficacy by increasing the yield of singlet dioxygen. Since the amount of internal conversion is expected to be reasonably consistent with a related family of dyes such as those described below, the lower the fluorescence quantum yield the greater the triplet quantum yield.

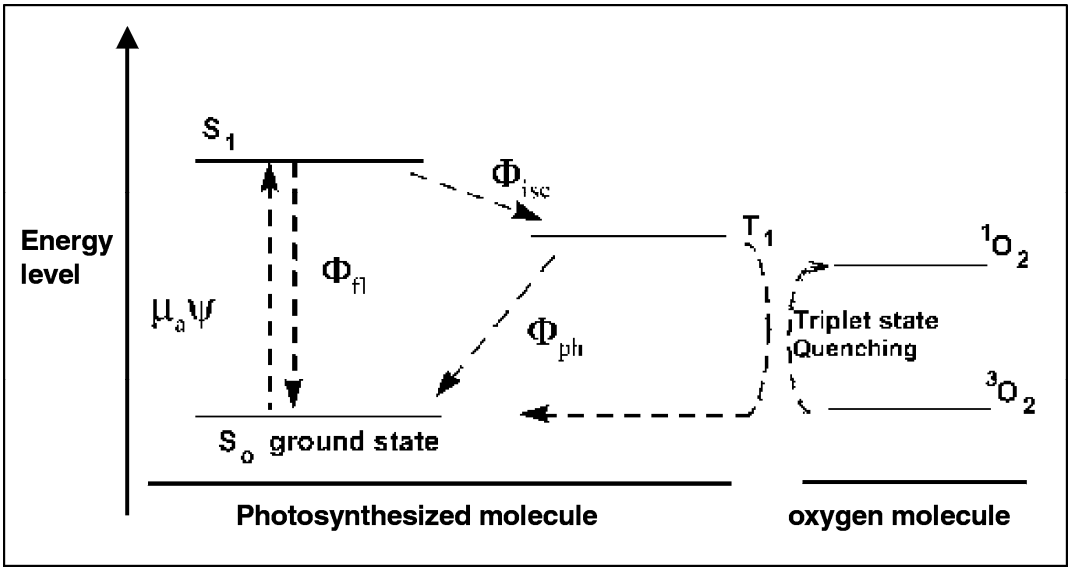

Figure 4.1. Zeblanski diagram for the sensitization of the formation of singlet dioxygen from the excited triplet state of a dye. (from www.ieee.org)

The oftentimes significantly greater fluorescence quantum yields of some chlorins and isobacteriochlorins make them suitable for use as fluorescent tags, and their use as therapeutics depends on the triplet quantum yield and sensitization of singlet oxygen formation. For example, a photosensitizer for PDT is meso-tetrakis(3'-hydroxyphenyl) chlorin. In general, the excited triplet state of PDT agents photosensitizes the formation of singlet oxygen which then causes damage to diverse cellular components – especially double bonds and heterocycles

Porphyrins with appended sugar moieties can have cytoxic activity[5]. The previously reported synthesis of non-hydrolysable thioglycosylated meso-arylporphyrins, also showed that the tetraglucose derivative ($PGlc_4$, Scheme1 1b) is a quite selective and effective PDT agent in vitro using several cell lines, such as MDA-MB-231 human breast cancer cells. In this chapter is reported an outline of the synthesis (performed by lab members Dr. Joao Tome and Ms Sunaina Singh), photophysical properties, and cell

uptake studies of the glycosylated chlorin ($CGlc_4$) and isobacteriochlorin ($IGlc_4$) analogues (Figure 4.3). The overall goal is to develop these compounds as cancer tags and therapeutics under normal, single photon, photodynamic conditions. In addition, bacteriochlorin ($BGlc_4$) is presented as a PDT agent with excellent photophysical properties, since its triplet quantum yield is hight but has a strong red absorption at 730 nm.

4.2 Experimental procedure

Synthesis and characterization: The reduction of $TPPF_{20}$ is carried out by a previously reported 1,3-dipolar cycloaddition reaction of an azomethine ylide with $TPPF_{20}$, to produce chlorin 2 and isobacteriochlorin 3 (Figure 4.3), but we scale up the reaction.. TLC indicates the two products are formed in yields of ca. 42% for 2 and 34% for 3 and 4; somewhat less than those reported. NMR and mass spectrometry are consistent with the previous report and attest to the purity of these intermediates. Preparative TLC and column chromatography were used to separate the compounds.

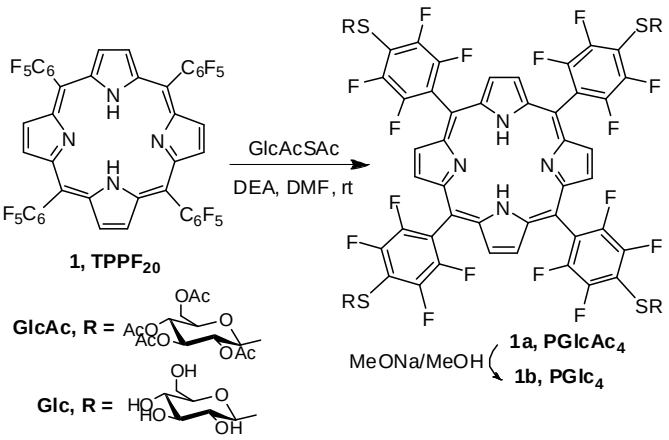

Figure 4.2. Synthesis of $PGlc_4$

The nucleophilic substitution of the thioglucose at the para position of the perfluorophenyl substituents of these three porphyrinoids is carried out by a modification of our previously reported. Thus, this new procedure was used to synthesized 2a ($CGlcAc_4$), 3a ($IGlcAc_4$), and 4 ($BGlcAc_4$), respectively from 2, 3 and 4 (Scheme 2).

Figure 4.3. Synthesis of $CGlc_4$, $IGlc_4$ and $BGlc_4$. Though the parent chlorin has a plane of symmetry, the bridgehead carbons of the fused N-methylpyrrolidine moiety are prochrial such that appending the glucose groups on the four meso aryl positions results in a diastereomeric pair at the chlorin 2 and 3 positions. For both the syn and anti forms of the bacteriochlorin there is a plane bisecting the fused N-methylpyrrolidines and two pairs of diastereomers are formed at the bridghead positions with addition of the glucose groups. The minor syn isomer of the isobacteriochlorin has a mirror plane, and there are two pairs of diasteriomers at the bridgehead carbons, whereas the anti isomer has only a c_2 axis so has a set of diastereomers before addition of the glucose groups. The mixture of diastereomers of the chlorin, the anti isomer of the isobacteriochlorin, and the anti isomer of the bacteriochlorin are used in the present work.

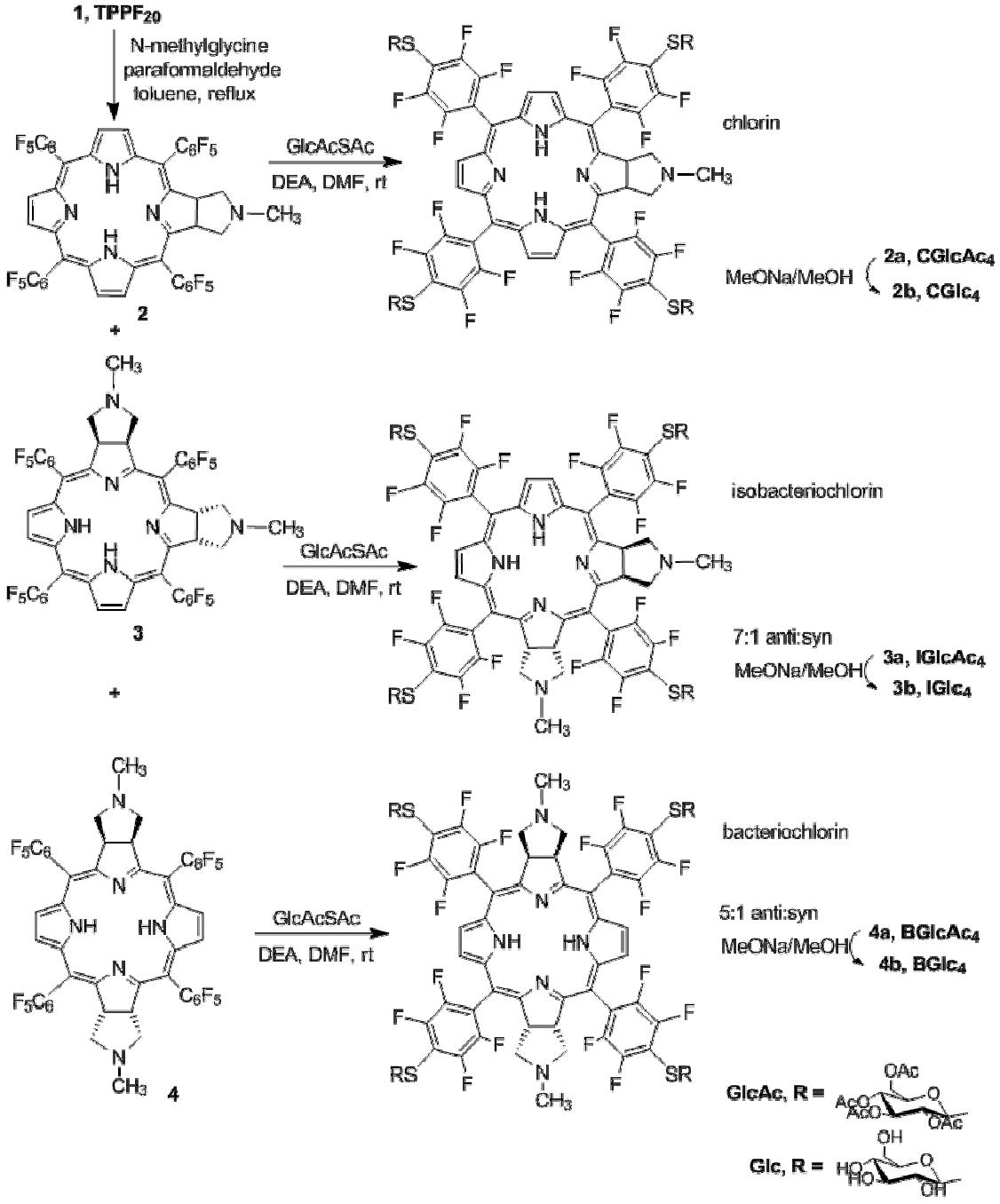

Note that for the bacteriochlorin and isobacteriochlorin, The carbohydrate protection groups are removed by treating 1a, 2a, 3a and 4a with sodium methoxide in dry methanol to obtain the glycoporphyrins 1b, 2b, 3b and 4b in ca. 95-98% yield (Figure

4.3). The detailed spectroscopic characterization by ^{1}H and ^{13}C NMR, high resolution mass spectrometry, and a discussion of the diastereomers of each compound will be given elsewhere. It should be noted that the mixture of diastereomers for 2b, anti 3b and anti 4b is used for all of the studies presented herein.

Cell Culture. Cells were maintained in DMEM, 10% bovine calf serum, 1% antimycotic, at 37^{0} C and 5% CO_2 atmosphere. Typically, ~2 x 10^{5} cells mL^{-1} were seeded in cell culture plates and allowed to grow for 24 hours. For experiments involving the porphyrin saccharide conjugate, $IGlu_4$, $PGlu_4$ or $CGlu_4$ was added to the cells 24 hours prior to the photodynamic experiments and biochemical assays to allow it to be taken up by the cells. The cultures were rinsed 2-3 times with fresh DMEM to remove any unbound porphyrinic compounds before proceeding to the various assays. Fluorescence microscopy indicates no unbound porphyrin remains.

Fluorescence spectroscopy Cells maintained in DMEM, 10% BCS, 1% antimycotic at 37 ºC and in 5% CO_2 atmosphere were plated in cell culture dishes. Compounds (dissolved in methanol) were added to the cultures to a final concentration of 1 or 2.5 μM such that there was never more than 0.5% methanol in the solution. After 20 h incubation, cells were washed with PBS 3 – 5 times and then visualized using a Nikon Optiphot 2 fluorescence microscope. Images were captured as JPEG files at 10X magnification, with excitation: 505 nm – 565 nm and emission at 565 nm – 685 nm. For each set of experiments, cells were cultured and the fluorescence images were taken under identical culture and microscopic conditions. For confocal microscopy, cells were then washed twice with PBS and incubated with a 4% paraformaldehyde solution in growth medium for 15 minutes at 37^{0} C under cell

growth conditions. Cells were then washed three times with PBS, mounted in Dako fluorescence mounting medium, and visualized using a Zeiss LSM510 laser scanning confocal microscope where images were captured. For MitoTracker green: excitation 476 nm, emission 490-510 nm; for $PGlu_4$: excitation at 633 nm, emission 650-670 nm.

Western blots. Cells were treated with porphyrin for 24 hours, rinsed and irradiated as described in above. After a period of time appropriate for the given experiment, cells were washed with cold PBS twice before lyses with RIPA buffer (50 mM Tris-HCl, 1% NP40, 0.25% Na-deoxycholate, 150 mM NaCl, 1 mM EDTA, 1 mM PMSF, 1 μg mL^{-1} aprotinin, leupeptin, and pepstatin each, 1 mM Na_3VO_4, and NaF). The lysates were gently rocked at 4^0 C for 25 minutes, centrifuged at maximum speed for 10 minutes, and the supernatant applied to a western blot. Equal amounts of protein were adjusted into gel-loading buffer (50 mM Tris-HCl, pH 6.8, 100 mM dithiothreitol, 2% SDS, 0.1% bromophenol blue, 10% glycerol), and heated for five minutes at 100^0 C prior to separation by SDS-polyacrylamide (8%) gel electrophoresis. After transferring to nitrocellulose membranes (Osmonics), membrane filters were blocked overnight at 4^0C with 5% non-fat dry milk in PBS. The nitrocellulose filters were washed three times for five minutes in PBS with 0.05% Tween-20 (Bio-Rad), before incubation with anti-PARP antibodies. Anti-mouse IgG conjugated with horseradish peroxidase was used as a secondary antibody. The bands were visualized using an enhanced chemiluminescent detection system (Amersham).

Fluorescence spectroscopy and Quantum Yield Calculations:

Fluorescence measurements were performed on dilute solutions, typically ~2 µM, of compounds in methanol, phosphate buffered saline and ethyl acetate. Samples were excited at the same band (around 500 nm) where absorbencies ≤ 0.1 and were within ~10% of each other. For emission spectra, both the excitation and detection monochrometors had a band pass of 1 nm. The corrected emission (for instrument response) and absorption spectra were using to calculate the quantum yield. Fluorescence quantum yields were determined for the chlorins, isobacteriochlorins, and bacteriochlorins in solution relative to TPP (in toluene), which as a fluorescence quantum yield of 0.11. The quantum yields are measured indirectly using TPP and as such these values may have some systematic error. All experiments were carried out on the same day, using identical concentrations to minimize any experimental errors. Figures 4.4 to 4.6 show the emission spectra, and figure 4.7 to 4.10 show UV-visible spectra

4.3 Results and discussions

Photophysical Properties. The deprotected glycosylated derivatives are used to evaluate uptake by K:Molv NIH 3T3 mouse fibroblasts (Figure 3.1). PBS (phosphate buffered saline, pH = 7.4), methanol or ethanol, and ethylacetate solvents were used to probe the photophysical properties since the glycoporphyrinoids may localize in aqueous, highly polar, or hydrophobic environments within cells. UV-visible spectral data in different solvents are summarized in Table 4.1, and the PBS data discussed.

The lowest energy Q band of chlorin $CGlc_4$ in PBS buffer at 649 nm has about 25-fold greater intensity than corresponding Q band of porphyrin $PGlc_4$ at 645 nm. For

isobacteriochlorin $IGlc_4$ in the same buffer, the lowest energy Q band at 645 nm is 5-fold greater than the porphyrin, and the band at 593 nm gains significantly in intensity. The $CGlc_4$ Soret band intensity decreases by 20%, broadens into two peaks, and the λ_{max} blue shifts by several nm. The Soret band splits into four peaks for $IGlc_4$ with a λ_{max} 25 nm to the blue of PGlc4. The spectral properties of the deprotected thioglycosylated compounds 2b, 3b, and 4b do not differ significantly from the protected 2a, 3a, and 4a intermediates in organic solvents.

Table 4.1. Photophysical Properties of Glycosylated Porphyrinoid Derivatives.

Cpd.		UV-visible	Emission	Quantum yield methanol[a]
PGlc4	ethanol	412, 505, 535, 586, 653	649, 701	0.05
	PBS buffer	410, 510, --- 576, 645(1)[b]	646, 691	0.03
	ethylacetate	412, 507, 450, 583, 655	649, 701	0.05
CGlc4	ethanol	406, 504, 532, 597, 651	653, 715	0.43
	PBS buffer	409, 506, 533, 597, 649(25)[b]	649, 707	0.17
	ethylacetate	406, 504, 531, 597, 651	653, 712	0.39
BGlc4	ethanol	374, 505, 673,732	737	0.06
IGlc4	ethanol	385, 508, 545, 586, 643	598, 646	0.70
	PBS buffer	385, 513, 548, 593, 645(5)[b]	606, 650	0.36
	ethylacetate	384, 510, 548, 589, 653	598, 646	0.60

[a] fluorescence experiments done in air, [b] relative intensity of lowest energy Q bands (see figures 1-6 below).

As expected, the fluorescence emission spectra for the three glycosylated porphyrinoids are notably different and have a strong solvent dependence (Table 4.1). There are negligible Stokes shifts for $PGlc_4$ and $CGlc_4$ in the three solvents. This likely indicates most specific solvent solute interactions are relegated to the sugar moieties. Notably, for the $IGlc_4$ in PBS, the strongest fluorescence band max is at 606 nm with a much weaker emission centered at 650 nm. Excitation spectra all indicate the presence of only the given compounds. The 0.17 and 0.36 fluorescence quantum yields for $CGlc_4$ and

for $IGlc_4$ in PBS are six times and twelve times that of the porphyrin analogue $PGlc_4$ (Figures 4.4 to 4.6). There is a small decrease in fluorescence quantum yield upon replacement of the para F by the thiocarbohydrate due to both electronic and heavy atom effects. The greater quantum yield of 2b than mTHPC, likely arises from the presence of the 16 F groups. Interestingly, the BGlc4 system with the 730 nm absorption band has a fluorescence quantum yield of about 0.05 and thus for the present we assume most of the excited state intersystem crosses to the triple manifold. Nonetheless, the fluorescence is sufficient to observe the uptake into cancer cell lines. Because 4b is a minor product, the anti/syn ratio smaller, and the set of diastereomers, this 4b was not extensively evaluated.

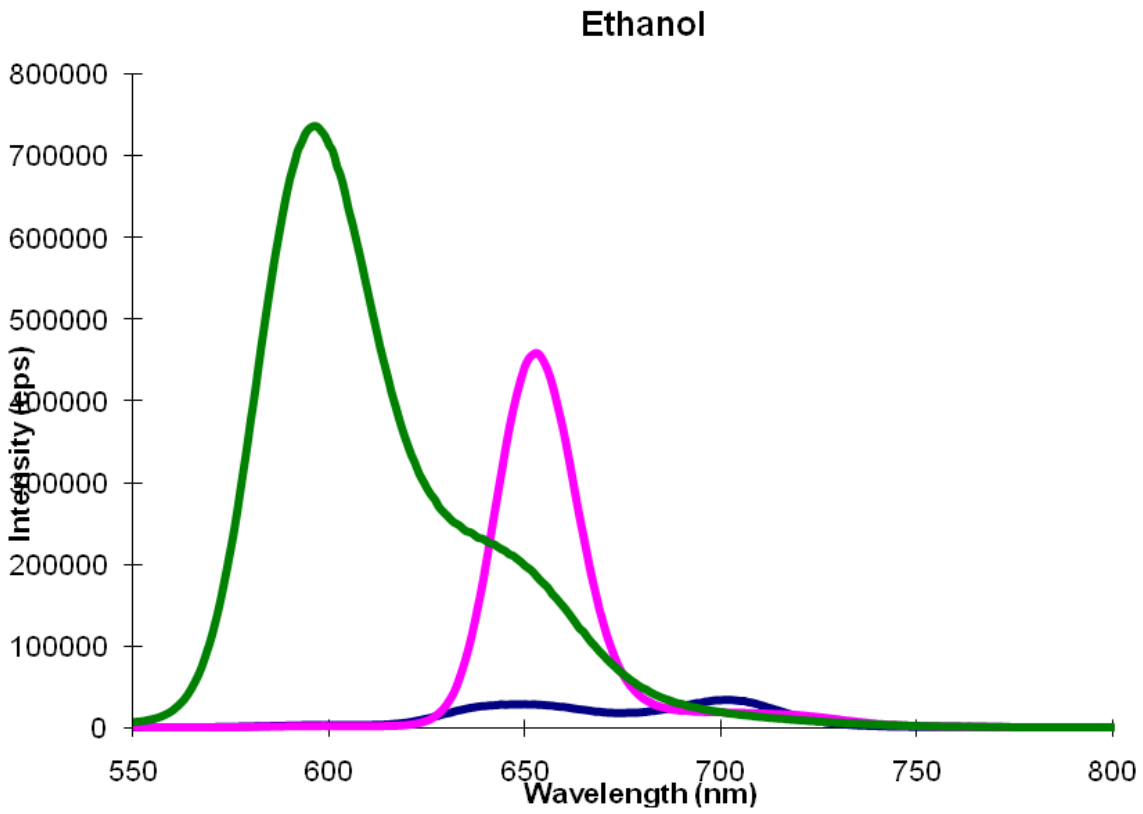

Figure 4.4. Emission spectra of the compounds in ethanol; excitation at 512 nm where the O.D. is ca. 0.05 for each compound. Green $IGlc_4$ Pink $CGlc_4$ Blue $PGlc_4$

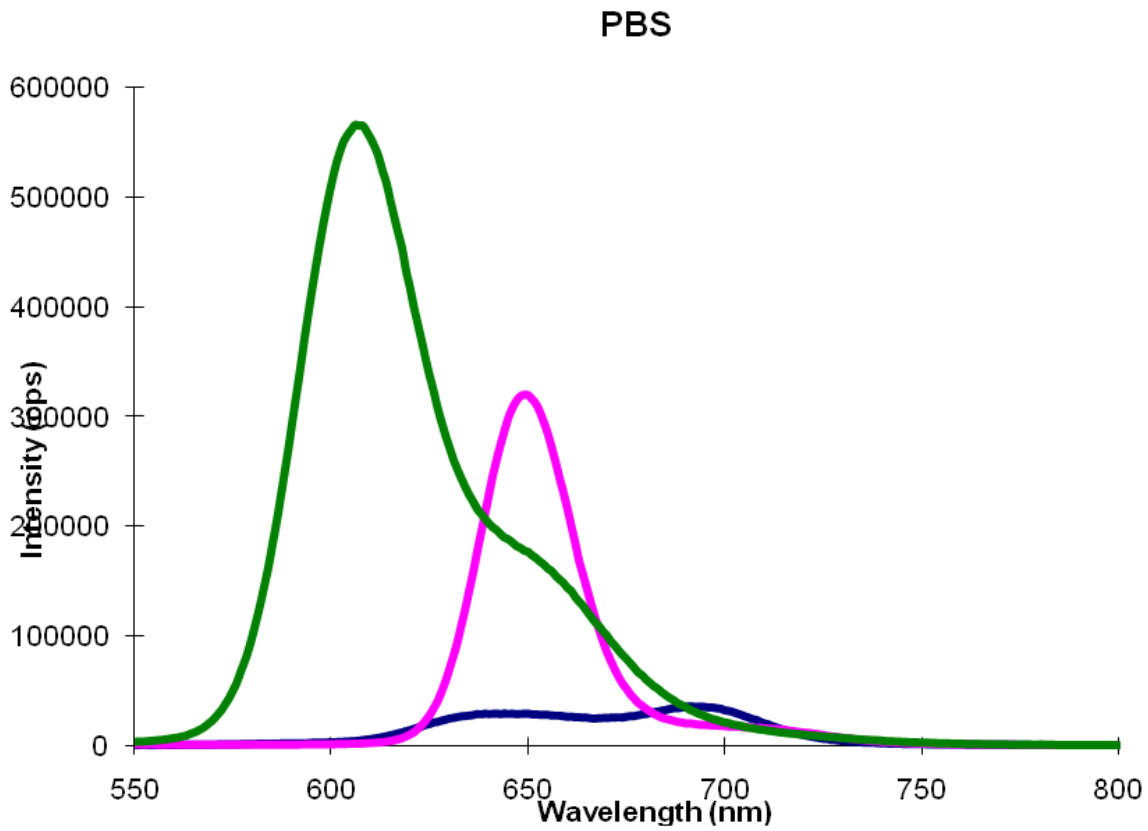

Figure 4.5. Emission spectra of the compounds in ethylacetate; excitation at 509 nm where the O.D. is ca. 0.098 for each compound. Green $IGlc_4$ Pink $CGlc_4$ Blue $PGlc_4$

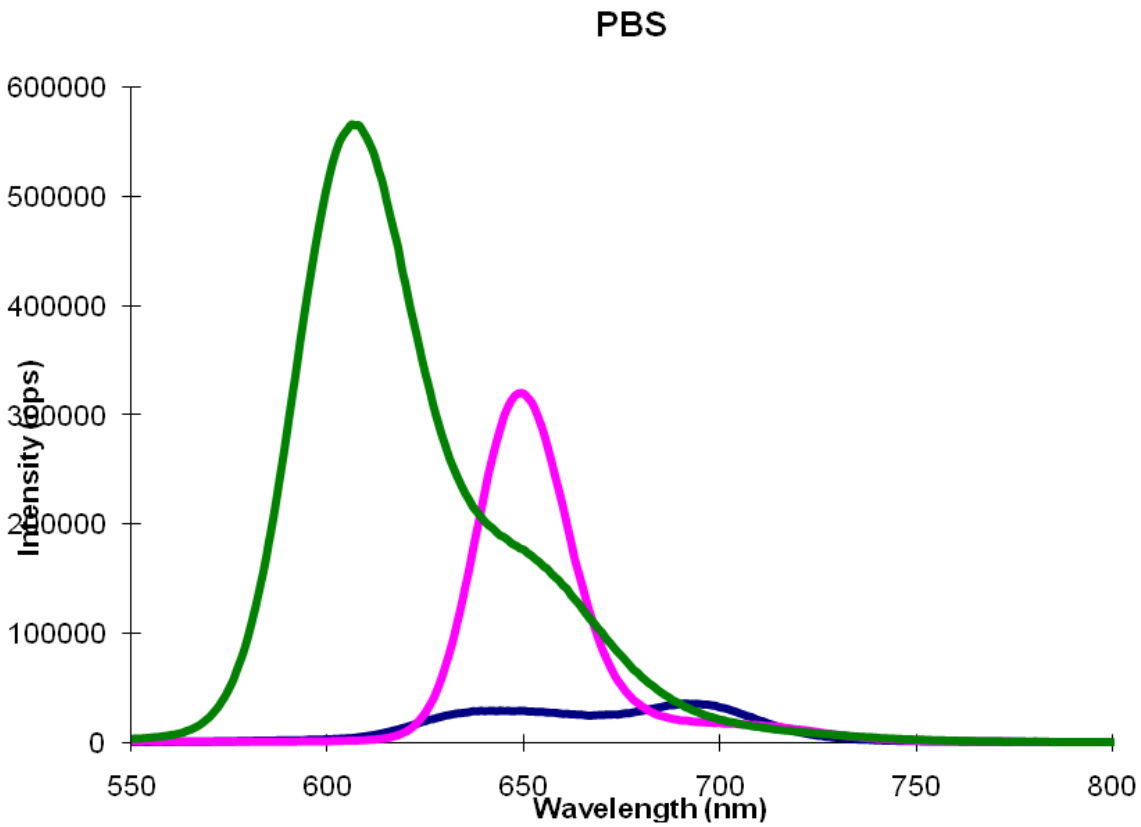

Figure 4.6. Emission spectra of the compounds in PBS; excitation at 512 nm where the O.D. is ca. 0.018 for each compound

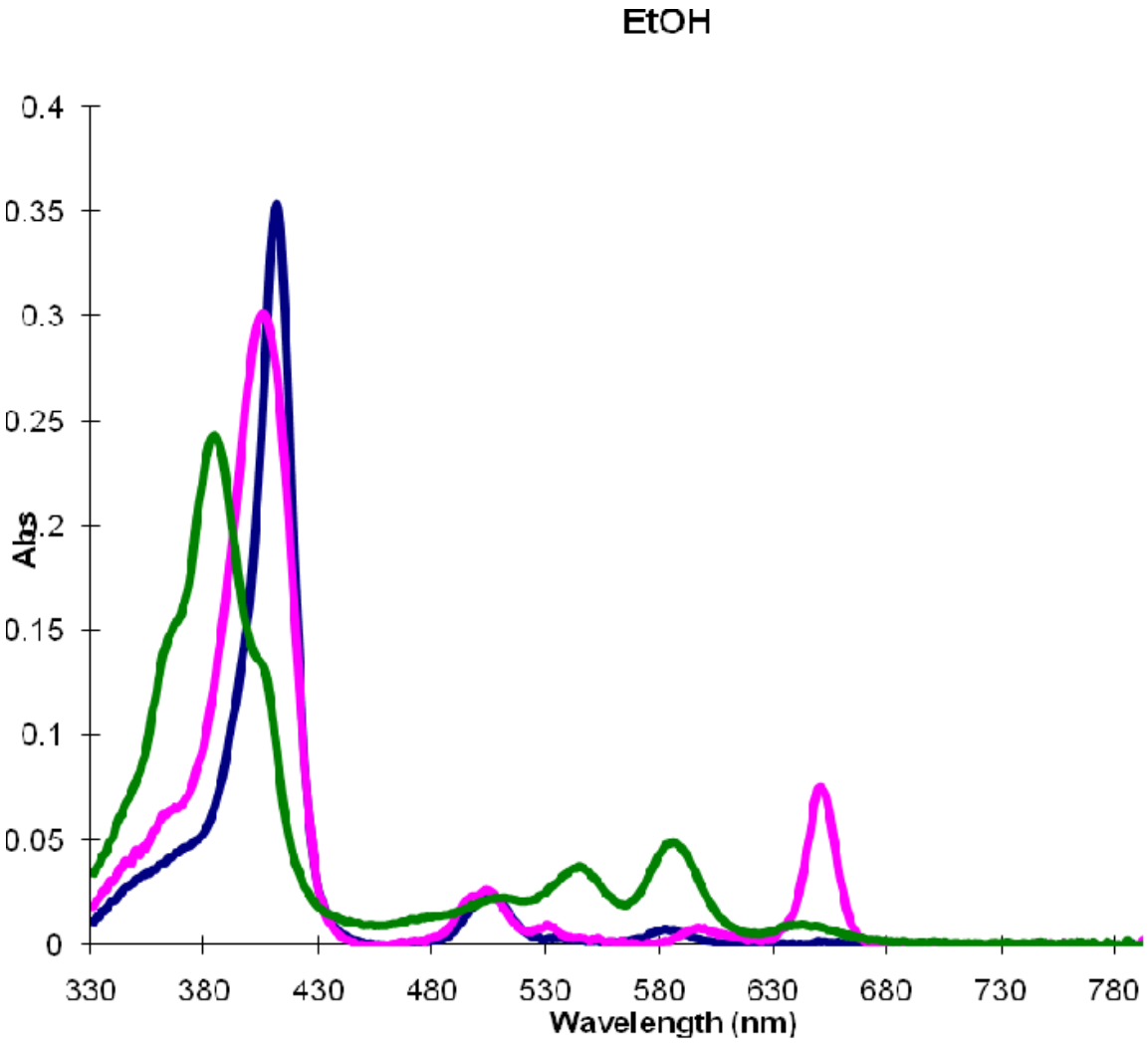

Figure 4.7. UV-visible spectra of the compounds, 1μ M in ethanol. Green $IGlc_4$ Pink $CGlc_4$ Blue $PGlc_4$

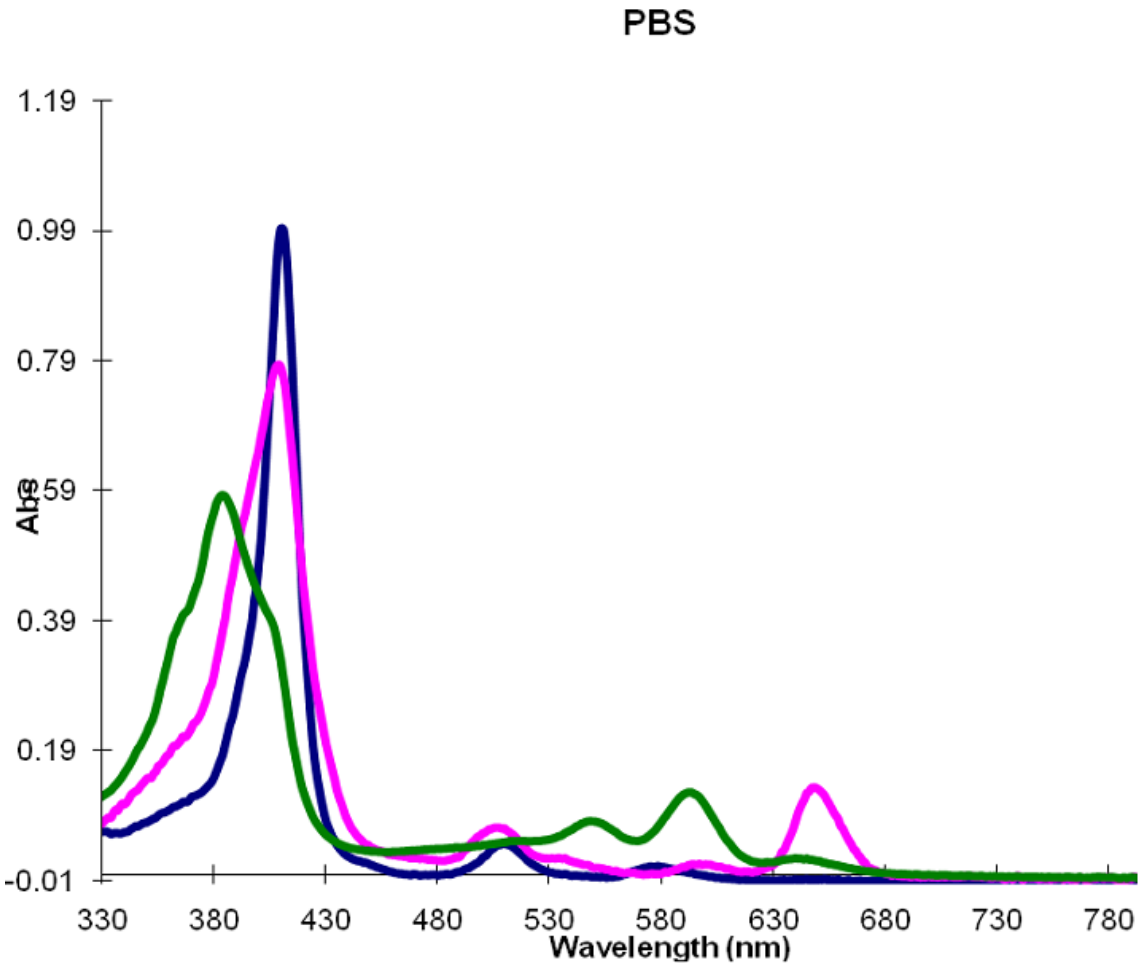

Figure 4.8. UV-visible spectra of the compounds, 4 μM in PBS. Green $IGlc_4$ Pink $CGlc_4$ Blue $PGlc_4$

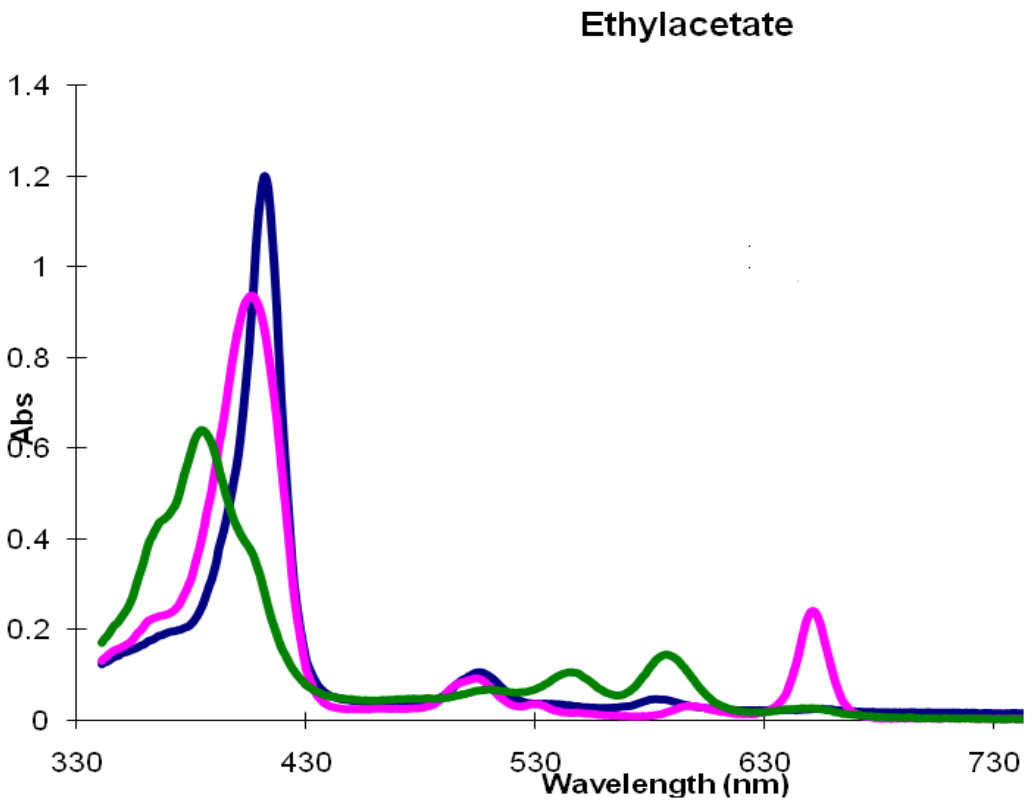

Figure 4.9. UV-visible spectra of the compounds, 4 μM in ethylacetate. Green $IGlc_4$ Pink $CGlc_4$ Blue $PGlc_4$

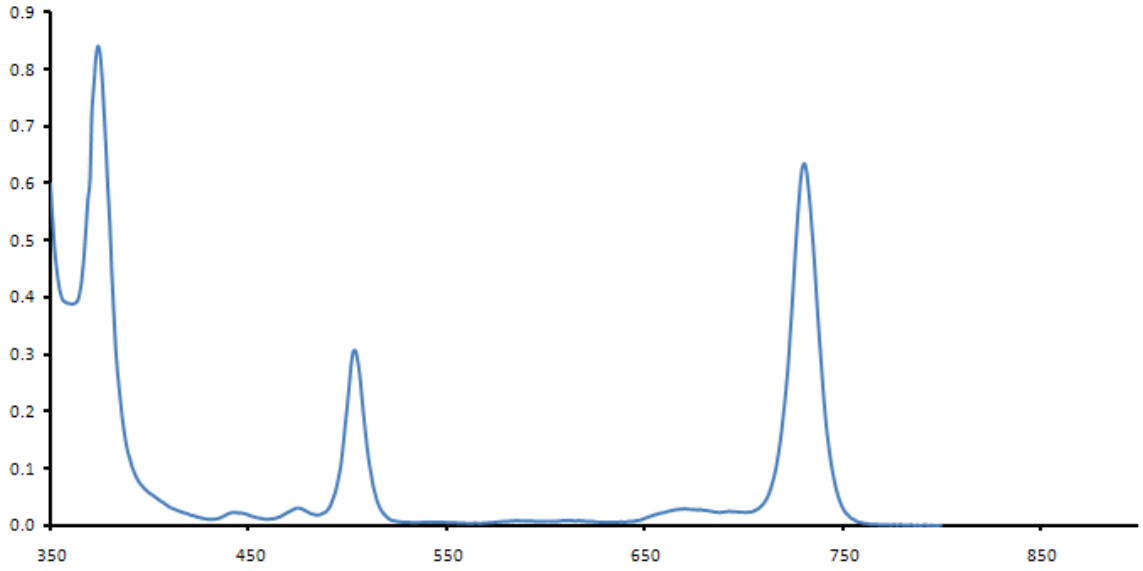

Figure 4.10. UV-visible and fluorescence of $BGlc_4$; 4 μM in ethanol.

K:Molv NIH 3T3 fibroblast cells were selected to evaluate these new thioglycosylated porphyrinoid derivatives because our previous studies with thioglycosylated porphyrin 1b $PGlc_4$ indicated good uptake and photodynamic effects on several cancer cell lines.[7] Our initial hypothesis was that the N-methyltetrahydropyrrole moieties used to make and stabilize the chlorins, bacteriochlorins, and isobacteriochlorins would have minimal effect on cell uptake, because these are sandwiched between the phenyl-sugars. Cells were incubated identically with 1 μM or 2.5 μM concentrations of $CGlc_4$, $IGlc_4$, and $PGlc_4$. The relative uptake and fluorescence was quantified by comparison of images taken by fluorescence microscopy under identical settings.[5] The unique spectral properties of $BGlc_4$ in terms of the 750 nm emission required the use of a different fluorescence microscope. At 2.5 μM, the relative integrated intensities for $PGlc_4$, $CGlc_4$ and $IGlc_4$ in the fluorescence micrographs are 1:2:7, respectively (Figure 4.11). In comparison to the quantum yields, this data indicates there are likely differences in uptake of the three compounds with this particular cell line. On TLC eluted with 3:2 ethyl acetate/methanol, the Rf of $PGlc_4$, $CGlc_4$, and $IGlc_4$ is 0.67, 0.48 and 0.26, respectively. Thus the differences in polarity, and maybe the propensity to aggregate in/on the cell[8] may result in differences in uptake. Detailed studies of the uptake and photodynamic effects in this and other cell lines will be reported elsewhere. The electronic spectra, fluorescence, and fluorescence microscopy studies all show that these compounds are robust to photobleaching. The remaining 16 F groups impart stability toward oxidative damage to the macrocycle and further enhance the photonic properties.

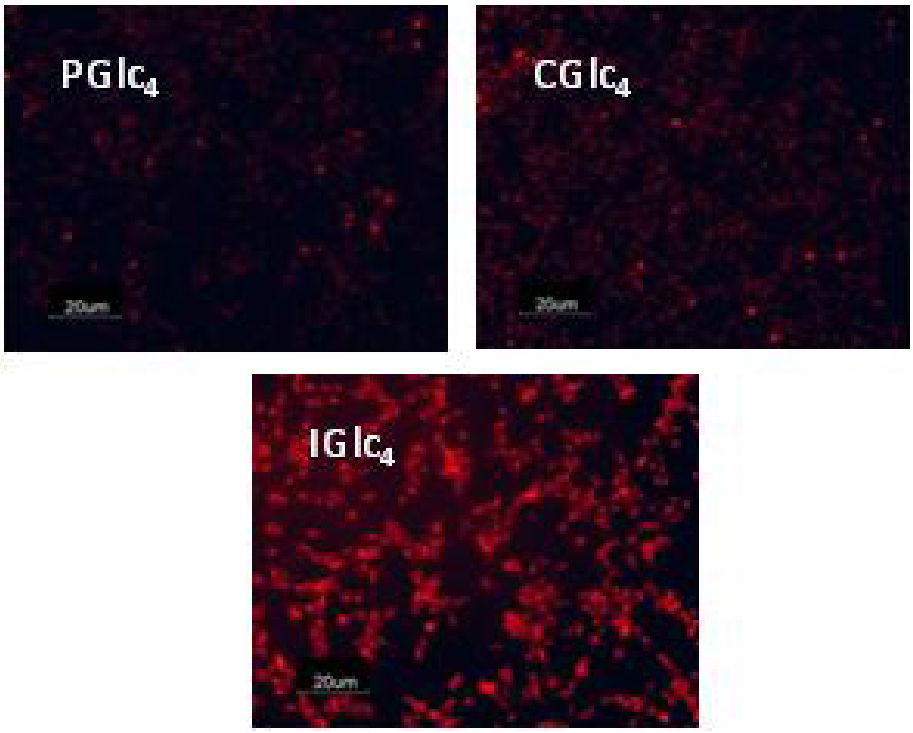

Figure 4.11. Fluorescence microscopy of K:Molv NIH 3T3 cells treated with 2.5 µM $PGlc_4$ (1b), $CGlc_4$ (2b), and $IGlc_4$ (3b). 3T3 NIH cells were incubated for 20 hrs with porphyrinoid, followed by removal of unbound dye from the cell culture by repeated rinsing, and the cells were imaged using standard methods. Images are taken under identical microscope setting and not enhanced; magnification 10X.

Though there may be differences in uptake between these compounds, we have shown that the $PGlc_4$ compound localizes in the endoplasmic reticulum because of the metabolic needs of this organelle.[9] The significantly greater fluorescence quantum yield of the IGlc4 system indicates that it can be used at ca. 25 nM concentrations to be detected under this condition. For PDT applications, sensitizers with strong red absorptions are generally considered better because these wavelengths penetrate deeper

into tissue. The optical cross section of $CGlc_4$ in the red region is significantly larger than the porphyrin or isobacteriochlorin analogues. Thus, if red light is used to activate the second generation dye $CGlc_4$, the increased light absorptivity more than compensates the reduced triplet quantum yield. Given the enhanced fluorescence quantum yield of $IGlc_4$ it is better suited for other tagging and sensor applications. Given the very strong 730 nm absorption of $BGlc_4$ and the low fluorescence quantum yield, this may be the best photosensitzer for PDT of the compounds described herein. However, a more efficient synthesis and purification of the isomers and diastereomers needs to be developed for the bacteriochlorin compounds to be used. The detailed photophysics of these compounds, including that in biological systems will be the subject of future studies.

4.4. Conclusions

Dual function photodynamic therapeutic and fluorescent tag. The much lower concentrations of the glycosylated chlorin ($CGlc_4$) and isobacteriochlorin ($IGlc_4$) indicate these compounds can be used as bioimaging and diagnostic tools. To demonstrate this, the compounds were tested with the same conditions as $PGlc_4$ (photodynamic therapy agent). The results confirm that the compounds result in much less damage to the cells compared to our PDT agent $PGlc_4$ under similar conditions.

In conclusion, both $CGlc_4$ and $IGlc_4$ have significantly enhanced fluorescence quantum yields compared to the $PGlc_4$, while the $BGlc_4$ derivative has a fluorescence quantum yield that is similar to the parent porphyrin. Thus $IGlc_4$ has greatest potential use as fluorescent tags, diagnostics, or imaging agents. The intermediate fluorescence of the $CGlc_4$ system may well serve as a dual purpose agent for targeting, detecting, and

treating diseased tissues. The $BGlc_4$ system has near optimal properties as the PDT agent, but new synthetic strategies are needed to make these compounds.

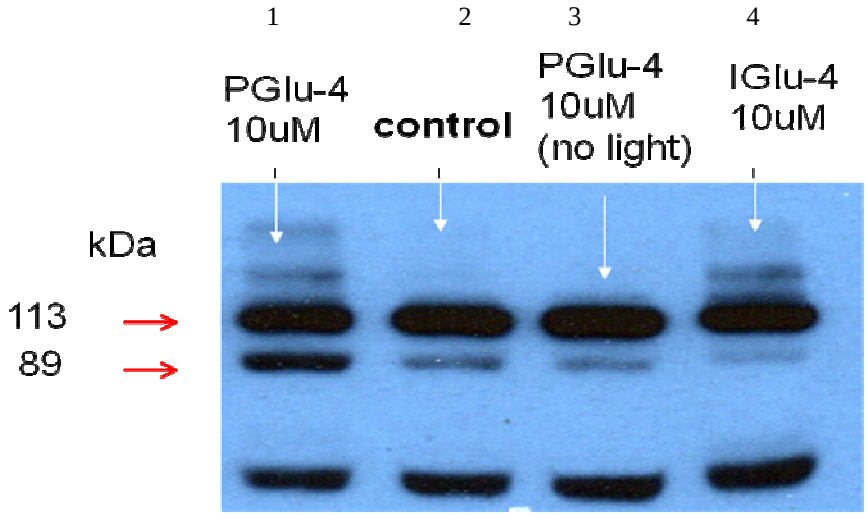

Figure 4.12. Western blot analysis for cleaved poly(ADP-ribose) polymerase (PARP) in MDA-MB-231 cells. The 89 KDa band indicates apoptosis. MDA-MB-231 cells were incubated 24 hours with $PGlu_4$ (used also as control) and IGlu-4. Cells were washed three times with porphyrin-free medium and irradiated under a 13 W fluorescent light (0.69mW cm^{-2}) for 25 min. Cells were collected three hours after irradiation. Lane 1 $PGlc_4$ (10 μM), lane 2 no porphyrin (control), lane 3 no light - $PGlc_4$ (10 μM), lane 4 $IGlc_4$ (10 μM). Protein content was measured after lysis and 100 μg of total protein were loaded in each lane of an SDS-PAGE.

Chapter 4 References

(1) Pushpan, SK; Venkatraman. S; Anand, VG; Sankar, J; Parmeswaran, D; Ganesan, S; Chandrashekar, TK Curr. Med. Chem. Anticancer Agents. 2002, 2: 187-207.

(2) Spikes, JD J. Photochem Photobiol B. 1990, 6: 259-274.

(3) Mauzerall, DC Clinic. Dermatology, 1998, 6: 195–201.

(4) Silva JN, Silva AM, Tomé JP, Ribeiro AO, Domingues MR, Cavaleiro JA, Silva AM, Neves MG, Tomé AC, Serra OA, Bosca F, Filipe P, Santus R, Morlière P. Photochem Photobiol Sci. 2008 Jul;7(7):834-43. Epub 2008 May 7

(5) Pandey, RK J. Porphyrins Phthalocyanines 2000, 4: 368-373.

(6) Silva, AMG.; Tome, AC; Neves, GPMS; Silva, AMS; Cavaleiro, JAS J. Org. Chem. 2005, 18;70(6) 2306-2314.

(7) Thompson, S; Chen, X; Hui, L; Toschi, A; Foster, D.A; Drain, CM Photochem. Photobiol. Sci. 2008, 7: 1415-1421.

(8) Samaroo, D; Vinodu, M; Chen, X; Drain, CM J. Comb. Chem. 2007, 9: 998-1011.

(9) Caramelo, J; Parodi, AJ Seminars in Cell and Developmental Biology, 2007, 18: 732-742.

Chapter 5

Two-Photon Microscopy using Tetraglycosylated Chlorin, Isobacteriochlorin, and Bacteriochlorin

Abstract

One of the main limitations of photodynamic therapy (PDT) is the damage produced to healthy tissue that has absorbed the dye – both in terms of tissues adjacent to the tumor exposed to therapeutic light doses and elsewhere in tissues exposed to high light conditions such as sunlight. This characteristic is presented because of the low specificity of photosensitizes (PS) currently in use. Thus, two means of increasing specificity in PDT are to increase the targeting of the dye to cancer tissues and to increase the localization of irradiation. Secondly, there is a significant need to develop dyes with greater optical cross sections in the red region of the spectrum, thereby allowing activation of the drug deeper inside tissues. For this reason, the use of dyes with significant two photon absorption (2PA) of red light may mitigate the disadvantage of collateral damage to nearby tissues by using a more specific, focused illumination. We reported the synthesis and biological activity of a tetraglycosylated porphyrin (P-Glc_4) starting from tetra-(perfluorophenyl)porphyrin ($TPPF_{20}$). Elimination of one or two of the double bonds on the pyrrole moieties of the macrocycle allows modulation of the photonic properties of the macrocycle, and the synthesis of three new tetraglycosylated derivatives were also described in the previous chapter: the chlorin ($ChlF_{20}$) and

tetraglycosylated chlorin ($CGlc_4$), the isobacteriochlorin ($IbcF_{20}$) and the tetraglycosylated derivative ($IGlc_4$), the bacteriochlorin (BcF_{20}) and the tetraglycosylated derivative ($BGlc_4$). Herein we report the photophysical properties these derivatives compared to the parent porphyrin. Using 2PA spectroscopy and microscopy, we show that the core macrocycles $TPPF_{20}$ and – $ChlF_{20}$ are not suitable for two photon microscopy, but IbcF20 and BcF_{20} are two photon active in the region of 760 nm to 860 nm. Further analysis indicates that BcF_{20} also has a one photon absorptivity in this region, while $IbcF_{20}$ has only 2PA properties.

5.1. Introduction

In the last decade 2PA research was mainly focused on the discovery and characterization of new molecules that have greater two photon cross sections,[1] for applications in optical technologies such as optical limiting, fluorescence techniques, lithographic micro fabrication, and biomedical applications[2]. Because porphyrins are a broad class of compounds with a diverse array of photonic properties, the 2PA properties have been intensely studied.[3] Unfortunately, most porphyrin derivates have low 2PA and lower fluorescence quantum yield,[4] so are poor chromophores for the aforementioned imaging applications. Consequentially, research on two-photon porphyrin materials contines to be focused on formation of multichromophore systems wherein the second chromophore served as the 2PA moiety.[5] Examples include the "2PA antenna- porphyrin complexes" that append auxiliary dyes to improve the two photon cross section, and the energy is transferred to a porphyrin core. Covalently coupling two or more porphyrin molecules via ethyne bridges at the meso positions also results in multichromophore

systems with 2PA cross sections,[6] but these systems may also have significant single photon absorptions in the same region.[7] Though the aforementioned advantages for photodynamic therapy using two-photon dyes are recognized, 2PA has had limited success thus far Two-photon PDT with 2PA dyes is, up to now, not well developed.[8]

.$PGlc_4$ (Scheme 1) has high selectivity to MDA-MB-231 breast cancer cells.[9] Furthermore, $PGlc_4$ was shown to be an effective PDT agent for MDA-MB-231 and several other cancer cell lines, and that under low light and low dye concentrations induces apoptosis.[10] It was also shown that $TPPF_{20}$ can serve as a core platform to make solution phase combinatorial libraries and appended with a variety of bio-targeting motifs[11]. Modification of the core porphyrin macrocycle is well known to significantly change the ground state and excited state properties. Elimination of one of the pyrrole double bonds in $TPPF_{20}$ results in a chlorin Chl. Eliminating two pyrrole double bonds on adjacent pyrroles yields the isobacteriochlorin Ibc, and on opposite pyrroles yields the bacteriochlorin Bc. However, methods for the effective synthesis of new porphyrinoid cores that can serve as platforms for further modification by appending biotargeting motifs are limited. A synthetic strategy to make these core porphyrinoid platforms starting from $TPPF_{20}$ was reported [12] and yields $ChlF_{20}$, $IbcF_{20}$, and BcF_{20} (Chapter 3). We have shown that the $ChlF_{20}$ and $IbcF_{20}$ can be appended with thioglusose to give $CGlc_4$, and $IGlc_4$ (Scheme 1) and that these are also taken up by cancer cells (chapter2 and 3).

The results presented in this chapter suggest that a single porphyrin dye molecule, as opposed to a multichromophoric system, can possess a sufficient two- photon cross section to be a good two photon imaging agent. Specifically, $IbcF_{20}$, BcF_{20}, $IGlc_4$ and

$BGlc_4$ have a sufficient 2PA to obtain high quality two photon images. These results also suggest that $IbcF_{20}$ is a good candidate for simultaneous imaging and PDT in animals.

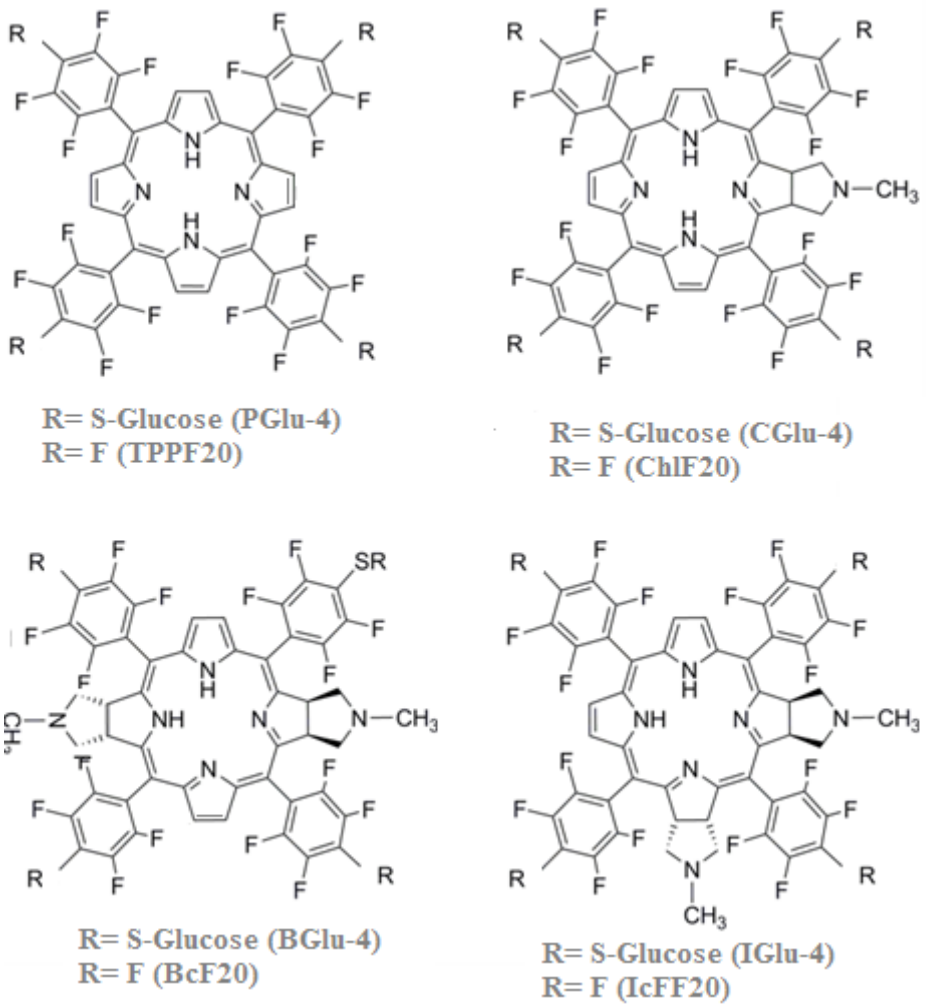

Figure 5.1. Structures of the six compounds.

5.2. Experimental procedures

Synthesis and characterization: All the compounds ($PGlc_4$, $CGlc_4$, $IGlc_4$, $BGlc_4$, $ChlF_{20}$, $IbcF_{20}$ and BcF_{20}) were synthesized and characterized as previously described in chapter 3.

Cell Culture. NIH 3T3 K:mol cells or CHO cells were maintained in DMEM, 10% fetal bovine serum, 1% antimycotic, at 37^0 C and 5% CO_2 atmosphere and F12, 5% bovine serum, 1% antimycotic, at 37^0 C and 5% CO_2 atmosphere respectively. Typically, ~2 x 10^5 cells mL^{-1} were seeded in cell culture plates and allowed to grow for 24 hours. For imaging or photodynamic therapy experiments, the compounds were added to the cells 24 hours prior to the experiments, unless otherwise noted. After incubation with the compound, the cultures were rinsed 2-3 times with fresh PBS to remove any unbound porphyrinic compounds before proceeding to the assays.

Two-photon imaging. Two-photon imaging was performing using a custom-built multiphoton imaging system in the laboratory of Professor Sushmita Muhkerjee at Cornell Medical College. The system consists of an Olympus BX61 upright microscope and a BioRad 1024 scan head. The specimens are excited using a tunable Ti-Sapphire laser (Mai Tai, Spectra-Physics), tuned to 860 nm. The laser power under the objective is controlled through a Pockel Cell (Conoptics). To avoid one photon process, 860 nm excitation light was used and the emitted light collected was between 500 nm and 670 nm. Note that the lowest energy optical absorption bands for the compounds in aqueous

media are: $PGlc_4$ 645 nm, $CGlc_4$ 649 nm, $IGlc_4$ 645 nm, $BGlc_4$ 730 nm. Thus, under these conditions, there is no single photon excitation of the compounds.

Two-photon cross section: 2PA measurements were done as previous described[13]: Briefly Ti–sapphire laser (Spectra-Physics Tsunami) pumped by a frequency doubled diode-pumped solid-state laser (Spectra-Physics Millennia) provided 90 fs operating at 82 MHz was used to probe the 2PA properties of the dyes, and a CW (continuous wave) laser was used for the single photon studies. Both lasers were operated at the same power (6 mW). Secondly, experiments concerning quadratic dependence with the laser power were obtained using the femto second laser. Experiments were performed at the same condition time with rhodamine G (standard) and calculations used an existing protocol.

5.3. Result and discussion

Our observations that cells treated with the $IGlc_4$ and $BGlc_4$ derivatives were observable in the two-photon microscope prompted us to further investigate these molecules and quantify the two photon absorption properties. Similar to previous studies on the $PGlc_4$ with MDA-MD-231[11] CHO cells were incubated overnight with $PGlc_4$, $CGlc_4$ and a mixture of $IGlc_4$ and $BGlc_4$ (5:1) at 10 μM final concentrations. The 5:1 mixture of the two compounds is a result of the synthetic methods (chapter two). As can be seen in Figures 1 to 3, only the 5:1 mixture of $IGlc_4$ and $BGlc_4$ appears to be active by two photon microscopy, or at least, some fluorescence light in the range of 500 nm to 670 nm is detected when the compounds are excited with 860 nm light.

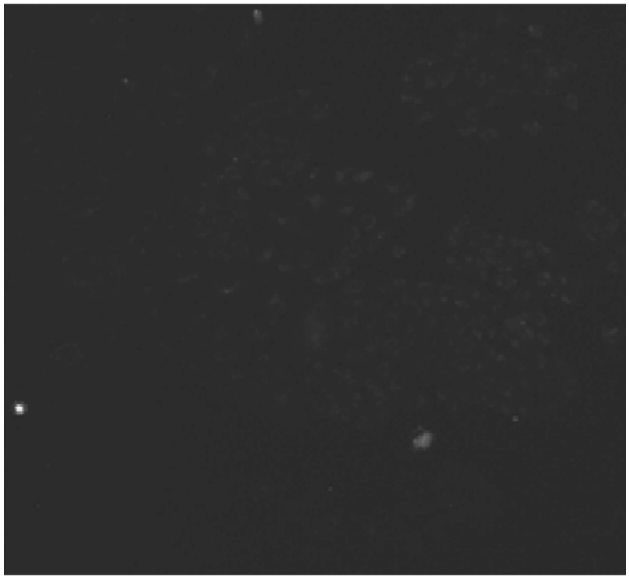

Figure 5.2. CHO cells were incubated with 10 μM $PGlc_4$ overnight. Two-photon microscope excitation light was at 860 nm, and the detector was set for 500 nm to 670 nm detection. The image data was collected for 1 s. The image is not manipulated.

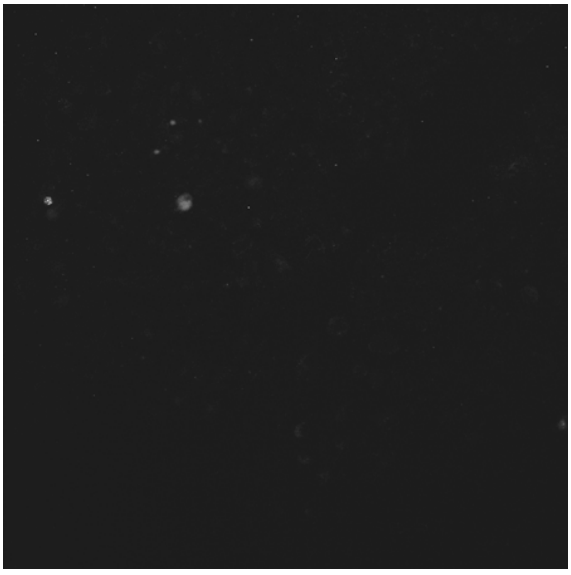

Figure 5.3. CHO cells were incubated with 10 μM $CGlc_4$ overnight. Two-photon microscope excitation light was at 860 nm, and the detector was set for 500 nm to 670 nm detection. The image data was collected for 1 s. The image is not manipulated.

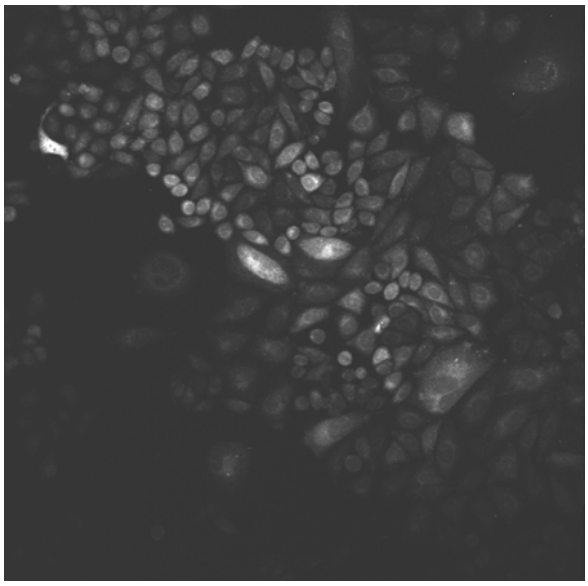

Figure 5.4. CHO cells were incubated with a 10 μM of a 5:1 mixture of $IGlc_4$: B Glc_4 overnight. Two-photon microscope excitation light was at 860 nm, and the detector was set for 500 nm to 670 nm detection. The image data was collected for 1 s. The image is not manipulated.

These result clearly show the possibility that either $IGlc_4$ or $BGlc_4$ are two-photon active. The 5:1 ratio of the glycosylated compounds was determined from the UV-visible spectra and the previously reported extinction coefficients of the isobacteriochlorin and bacteriochlorin, $IbcF_{20}$ and BcF20 respectively. In order to delineate the contributions of each compound to the observed two-photon microscopy data, we returned to the $IbcF_{20}$ and BcF_{20} mixture, separated the isomers, and re-evaluated the photophysical properties, and two-photon microscopy. Because the long-term goal is to use the different porphyrinoids as core platforms to append an array of bio-targeting motifs, the photophysical properties of these were investigated. Thus, from this point onwards the

experiments were performed only with the core $IbcF_{20}$ and BcF20 platforms rather than the glycosylated derivatives.

After $IbcF_{20}$ and BcF_{20}were separated, cells were incubated under the same conditions with each compound. UV-visible spectra show that none of the compounds absorb at the 860 nm excitation use in the two-photon microscopy. Since the fluorescence of BcF_{20} begins around 720 nm and the detector is set up from 500 nm until 670 nm, significant fluorescence of this compound is not observed. As expected, $IbcF_{20}$ is two photon active as can be observed in figure 4.

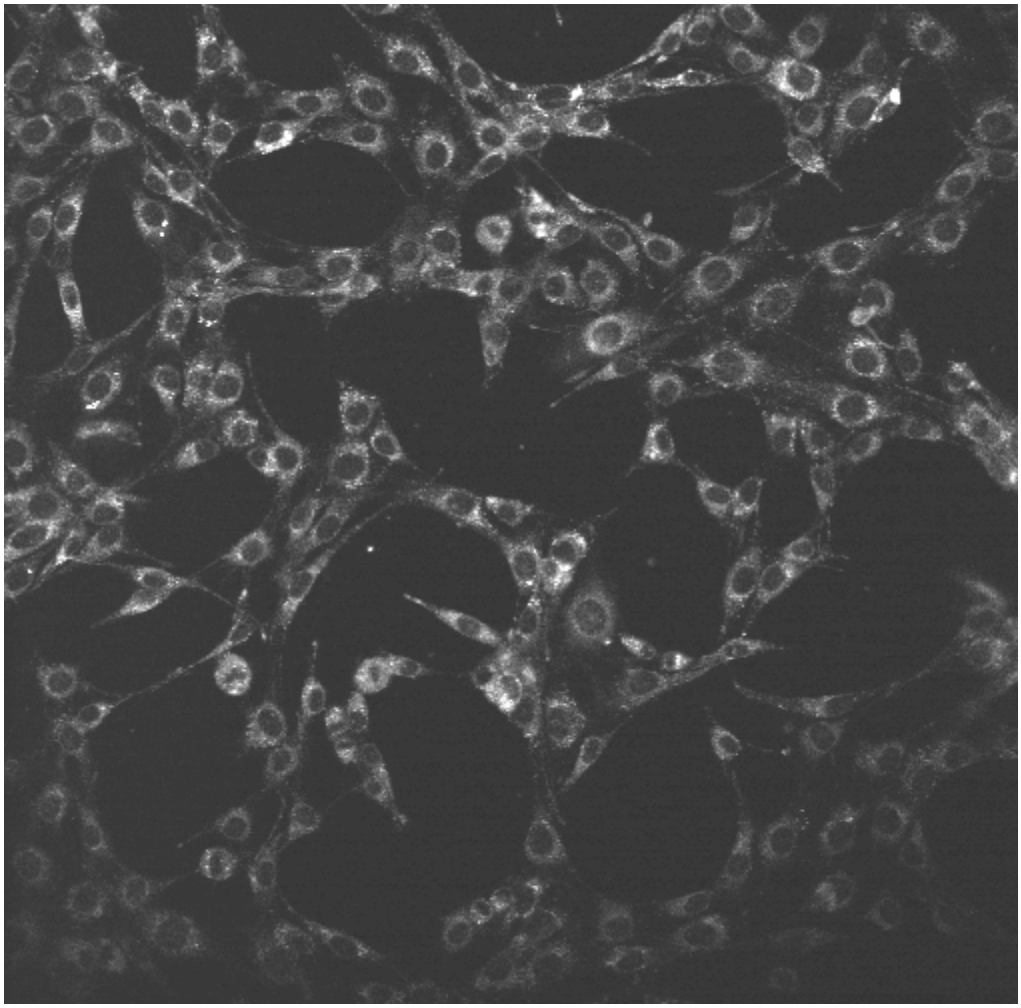

Figure 5.5. NIH 3T3 K:mol cells were incubated with 10 μM of $IbcF_{20}$ overnight. Two-photon microscope excitation light was at 860 nm, and the detector was set for 500 nm to 670 nm detection. The image data was collected for 1 s. The image is not manipulated.

Two photon fluorescence versus One photon fluorescence

Although the one photon absorbance spectra of $IbcF_{20}$ and BcF_{20} show no absorbance peaks around 860 nm (figures 5.6 and 5.7), both compounds were excited using CW laser and femtosecond laser to insure that the absorption process is due two

photon process only. The CW laser is typically used to excite compounds with one photon, while the femtosecond laser is utilized to produce the excitation by two photons[13]. The difference between the two ways of excitation is due the dependence of the two photon efficiency on the instantaneous irradiance.

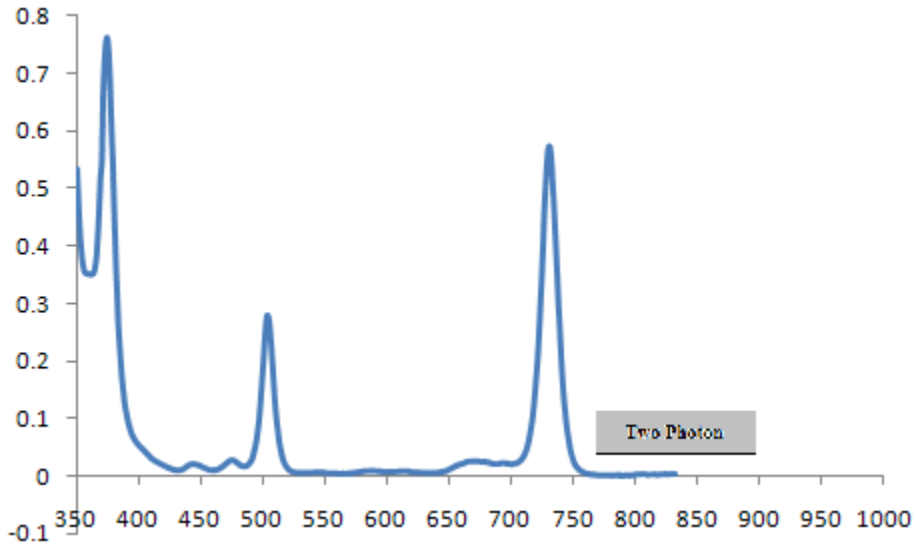

Figure 5.6. UV-visible spectra of the BcF_{20}compound, 1µ M in ethanol.

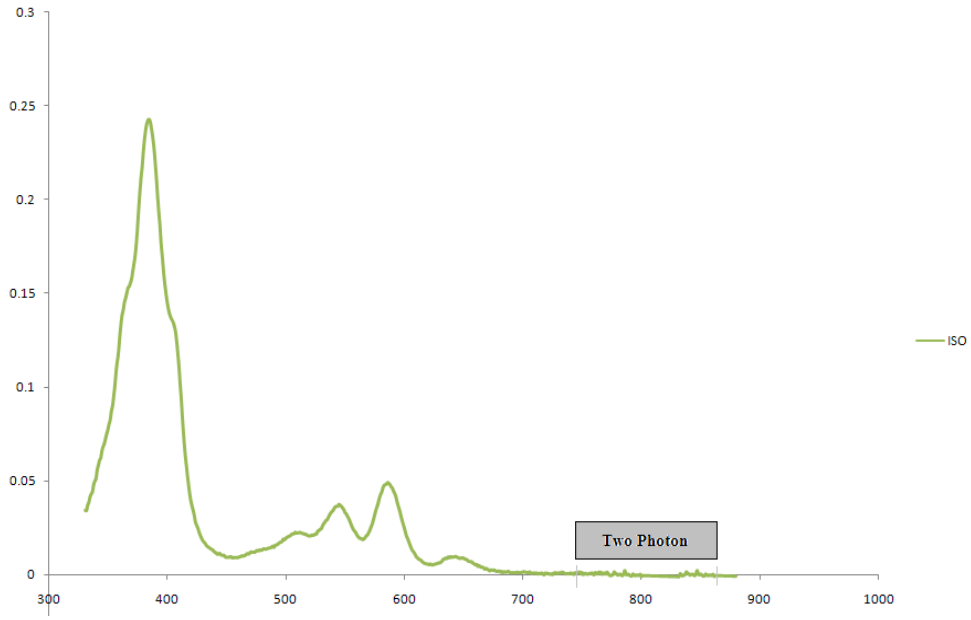

Figure 5.7. UV-visible spectra of the $IbcF_{20}$compounds, 1µ M in ethanol.

The powers of both modes used in the following were the same. The results are expressed in the following table for the rhodamine 6G standard used for calculation of the 2PA properties.

Table 5.1 Wavelength vs integrated area (A.U.) for R6G.

Wavelength	Femtosecond Laser	CW Laser
760nm	39916720	0
780nm	145011030	0
800nm	30758521	0
820nm	8564341	0
840nm	50934864	0
860nm	681493	0
880nm	174537	0

Our two photon reference, R6G, is not exited at all when the CW laser is used. On the other hand, excitation is produced (and fluorescence light is measured) when a femtosecond laser is used instead. Similar results are obtained for $IbcF_{20}$, indicating that $IbcF_{20}$ is two photon active, and no one photon absorption is presented. The results are presented in the following table.

Table 5.2 Wavelength vs. integrated area (A.U.) for $IbcF_{20}$

Wavelength	Femtosecond Laser	CW Laser
760nm	76390	0
780nm	3008379	0
800nm	289240	0
820nm	69493	0
840nm	841539	0
860nm	296746	0
880nm	44659	0

The mixed results are obtained when BcF_{20} is exited using a similar set up. The one photon absorption can be observed from 760 nm until 880 nm. It is very interesting that when 760 nm, 780 nm or 800 nm wavelengths are used, the one photon process dominates the excitation process. Concerning lower energy wavelengths (820 nm, 840 nm, 860 nm and 880 nm) the combination both two photon and one photon absorption is presented. The results are expressed in the following table.

Table 5.3 Wavelength vs integrated area (A.U.) for $BbcF_{20}$

Wavelength	Femtosecond Laser	CW Laser
760nm	427192460	427192460
780nm	427192460	427192460
800nm	10134667	10134667
820nm	7142291	3188409
840nm	10063471	6598879
860nm	1076278	384684
880nm	35527	22199

The combination of both absorption processes is presented in the case of BcF_{20} because of the lower energy absorption peak around 730 nm. Laser excitation with energies close to 730 nm (760 nm to ca. 800 nm) may possibly excite the molecule by one photon process wherein there is a very small, but significant tail on the red edge of the absorption band, or there is a small band centered at ca. 830 nm (see Figure 5). An anti-Stokes effect is also possible wherein the molecule gets vibration and rotational excitation from the basal level from the room temperature energy, thus allowing excitation of the molecule with a lower energy than is normally expected. Neither the small tail or the absorption band, nor the anti-Stokes effect is observed with the $IbcF_{20}$

compound because its lowest energy absorption peak is located at 600 nm, which is far enough away from the lower energy laser used (760 nm). Thus $IbcF_{20}$ can only have a 2PA at wavelengths greater than 760 nm.

Quadratic dependence with laser power

Two Photon absorbance processes imply that the fluoresces light increases quadraticly versus increasing laser power, and not linearly as it is for one photon emission. This behavior arises from the fact that two photons are absorbed in the same quantum event. Using a femtosecond laser, BcF_{20} and $IbcF_{20}$ were exited at a 860 nm wavelength, and the fluorescence light measured while the laser power was changed. Together with both compounds, rhodamine 6G was measured under the same conditions as a two photon reference compound. The following graph illustrates the fluorescence dependence of the three compounds on the laser power using 860 nm excitation.

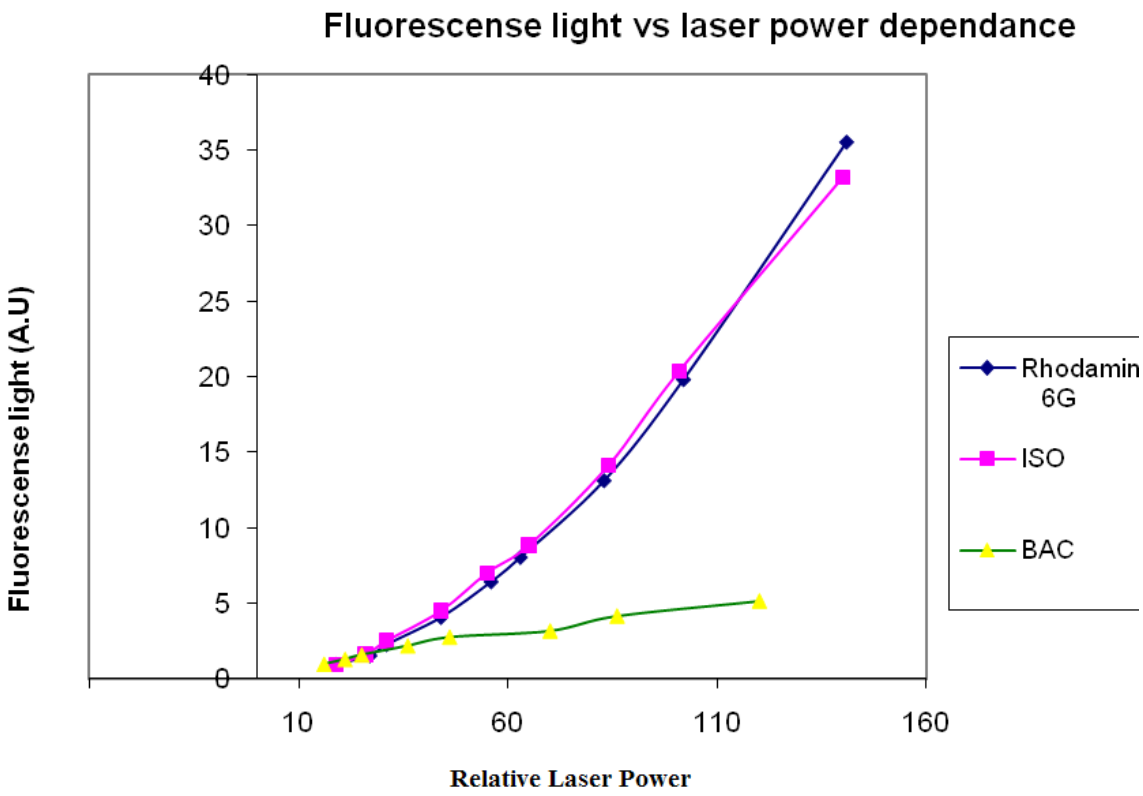

Figure 5.8. Dependence of light emitted versus laser power. Excitation: 860 nm. Light collected: 500 nm to 800 nm. Pink = IbF_{20}, blue = rhodamine 6G, yellow = BcF_{20}.

As can be appreciated from graph 1, $IbcF_{20}$ has a clear quadratic dependence on the laser power that is similar to the rhodamine 6G standard, while BcF_{20} shows a linear dependence on the laser power. These results confirm that $IbcF_{20}$ is indeed 2-photon active, and that BcF_{20} either has no 2PA or the single photon processes dominate the observed fluorescence.

Two photon cross sections (2PA) are difficult to measure consistently and accurately because of the large flux of photons needed from the femtosecond laser can vary significantly. For this reason, all the 2PA calculations are based in the fluorescence

light emitted when the sample is excited by two photons and assuming this is directly proportional to the photons absorbed. Using the same laser power for the sample and for the two photon reference, it is possible to calculate with reasonable precision the 2-photon cross section. The only assumption is the quantum yields of both samples are the constant as a function of the wavelength. Our reference for two photon is rhodamine 6G in methanol at 110 μM (Quantum Yield = 0.93). $IbcF_{20}$ was dissolved in DMSO at the same concentration (Quantum Yield = 0.15).

The cross section (σ) of $IbcF_{20}$ was calculated for each wavelength using the following equation:

$$\sigma s(\lambda) = \frac{F(\lambda) \times QYr \times nr}{Fr(\lambda) \times QY \times n} \sigma r(\lambda)$$

Where F(λ), Fr(λ), QY, QYs and σr are the two photon fluorescence of the sample, two photon fluorescence of the reference, quantum yield, quantum yield of the reference, and the reference cross section, nr and n are the reflective index of the solvents. The cross sections obtained are expressed in the following table 4. Two-photon cross-sections for molecular systems are expressed in Goeppert-Mayer (GM) units, where 1 GM is 10^{-50} cm^4 s $photon^{-1}$. GM units arise from the product of two cross sectional areas (one for each photon, in cm^2) and a time (when two photons simultaneously interact with the sample). The large scaling factor allows for convenient comparisons of the molecular systems.

Wavelength	Cross section (GM)
760	1.7
780	7.5
800	3.2
820	3.1
840	3.2
860	24.5
880	6.1

Table 5.4. Two photon cross section values of $IbcF_{20}$

Photobleaching in cells

Photo bleaching is also observed in two photon process. The photo stability of the fluorescent imaging agent and/or PDT photosensitizer is very important, since a longer photo stability would allow imaging over a greater amount of time or multiple images to be taken, and from a therapeutic perspective, the stability of the sensitizer to photo bleaching increases the efficacy of the dye.

To investigate the photo stability of $IbcF_{20}$, 25 scans were performed using the two photon microscope and the first image (obtained from the first scan) was compared with the last image (obtained from the last scan). As can be appreciated form the images in Figure 5.9, $IbcF_{20}$ is not photo bleaching to a great extent. Thus this core platform may

be an excellent choice for both therapeutic and imaging applications where one needs to follow cells or biochemical processes over time.

Figure 5.9. After 3T3 NIH cells were incubated with $IbcF_{20}$ for 24 hours and rinsed with buffer, the 2-photon microscopy was done repeatedly to examine the photo stability of the compounds under these conditions. Excitation was a 860 nm, and detection between 500 nm and 670 nm. Top the 2-photon microscopic image after one scan, and the same sample after 25 scans.

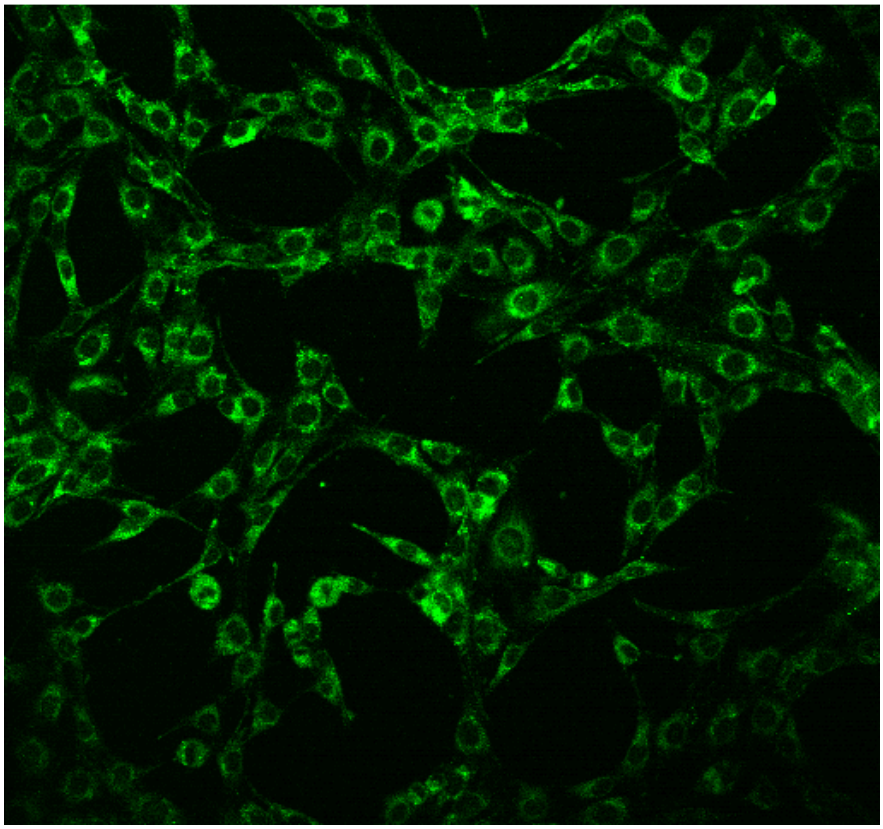

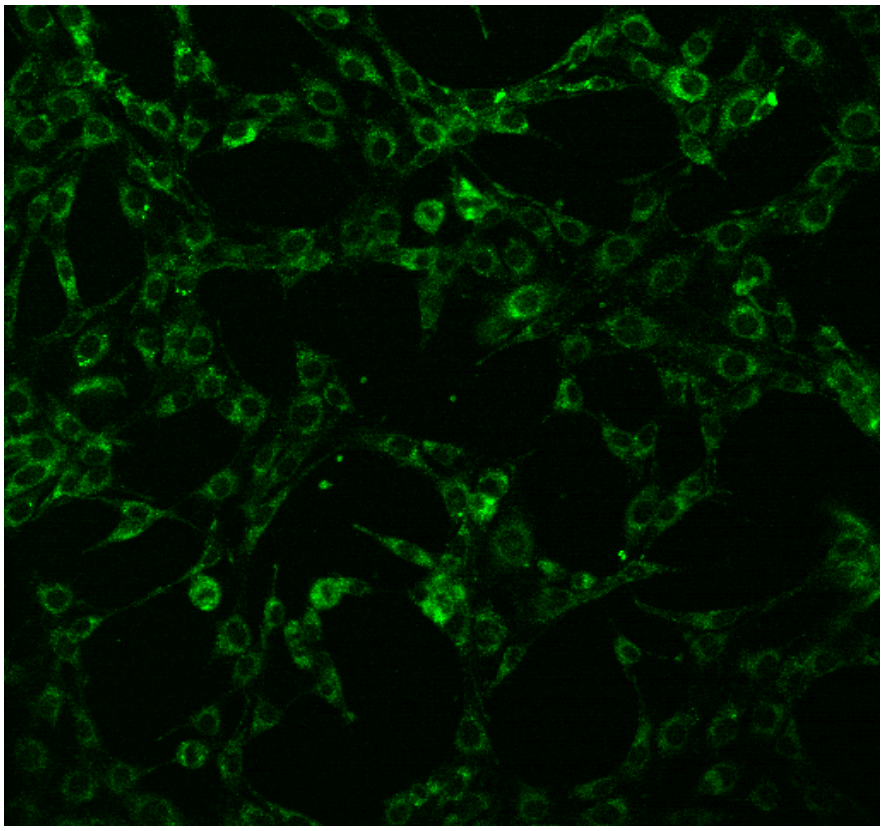

5.4. Conclusions

The two photon absorption proprieties of two compounds were presented in this chapter. $IbcF_{20}$ is two photon active in the range analyzed (760 nm to 880 nm), while BcF_{20} is largely a one photon dye that may have small contributions from two photon processes.

Both compounds are considered good chromophores for the next generation of photosensitizer for PDT. The first generation includes the porphyrin oligomers formulated as Photofrin (the first photosensitizer approved for clinical use). One disadvantage of the first generation systems (poor light absorption at wavelengths that penetrate deeper into tissues, and the lack of exocyclic targeting motifs that direct the compound to cancer cells or other cells) is reduced in the second generation of photosensitizer (e.g. 5,10,15,20-tetrakis(3-hydroxypheny)chlorin) in that there is a stronger red absorption. There are other second generation choromophores for other applications, such as the chlorin Visudyne® [13] used for wet macular degeneration. However, these compound in clinicl use or trials generally lack organic moieties that are designed to direct the choromphore to specific cell types, tissues, or other organisms for uses as antibiotics. Thus, the appending of the sugars will make these compounds more biocompatible and have cancer-targeting properties.

The strong red absorption bands are advantages of the both bacteriochlorin and isobacteriochlorin platforms in terms of single photon processes for sensitizer applications. The 2PA properties of $IbcF_{20}$, while not large compared to the multichronmophore systems reported, are sufficient for imaging applications and perhaps for therapeutic applications. One advantage also may be that the present systems are significantly smaller in terms of molecular size; therefore may be better taken up into cell and tissues. Based on our new knowledge of the BcF_{20} and $IbcF_{20}$ systems, perhaps other bacteriochlorins and isobacterioschlorins have the potential for an array of applications.

Another point that should be mentioned is the paucity of work done using robust dyes as contrast and imaging agents for two photon microscopy – especially dye appended with targeting motifs. The main reason is that most compounds have low quantum yields compared to isobacteriochlorins. The 2-photon microscopy is enabled by the fact that $IbcF_{20}$ combines a high quantum yield of ca. 30% with a 25 GM 2PA cross section. Future research must be conducted to reach several different objectives. First of all, $IbcF_{20}$ is just the core platform, upon which many different targeting motifs can be attached, so that two photon active dyes with significantly improved selectivity and uptake by cancer cells are possible. This will result in more efficacious molecules for PDT applications and imaging applications. It may be advantageous to use a combination of two or all three of systems discussed herein (chlorine, isobacteriochlorin, and bacteriochlorin) where each brings a specific photonic property.

Currently our group, in collaboration with Cornell University Medical College, is focusing on the possibility of detecting cells that were incubated overnight with $IbcF_{20}$ and injected intra-dermally in mice skin by two photon microscopy. Our preliminary

positive results show for the first time that two photon microcopy is suitable to excite a molecule and detect the fluorescence light emitted in vivo. This result opens the possibility to perform two photon photodynamic therapy in vivo, something that still not performed with good results. On the other hand, although neither the chlorin nor BcF_{20} is suitable for two photon imaging or two photon photodynamic therapy since the compound possesses several advantages as a one photon photosensitizer (chapter 2).

Chapter 5 References

(1) Dy, J; Ogawa, K; Satake, A; Ishizumi, A; Kobuke, Y Chem. Eur. J. 2007, 13: 3491-3500.

(2) Hanninen P, Soukka J, Soini JT.Ann N Y Acad Sci. 2008;1130:320-6. Review

(3) Drobizhev, M; Karotki, A; Kruk, M; Rebane, A Chem. Phys. Let. 2002, 355: 175-182.

(4) Mir, Y; Lier, J; Allard, J; Morris, D; Houde, D Photochem. Photobiol. Sci. 2009, 8: 391-395.

(5) Leupold, D; Teuchner, K; Ehlert, J; Irrgang, K; Renger, G; Lokstein, H J. Biol. Chem. 2006, 281: 25381- 25387.

(6) Dhistedt, E; Collins, H; Balaz, M; Kuimova, M; Khurana, M; Wilson, B; Philips, D; Anderson, HL Org. Biomol. Chem. 2009, 7: 897-904.

(7) Fisher, JA; Susumu, K; Therien, MJ; Yodh, AG; J. Chem. Phys. 2009, 130: 134506

(8) Starkey, JR; Rebane, AK; Drobizhev, MA; Meng, F; Gong, A; Elliott, A; McInnerney, K; Spangler, CW. Clin. Cancer. Res. 2008, 14: 6564-6573.

(9) Thompson, S; Chen, X; Hui, L; Toschi, A; Foster, DA; Drain, CM Photochem. Photobiol. Sci. 2008, 7: 1415-1421.

(10) Chen, X; Hui, L; Foster, DA; Drain, CM Biochemistry 2004, 43: 10918-10929.

(11) Pasetto, P; Chen, X; Drain, CM; Franck, RW Chem. Commun. 2001, 81-82.

(12) Samaroo, D; Vinodu, M; Chen, X; Drain, CM J. Comb. Chem. 2007, 9: 998-1011.

(13) Khurana, M; Collins, HA; Karotki, A; Anderson, HL; Cramb, DT; Wilson, BC Photochem. Photobiol. 2007, 83: 1441–1448.

Chapter 1 References

1) Croce, CM New England J. Med. 2008, 358: 502-511.
2) Cancer Facts and figures Am. Cancer Soc. 2002.
3) Sawyers CL Nature 2008, 452: 548-552.
4) Mitton D, Ackroyd R Photodiagnosis Photodyn Ther. 2008, 5:103-11.
5) Wilson, BC; Patterson, MS Physics in Medicine and Biology 2008, 53: R61–R109.
6) Buytaert, E; Dewaele, M; Agostinis P Biochim. Biophys. Acta 2007, 1776: 86-107.
7) Henderson, BW; Dougherty, TJ Photochem. Photobiol. 1992, 55: 145-157.
8) Danial NN, Korsmeyer SJ. Cell. 2004, 116:205-19. (a review)
9) Silvestris F, Ribatti D, Nico B, Silvestris N, Romito A, Dammacco F. Ann Ital Med Int. 1995, 10:7-13.
10) Seitz SJ, Schleithoff ES, Koch A, Schuster A, Teufel A, Staib F, Stremmel W, Melino G, Krammer PH, Schilling T, Müller M. Int. J. Cancer. 2009, 26:1-51
11) Thompson, S; Chen, X; Hui, L; Toschi, A; Foster, DA; Drain, CM Photochem. Photobiol. Sci. 2008, 7: 1415-1421.
12) Minamikawa, T; Sritana, A; Willians, D; Bowser, J; Hill, S; Nsgley, PJ. Cell Sci. 1999, 112: 2419-2430.
13) Edinger, A; Thompson, C Curr. Opin. Cell. Biol. 2004, 5: 752-762.
14) Fabris, C; Valduga, G; Moitto, G; Borsetto, G; Loi, G; Gabrisa, S; Reddi, E; Cancer Res. 2001, 61: 7495-7500.

Chapter 2 References

15) Kroemer, G; Dallaporta, B; Resche-Rigon, M Annu. Rev. Physiol., 1998, 60: 619-642.

16) Lawen, A BioEssays, 2003, 25: 888-896.

17) Sternberg, ED; Bruckner, C; Dolphin, D Tetrahedron, 1998, 54: 4151-4202.

18) Osterloh, J; Vicente, MGH J. Porphyrins Phthalocyanines, 2002, 6: 305-324.

19) Chen, X; Drain, CM, Drug Design Reviews 2004, 1: 215-234.

20) Chen, X; Hui, L; Foster, DA; Drain, CM Biochem., 2004, 43: 10918-10929.

21) Xu, C; Bailly-Maitre, B; Reed, JC J. Clin. Invest. 2005, 115: 2656-2664.

22) I. Yslas, M. G. Alvarez, C. Marty, G. Mori, E. N. Durantini, Rivarola V, Toxicology, 2000, 149, 69-74.

23) E. A. Slee, C. Adrain, S. J. Martin, Cell Death and Differentiation, 1999, 6: 1067-1074.

24) W. Yu, H. Wang, M. F. Poitras, C. Coombs, W. J. Bowers, H. J. Federoff, G. G. Poirier, T. M. Science, 2002, 297: 259-263

25) B. S. P. Reddy, S. M. Sondhi and J. W. Lown, Pharmacology & Therapeutics, 1999, 84: 1-111.

26) Caramelo, J; Parodi, AJ Seminars in Cell and Developmental Biology, 2007, 18: 732-742.

27) Thompson, S; Chen, X; Hui, L; Toschi, A; Foster, DA. Drain, CM Photochem. Photobiol. Sci. 2008, 7: 1415-1421.

28) Pino, SC; O'Sullivan-Murphy, B; Lidstone, EA; Yang, C; Lipson, KL, Jurczyk, A; diIorio, P; Brehm, MA; Mordes, JP; Greiner, DL; Rossini, AA; Bortell, R PLoS ONE. 2009; 4 (5):e5468

29) Buytaert, E; Dewaele, M; Agostinis, P Biochim Biophys Acta. 2007, 1776: 86-107.

30) Sun, GD; Kobayashi, T; Abe, M; Tada, N; Adachi, H; Shiota, A; Totsuka, Y; Hino O Biochem. Biophys. Res. Commun. 2007, 360: 181-187.

Chapter 3 References

31) Thompson, S; Chen, X; Hui, L; Toschi, A; Foster, DA; Drain, CM. Photochem. Photobiol. Sci. 2008, 7:1415-1421.

32) Kessel, D; Luo, Y; Deng, Y; Chang, CK Photochem. Photobiol. 1997, 65: 422-426.

33) Kessel, D; Vicente, MG; Reiners, JJ; J, Autophagy 2006, 2: 289-290.

34) Buytaert, E; Dewaele, M; Agostinis, P; Biochim. Biophys. Acta. 2007, 1776: 86-107.

35) Berg K, Folini M, Prasmickaite L, Selbo PK, Bonsted A, Engesaeter B, Zaffaroni N, Weyergang A, Dietze A, Maelandsmo GM, Wagner E, Norum OJ, Høgset A.; Curr. Pharm. Biotechnol. 2007, 8: 362-372.

36) Markovits, J; Roques, BP; Le Pecq, JB; Anal. Biochem. 1979, 94: 259-264.

37) Dunn, WA; Hubbard, AL; Aronson, NN J. Biol. Chem., 1980, 255: 5971-5978.

38) Zucker, SD; Goessling, W; Bootle, EJ; Sterritt, C. J. Lipid Res. 2001, 42: 1377-1388

39) Weissleder, R; Tung, CH; Mahmood, U; Bogdanov, A. Nat. Biotechnol. 1999, 17: 375–378.

40) Pagano, M; Clynes, MA; Masada ,N; Ciruela, A; Ayling, LJ; Wachten, S; Cooper, DM Am. J. Physiol. Cell Physiol. 2009; 296: C607-619.

41) Leth-Larsen, R; Lund, R; Hansen, HV; Laenkholm, A-V; Tarin, D; Jensen, ON; Ditzel, HJ Mol. Cellular Proteomics 2009, 8:1436-1449.

42) Chen, X; Hui, L; Foster, DA; Drain, CM. Biochemistry 2004, 43: 10918-10929.

43) Samaroo, D; Vinodu, M; Chen, X; Drain, CM. J. Comb. Chem. 2007, 9: 998-1011.

44) Castaneda F, Burse A, Boland W, Kinne RK. Int. J. Med. Sci. 2007, 4: 131-139.

45) Fritsch C, Lang K, Neuse W, Ruzicka T, Lehmann P. Skin Pharmacol. Appl. Skin Physiol. 1998, 11: 358-373.

46) Dougherty TJ, Gomer CJ, Henderson BW, Jori G, Kessel D, Korbelik M, Moan J, Peng Q. J. Natl .Cancer Inst. 1998, 90: 889-905.

47) Rastogi, S; Banerjee, S; Chellappan, S; Simon, GR Cancer Let. 2007, 257: 244-251.

Chapter 4 References

48) Pushpan, SK; Venkatraman. S; Anand, VG; Sankar, J; Parmeswaran, D; Ganesan, S; Chandrashekar, TK Curr. Med. Chem. Anticancer Agents. 2002, 2: 187-207.

49) Spikes, JD J. Photochem Photobiol B. 1990, 6: 259-274.

50) Mauzerall, DC Clinic. Dermatology, 1998, 6: 195–201.

51) Silva JN, Silva AM, Tomé JP, Ribeiro AO, Domingues MR, Cavaleiro JA, Silva AM, Neves MG, Tomé AC, Serra OA, Bosca F, Filipe P, Santus R, Morlière P. Photochem Photobiol Sci. 2008 Jul;7(7):834-43. Epub 2008 May 7

52) Pandey, RK J. Porphyrins Phthalocyanines 2000, 4: 368-373.

53) Silva, AMG.; Tome, AC; Neves, GPMS; Silva, AMS; Cavaleiro, JAS J. Org. Chem. 2005, 18;70(6) 2306-2314.

54) Thompson, S; Chen, X; Hui, L; Toschi, A; Foster, D.A; Drain, CM Photochem. Photobiol. Sci. 2008, 7: 1415-1421.

55) Samaroo, D; Vinodu, M; Chen, X; Drain, CM J. Comb. Chem. 2007, 9: 998-1011.

56) Caramelo, J; Parodi, AJ Seminars in Cell and Developmental Biology, 2007, 18: 732-742.

Chapter 5 References

57) Dy, J; Ogawa, K; Satake, A; Ishizumi, A; Kobuke, Y Chem. Eur. J. 2007, 13: 3491-3500.

58) Hanninen P, Soukka J, Soini JT.Ann N Y Acad Sci. 2008;1130:320-6. Review

59) Drobizhev, M; Karotki, A; Kruk, M; Rebane, A Chem. Phys. Let. 2002, 355: 175-182.

60) Mir, Y; Lier, J; Allard, J; Morris, D; Houde, D Photochem. Photobiol. Sci. 2009, 8: 391-395.

61) Leupold, D; Teuchner, K; Ehlert, J; Irrgang, K; Renger, G; Lokstein, H J. Biol. Chem. 2006, 281: 25381- 25387.

62) Dhistedt, E; Collins, H; Balaz, M; Kuimova, M; Khurana, M; Wilson, B; Philips, D; Anderson, HL Org. Biomol. Chem. 2009, 7: 897-904.

63) Fisher, JA; Susumu, K; Therien, MJ; Yodh, AG; J. Chem. Phys. 2009, 130: 134506

64) Starkey, JR; Rebane, AK; Drobizhev, MA; Meng, F; Gong, A; Elliott, A; McInnerney, K; Spangler, CW. Clin. Cancer. Res. 2008, 14: 6564-6573.

65) Thompson, S; Chen, X; Hui, L; Toschi, A; Foster, DA; Drain, CM Photochem. Photobiol. Sci. 2008, 7: 1415-1421.

66) Chen, X; Hui, L; Foster, DA; Drain, CM Biochemistry 2004, 43: 10918-10929.

67) Pasetto, P; Chen, X; Drain, CM; Franck, RW Chem. Commun. 2001, 81-82.

68) Samaroo, D; Vinodu, M; Chen, X; Drain, CM J. Comb. Chem. 2007, 9: 998-1011.

69) Khurana, M; Collins, HA; Karotki, A; Anderson, HL; Cramb, DT; Wilson, BC Photochem. Photobiol. 2007, 83: 1441–1448.